ΔΙΑΤΜΗΜΑΤΙΚΟ ΜΕΤΑΠΤΥΧΙΑΚΟ ΠΡΟΓΡΑΜΜΑ ΣΠΟΥΔΩΝ

"ΕΓΚΕΦΑΛΟΣ & ΝΟΥΣ"

ΤΜΗΜΑ ΙΑΤΡΙΚΗΣ

ΠΑΝΕΠΙΣΤΗΜΙΟ ΚΡΗΤΗΣ

Ποσοτική χαρτογράφηση φλοιϊκών εγκεφαλικών περιοχών πιθήκου που εμπλέκονται στην οφθαλμοκινητική συμπεριφορά: *in vivo* λειτουργική απεικόνιση με τη χρήση της αυτοραδιογραφικής μεθόδου [^{14}C]-δεοξυγλυκόζης

Διδακτορική Διατριβή

Σοφία Μπακόλα

Επιβλέπουσα: καθ. Ε. Σαββάκη

Ηράκλειο, 2007

Interdisciplinary Graduate Programme
in Brain and Mind Sciences
Faculty of Medicine
University of Crete

Quantitative Mapping of Monkey Cortical Areas during Oculomotor Behavior: *in vivo* Functional Imaging with the Autoradiographic Method of [^{14}C]-deoxyglucose

Doctoral Thesis

by Sophia Bakola
under the supervision of Prof. H.E. Savaki

Heraklion, 2007

TABLE OF CONTENTS

ΕΥΧΑΡΙΣΤΙΕΣ

Η παρούσα διατριβή εκπονήθηκε στα πλαίσια του Διατμηματικού Μεταπτυχιακού Προγράμματος Σπουδών "Εγκέφαλος & Νους", στο τμήμα Ιατρικής του Πανεπιστημίου Κρήτης. Οφείλω να ευχαριστήσω τα μέλη του Προγράμματος, διδάσκοντες και διδασκόμενους, που παρείχαν ένα γόνιμο περιβάλλον συμμετοχής και ανταλλαγής απόψεων.

Είχα την τύχη να εργαστώ υπό την καθοδήγηση της Ελένης Σαββάκη. Η ενεργητικότητα, το πάθος και η άρτια επιστημονική της κατάρτιση αποτέλεσαν σημεία αναφοράς στην εργαστηριακή μου πορεία. Της είμαι ευγνώμων για όσα μου δίδαξε και όσα προσπάθησε να μου διδάξει, κυρίως την τήρηση προκαθορισμένων ημερομηνιών κατά την παράδοση εργασιών.

Ευχαριστώ τον Αντώνη Μοσχοβάκη για την εξαιρετική συνεργασία σε κάθε στάδιο της πορείας μου. Στάθηκε εμπνευσμένος δάσκαλος και πολύτιμος σύμβουλος.

Ευχαριστώ την Κατερίνα Δερμών για την πολυετή συμπαράστασή της. Με δέχθηκε στο εργαστήριό της ως προπτυχιακή φοιτήτρια Βιολογίας φέρνοντάς με σε επαφή με τον γοητευτικό χώρο των Νευροεπιστημών.

Τους Αντώνη Μοσχοβάκη και Κατερίνα Δερμών ευχαριστώ επιπλέον για τη συμμετοχή τους στην Τριμελή Συμβουλευτική Επιτροπή.

Ευχαριστώ τον Γιάννη Δαλέζιο για τις ουσιαστικές υποδείξεις στην στατιστική ανάλυση των πειραματικών δεδομένων αλλά και για τις ενδιαφέρουσες συζητήσεις εντός και εκτός εργαστηρίου.

Ευχαριστώ τον Βασίλη Ράο για την ανιδιοτελή συμπαράσταση και πολύτιμη βοήθεια σε όλα τα στάδια εκπόνησης της εργασίας. Με την θεωρητική και τεχνική του κατάρτιση κατάφερε να δώσει λύσεις σε πολλά από τα προβλήματα που συνάντησα.

Ευχαριστώ την Helen Barbas από το Πανεπιστήμιο της Βοστόνης και τον Arnaud Falchier από το εργαστήριο του Henry Kennedy στο INSERM, Bron, Γαλλία, για την βοήθεια στην κυττοαρχιτεκτονική αναγνώριση των περιοχών της ενδοβρεγματικής και άνω κροταφικής αύλακας, αντίστοιχα.

Ευχαριστώ τους φίλους μεταπτυχιακούς φοιτητές με τους οποίους μοιραστήκαμε τον εργαστηριακό χώρο, ιδιαιτέρως τους Γωγώ Γρηγορίου, Λίνα Παπαδάκη, Μίνα Ευαγγελίου, Μάνο Κάττουλα και Κώστα Χατζηδημητράκη. Η βοήθειά τους συνέβαλε ώστε η καθημερινότητα να γίνεται πιο διασκεδαστική.

Ευχαριστώ τις Μαρία Παγωμένου, Μαρία Κεφαλογιάννη και Τένια Κουμάκη για την εξαιρετική τεχνική υποστήριξη.

Ευχαριστώ την Μαρία Ματαλλιωτάκη για την γραμματειακή υποστήριξη.

Ευχαριστώ τους συν-συγγραφείς των δημοσιευμένων επιστημονικών άρθρων για την βοήθεια στην συγγραφή της παρούσας εργασίας.

Ευχαριστώ την Michela Gamberini από το Πανεπιστήμιο της Μπολόνια για τη βοήθεια κατά την προετοιμασία της παρουσίασης της διατριβής.

Τέλος, ευχαριστώ τα μέλη της Επταμελούς Εξεταστικής Επιτροπής (Ε. Σαββάκη, Α. Μοσχοβάκη, Κ. Δερμών, Α. Γραβάνη, Κ. Χριστάκο, Γ. Δαλέζιο, Β. Ράο) για τον κόπο και την ευθύνη που ανέλαβαν.

Πηγές χρηματοδότησης:

FP5-grant QLRT-2001-00746,
FP6-grant IST-027574,
ΓΓΕΤ-01ΕD111,
Ιατρικό Κρήτης

Δημοσιευμένα άρθρα:

Bakola S, Gregoriou GG, Moschovakis AK, Savaki HE. (2006). Functional imaging of the intraparietal cortex during saccades to visual and memorized targets. *Neuroimage*. **31**(4):1637-49.

Bakola S, Gregoriou GG, Moschovakis AK, Raos V, Savaki HE. (2007). Saccade-related information in the superior temporal motion complex: quantitative functional mapping in the monkey. *J Neurosci.* **27**(9):2224-9.

ABBREVIATIONS

2D	two-dimensional	δισδιάστατος, -η, -ο
2DG	[^{14}C]-deoxyglucose	[^{14}C]-δεοξυγλυκόζη
2DG6P	[^{14}C]-deoxyglucose-6-phosphate	[^{14}C]-δεοξυγλυκόζη-6-φωσφορική
A	anterior	πρόσθιος, -α, -ο
Cd	monkey, control in the dark	πίθηκος ελέγχου στο σκοτάδι
Cf	monkey, fixation control	πίθηκος ελέγχου που εκτελούσε τη συμπεριφορά «εστίαση βλέμματος σε κεντρικό οπτικό στόχο»
D	dorsal	ραχιαίος, -α, -ο
Hd	monkey, horizontal memory-guided saccade task	πίθηκος που εκτελούσε τη συμπεριφορά «οριζόντιες σακκαδικές κινήσεις προς απομνημονευμένους στόχους»
Hl	monkey, horizontal visually-guided saccade task	πίθηκος που εκτελούσε τη συμπεριφορά «οριζόντιες σακκαδικές κινήσεις προς οπτικούς στόχους»
LCGU	local cerebral glucose utilization	τοπική κατανάλωση γλυκόζης στο φλοιό
Od	monkey, oblique memory-guided saccade task	πίθηκος που εκτελούσε τη συμπεριφορά «πλάγιες σακκαδικές κινήσεις προς απομνημονευμένους στόχους»
Ol	monkey, oblique visually-guided saccade task	πίθηκος που εκτελούσε τη συμπεριφορά «πλάγιες σακκαδικές κινήσεις προς οπτικούς στόχους»
P	posterior	οπίσθιος, -α, -ο
SD	standard deviation	σχετική απόκλιση
Sd	monkeys, memory-guided saccade tasks	πίθηκοι που εκτελούσαν τη συμπεριφορά «σακκαδικές κινήσεις προς απομνημονευμένους στόχους»
Sl	monkeys, visually-guided saccade tasks	πίθηκοι που εκτελούσαν τη συμπεριφορά «σακκαδικές κινήσεις προς οπτικούς στόχους»
V	ventral	κοιλιακός, -ή, ό

areas, zones, nuclei		*περιοχές, ζώνες, πυρήνες*
5	area 5, complex	περιοχή 5, σύμπλεγμα
5IP	medial intraparietal bank	έσω όχθη ενδοβρεγματικής αύλακας
7	area 7, complex	περιοχή 7, σύμπλεγμα
7a	visual area 7a	οπτική περιοχή 7
7IP	lateral intraparietal bank	πλάγια όχθη ενδοβρεγματικής αύλακας
7IPa	lateral intraparietal bank, anterior	πλάγια όχθη ενδοβρεγματικής αύλακας, πρόσθια
7IPm	lateral intraparietal bank, middle	πλάγια όχθη ενδοβρεγματικής αύλακας, μέση
7IPp	lateral intraparietal bank, posterior	πλάγια όχθη ενδοβρεγματικής αύλακας, οπίσθια
DLPN	dorsolateral pontine nuclei	ραχιαίοι-πλάγιοι πυρήνες της γέφυρας
FEF	frontal eye field	πρόσθια οφθαλμικά πεδία
FST	floor of superior temporal	δάπεδο της άνω κροταφικής αύλακας
FSTd	floor of superior temporal, dorsal	δάπεδο της άνω κροταφικής αύλακας,

		ραχιαίο
FSTv	floor of superior temporal, ventral	δάπεδο της άνω κροταφικής αύλακας, κοιλιακό
IPa	area IPa, Cusick et al. (1995)	περιοχή IPa, Cusick et al. (1995)
LIPd	lateral intraparietal area, dorsal	πλάγια ενδοβρεγματική αύλακα, ραχιαία
LIPv	lateral intraparietal area, ventral	πλάγια ενδοβρεγματική αύλακα, κοιλιακή
LOP	lateral occipital parietal zone, Lewis and van Essen (2000b)	πλάγια ινιακή βρεγματική ζώνη, Lewis and van Essen (2000b)
MC	motion complex	σύμπλεγμα ανάλυσης κινούμενων οπτικών ερεθισμάτων
MST	medial superior temporal area	έσω άνω κροταφική περιοχή
MSTd	medial superior temporal area, dorsal	έσω άνω κροταφική περιοχή, ραχιαία
MSTl	medial superior temporal area, lateral	έσω άνω κροταφική περιοχή, πλάγια
MT/V5	middle temporal area/ visual area 5	μέση κροταφική περιοχή/ οπτική περιοχή 5
MTf	middle temporal area, foveal	μέση κροταφική περιοχή, κεντρικό τμήμα
OAa	area OAa in the lower bank of the STs, Seltzer and Pandya (1978)	περιοχή OAa στην κάτω όχθη της άνω κροταφικής αύλακας, Seltzer and Pandya (1978)
PGa	area PGa in the upper bank of the STs, Seltzer and Pandya (1978)	περιοχή PGa στην άνω όχθη της άνω κροταφικής αύλακας, Seltzer and Pandya (1978)
PIT	posterior inferotemporal area, Felleman and van Essen (1991)	οπίσθια κάτω κροταφική περιοχή, Felleman and van Essen (1991)
PO	parietal-occipital area	περιοχή βρεγματοϊνιακή
SC	superior colliculus	άνω διδύμιο
SEF	supplementary eye fields	συμπληρωματικά οφθαλμικά πεδία
STP	superior temporal polysensory area	άνω κροταφική πολυαισθητική περιοχή
TEO	area temporoccipital, Boussaoud et al (1991)	κροταφική-ινιακή περιοχή, Boussaoud et al (1991)
TF	Temporal area F, von Bonin and Bailey (1947)	κροταφική περιοχή F, von Bonin and Bailey (1947)
TPO	temporal parietal occipital area	κροταφική βρεγματική ινιακή περιοχή
TPOc	temporal parietal occipital area, caudal	κροταφική βρεγματική ινιακή περιοχή, οπίσθια
TPOi	temporal parietal occipital area, intermediate	κροταφική βρεγματική ινιακή περιοχή, ενδιάμεση
TPOr	temporal parietal occipital area, rostral	κροταφική βρεγματική ινιακή περιοχή, πρόσθια
V1	visual area 1	οπτική περιοχή 1
V2	visual area 2	οπτική περιοχή 2
V3	visual area 3	οπτική περιοχή 3
V3A	visual area V3A	οπτική περιοχή 3α
V4	visual area 4	οπτική περιοχή 4
V4A	visual area V4A, Zeki (1971b)	οπτική περιοχή 4A, Zeki (1971b)
V4t	V4 transitional area	μεταβατική οπτική περιοχή 4
V4ta	V4 transitional area, anterior	μεταβατική οπτική ζώνη 4, πρόσθια
V4tp	V4 transitional area, posterior	μεταβατική οπτική ζώνη 4, οπίσθια

V6	visual area 6	οπτική περιοχή 6
VIP	ventral intraparietal area	κοιλιακή ενδοβρεγματική περιοχή
sulci		*αύλακες*
As	arcuate sulcus	τοξοειδής αύλακα
Cs	central sulcus	κεντρική αύλακα
IOs	inferior occipital sulcus	κάτω ινιακή αύλακα
IPs	intraparietal sulcus	ενδοβρεγματική αύλακα
Ls	lateral (Sylvian) sulcus	πλάγια αύλακα
Lus	lunate sulcus	μηνοειδής αύλακα
POs	parieto-occipital sulcus	βρεγματική-ινιακή αύλακα
Ps	principal sulcus	κύρια αύλακα
STs	superior temporal sulcus	άνω κροταφική αύλακα

INTRODUCTION

Oculomotor pathways

Intense research in systems neuroscience seeks to explain the neural basis of behavior providing ultimately a link between the mental and the physic. Inter-disciplinary approaches lead to the localization of function in brain areas so that now we are endowed with over 32 cortical areas implicated in visual processing (Felleman and Van Essen, 1991). Scientific toil aims to expose the critical information analyzed and stored within each node of an intricate network of connections, especially as one moves away from the centers of sensory input and motor output. Perhaps the most stimulating line of work investigates whether and how the discharge of single neurons or groups of neurons relates to complex behaviors, attentions, intentions, perceptions and decisions (Schall, 2004).

A fascinating system to address these questions is the oculomotor system. Fascination partly stems from its seemingly simplicity: the eye moves with only a few degrees of freedom by few muscles, it has a constant load and eye movements can be accurately measured in the laboratory. Extensive research indicates a constellation of brain regions responsible for eye movements that spread over the brainstem, the cerebellum, the basal ganglia,

the thalamus and the cortex (Fuchs et al., 1985; Moschovakis et al., 1996; Ilg, 1997; Tehovnik et al., 2000; Krauzlis, 2005). Two types of eye movements responsible for conjugate shifts of the line of sight have been described (Dodge, 1903, in Rashbass, 1961). Fast or saccadic movements use spatial information to redirect the line of sight to a peripheral target. Slow or smooth pursuit movements use motion information to match eye velocity to target velocity. Traditional views hold that different oculomotor circuits mediate saccadic and pursuit function. The superior colliculus (SC) in the midbrain, the frontal eye field (FEF) and the supplementary eye field (SEF) in the frontal lobe, and the lateral intraparietal area (LIP) in the parietal lobe are of particular importance for saccades (Robinson and Fuchs, 1969; Wurtz and Goldberg, 1972; Schlag and Schlag-Rey, 1987; Andersen et al., 1990). In contrast, the areas of the motion complex (MC) in the temporal lobe are of particular importance when it comes to pursuit (Komatsu and Wurtz, 1988a). Skepticism towards such a dichotomy was raised by more recent evidence suggesting that the same networks and, in some cases, the same neurons are activated during both pursuit and saccades (Krauzlis, 2004). For example, the rostral portion of the SC encodes an error signal that could be used in multiple movements (Krauzlis et al., 1997). Also, the involvement of the saccade-related cortical areas FEF, SEF and LIP in smooth pursuit has been broadly documented (Gottlieb et al., 1993; Heinen, 1995; Bremmer et al., 1997a; Tanaka and Lisberger, 2002). On the other hand, evidence on the involvement of the pursuit-related superior temporal MC in saccades is mainly circumstantial (Newsome et al., 1985; Dursteler and Wurtz, 1988) and largely questionable (Schiller and Lee, 1994). In this view, the strong reciprocal connections between area LIP and the middle temporal area (MT) are described as "puzzling" (Lewis and Van Essen, 2000b).

These observations triggered our interest in the current study. We aimed to map cortical activity in monkeys making repetitive visually-guided and

memory-guided saccades. Oculomotor behavior in the presence or absence of visual stimulation would reveal the distinct areas involved in sensory processing and/or motor execution. To this end, we employed the quantitative autoradiographic method of [^{14}C]-deoxyglucose (2DG; Sokoloff et al., 1977) that has provided a valuable tool in mapping neuronal pathways activated under different behavioral paradigms (Savaki, 1999). The method allows for the simultaneous measurement of local rates of cerebral glucose consumption, coupling energy metabolism with functional activity. Applications in primates include studies on the visuotopic organization and functional response properties in several cortical areas (e.g. Tootell et al., 1982; Geesamen et al., 1997; Gregoriou and Savaki, 2001; Vanduffel et al., 2002; Moschovakis et al., 2004).

Our analysis focused on the posterior parietal and superior temporal cortical areas (Fig. 1), both important nodes of the oculomotor network. These regions occupy intermediate positions between the centers of visual input and motor output. As we outline in the following sections, they possess the neural machinery to receive and/or process signals related to oculomotor behavior.

Posterior Parietal Cortex

The posterior parietal cortex lies in the caudal part of the parietal lobe and is composed of Brodmann's cytoarchitectonic areas 5, medially, and 7, laterally (Garey, 1999), divided by the intraparietal sulcus (IPs). Lesions in the posterior parietal cortex have long been described to cause a variety of visuomotor disorders. In the early 20th century, biparietal lesion in humans was reported to cause inability to look to peripheral targets ("psychic paralysis of gaze"), optic ataxia and simultagnosia, a syndrome that became known as Balint's syndrome (Hecaen and de Ajuriaguerra, 1954). More recently, functional studies in humans investigated subregions within the posterior parietal cortex, implicated

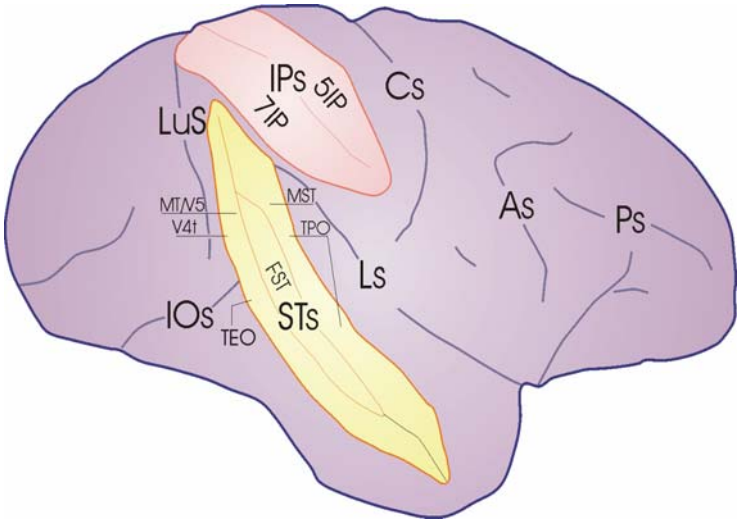

Figure 1. *Lateral view of the macaque brain. The intraparietal (IPs, pink) and superior temporal (STs, yellow) sulci are unfolded, exposing the areas studied. As, arcuate sulcus; Cs, central sulcus; IOs, inferior occipital sulcus; Ls, lateral sulcus; Lus, lunate sulcus; Ps, principal sulcus. FST, floor of the STs; MST, area medial superior temporal; MT/V5, area middle temporal/ visual area 5; TEO, area TEO; TPO, area temporal-parietal-occipital; V4t, area V4 transitional; 5IP, medial bank, 7IP, lateral bank of the IPs, respectively.*

in the visual guidance of movements (Anderson et al., 1994; Paus et al., 1995; Muri et al., 1996; Connolly et al., 2000; DeSouza et al., 2000; Tobler et al., 2001; Pierrot-Deseilligny et al., 2004).

One of the most studied areas in the macaque posterior parietal cortex is LIP which is engaged in eye movement control (Andersen et al., 1990). As the name implies, area LIP lies within the depths of the lateral bank of the IPs. Due to differences in myelination patterns and connectivity, LIP was further subdivided into a light myelinated dorsal part (LIPd) and a denser myelinated ventral part (LIPv) (Blatt et al., 1990). The visuotopic organization has been described in both anesthetized and awake monkeys (Blatt et al., 1990; Ben Hamed et al., 2001). These studies report a crude topographic representation of the contralateral visual field. In parallel with myelin demarcation, neurons representing the central visual field are found to reside mainly in LIPd whereas contralateral peripheral visual locations are represented in LIPv.

Area LIP has an extensively rich set of connections with visual and oculomotor areas. It is connected to prestriate areas V2, V3, and V4 (Seltzer and

Pandya, 1986; Cavada and Goldman-Rakic, 1989a; Andersen et al., 1990; Blatt et al., 1990; Baizer et al., 1991). Connections include the areas of the dorsal parieto-occipital cortex V3A and V6/PO (Colby et al., 1988; Baizer et al., 1991; Galletti et al., 2001). It is also reciprocally interconnected with areas VIP and 7a in the parietal cortex (Seltzer and Pandya, 1986; Cavada and Goldman-Rakic, 1989b; Blatt et al., 1990). Connections with temporal areas include the motion areas MT, MST and FST, as well as the caudal and intermediate parts of TPO (TPOc and TPOi) and area TEO (Andersen et al., 1990; Blatt et al., 1990; Boussaoud et al., 1990; Distler et al., 1993; Webster et al., 1994; Bullier et al., 1996; Lewis and Van Essen, 2000a). Projections from area LIP are directed to cortical and subcortical oculomotor centers such as the frontal eye fields (FEF) and the superior colliculus (SC) (Barbas and Mesulam, 1981; Asanuma et al., 1985; Lynch et al., 1985; May and Andersen, 1986; Andersen et al., 1990; Schall et al., 1995; Stanton et al., 1995; Bullier et al., 1996; Petrides and Pandya, 1999). Finally, we should note that LIP projects to the parahippocampal area TF that contributes to memory function (Suzuki and Amaral, 1994). The bulk of these studies highlights a differential connectivity pattern for the LIP subdivisions reviewed in Lewis and Van Essen (2000a). LIPd is strongly connected to areas emphasizing the central visual field, i.e. V4, V4ta, TEO and to ventral frontal eye fields, which control small-amplitude saccades. LIPv connections, on the other hand, involve the peripheral representations of visuotopic areas (V2, V3, V4, V4tp), motion areas MT and MST and the dorsal FEF implicated in large-amplitude saccades.

Physiological evidence supporting a role in saccade execution was provided by single-unit recordings in primates that described the visual and saccade-related properties of posterior parietal cortex. Early recordings of Mountcastle and colleagues (Mountcastle et al., 1975; Lynch et al., 1977) revealed neurons that respond during visually-guided saccades, suggesting a motor command function for this area. At about the same time, Robinson and

colleagues interpreted parietal function as sensory and attentional by recording enhanced visual responses when a stimulus was made behaviorally significant (Robinson et al., 1978; Bushnell et al., 1981). These initial observations would fuel a long and interesting debate regarding the decoding of parietal signals. However, the first investigations failed to distinguish LIP from the adjacent gyral cortex. Later recordings targeting specifically area LIP confirmed and expanded its visuo-oculomotor properties describing three cardinal features. First, robust visual responses were recorded from the majority of LIP neurons when a light stimulus excites their response field (Gnadt and Andersen, 1988; Andersen et al., 1990; Barash et al., 1991a; Colby et al., 1996). Second, saccade-related discharge was also present, usually occurring in the same neurons that were visually responsive. A common observation was that sensory and motor fields in each neuron were almost perfectly aligned (Barash et al., 1991b). More significantly, in about half of the neurons this signal was an early component of motor response, appearing well before saccade execution (Gnadt and Andersen, 1988). Oculomotor activation in the absence of a visual target is reported in only one study (learned saccade task, Colby et al., 1996). Third, by introducing a delay period between stimulus presentation and saccade execution many neurons displayed sustained "memory" activity while the animal had to withhold eye movements (Gnadt and Andersen, 1988). The above mentioned characteristics led to ambiguous interpretations of the precise role of area LIP in representing visual targets and preparing saccades [reviewed in Colby and Goldberg (1999); Andersen and Buneo (2002)]. On the one hand, emphasis is placed on the visual responses by proposing that area LIP contains a map of selective spatial locations irrespective of any action toward them. Experimental evidence in support is provided by the observation that visual response during fixation is further enhanced with the attentional load of the task in a particular location without overt eye movements (Colby et al., 1996). Further, LIP neurons are particularly excited by the abrupt appearance of novel stimuli that are

brought onto their receptive field by a saccade (Gottlieb et al., 1998). In addition, responses are stronger when a saccade is made to a visual stimulus than when a saccade is made in the same spatial location without a visual stimulus (Kusunoki et al., 2000). In the same context, responses are stronger to stimuli regardless of the direction of saccade (Gottlieb and Goldberg, 1999). It is argued therefore that salient stimuli weigh more in LIP neurons response than the execution of eye movements. On the other hand, experimental evidence supports that the discharge of LIP is related to early plans for saccade eye movements. Employing a variation of the double-saccade paradigm (Mays and Sparks, 1980), which requires the execution of two sequential saccades to briefly presented targets, it was shown that sustained activity was higher for saccades into the neuron's motor field. In contrast, many neurons had less memory activity of the visual stimulus when saccades were directed away from the motor field (Mazzoni et al., 1996a). Moreover, response patterns remained the same for saccades to visual and to auditory targets (Bracewell et al., 1996; Mazzoni et al., 1996b) although auditory stimulation alone does not activate LIP neurons (Grunewald et al., 1999). When either saccades or reaches were planned, activity in LIP was specific for the type of movement (Snyder et al., 1997; 1998). A different study showed that signals sent to the SC by LIP carry both visual and saccade-related information (Paré and Wurtz, 1997). In addition, electrical microstimulation of area LIP neurons evokes saccades albeit at high thresholds (Shibutani et al., 1984; Thier and Andersen, 1998). Moreover, tasks with a cognitive dimension revealed that between sensory activation and movement execution LIP participates in complex perceptual processes (Shadlen and Newsome, 1996; Platt and Glimcher, 1997).

In summary, the visual, saccadic and memory signals carried by area LIP neurons support its role in oculomotor behavior and spatial representation. Modulation of neuronal discharge with increasingly difficult tasks suggests that

LIP may be involved in the integration of sensory signals to guide motor actions.

Temporal cortex

From the extensive research on the visual areas of the STs a somewhat different picture has emerged. A great deal of attention targeted the motion areas of the MC located in the caudal portion of the STs. This consists of area MT/V5, situated in the posterior (lower) bank (Allman and Kaas, 1971; Zeki, 1974; Gattass and Gross, 1981; Van Essen et al., 1981), area MST in the anterior (upper) bank and area FST in the fundus and floor (Maunsell and Van Essen, 1983a; Desimone and Ungerleider, 1986; Boussaoud et al., 1990). MT/V5 was initially described in macaques on the grounds of the large projection it receives from the central field representation of the striate cortex (Zeki, 1971a). This report was soon followed by the description of its physiological properties (Zeki, 1974). MST and FST were originally referred to as a unified area (MST) medially to MT, receiving projections from the latter (Maunsell and Van Essen, 1983a). Studies on the myeloarchitecture and response properties revealed that the MT-projection zone consisted of two areas: MST, anterior, and FST, ventrally to MT (Desimone and Ungerleider, 1986). All three areas display response characteristics related to oculomotor function. Area MT contains a topographic representation of the contralateral visual field with a large area devoted to foveal vision (Van Essen et al., 1981). The defining characteristic of MT neurons is their selectivity for the direction of stimulus motion, with 65% up to 90% of neurons being directionally selective (Dubner and Zeki, 1971; Maunsell and Van Essen, 1983b; Albright, 1984; Rodman and Albright, 1987; Erickson et al., 1989; Cheng et al., 1994). All directions of motion are evenly distributed among the MT neuronal population (Kruse et al., 2002). Average neuronal response to the preferred

direction has been reported to be approximately 11 times higher than to the null direction (Maunsell and Van Essen, 1983b). However, MT neurons exhibit broad directional tuning, with mean bandwidth (width of directional tuned curve at half-maximal height) of about 90° (Albright, 1984). Neurons with similar directional tuning tend to be organized so that gradual changes of preferred motion direction are represented along columns (Albright et al., 1984). When tested with moving stimuli at different speeds, MT neurons responded to a range from 0.5 to 512 deg/sec (Maunsell and Van Essen, 1983b; Mikami et al., 1986; Lagae et al., 1993). Within this range, the most common preferred speed was about 40 deg/sec (Rodman and Albright, 1987). In contrast to the functional architecture for direction of motion, columnar organization for speed does not exist in MT, even though speed tuned neurons are clustered (Liu and Newsome, 2003). Area MT neurons encode global motion and thus resolve the aperture problem arising from local ambiguities of motion perception when two superimposed components move orthogonal to each other (Movshon and Newsome, 1996). Moreover, MT neurons integrate motion information in a roughly linear way. When multiple directions of motion are presented within their receptive fields the typical response is the scaled average of the individual component motion directions (Recanzone et al., 1997; van Wezel and Britten, 2002). Enhanced responses were elicited from MT neurons when their response field overlapped an attended portion of visual space (Treue and Maunsell, 1996; 1999). Discharge was further augmented when attention was directed to the one of a pair of competing stimuli that moved in the preferred direction.

Neurons in areas MST and FST have larger receptive fields compared to those reported for MT (Desimone and Ungerleider, 1986; Fiorani et al., 1989; Raiguel et al., 1997). While the receptive fields of FST include the fovea, those of MST are eccentric and usually do not include the central visual field (Erickson et al., 1989). In three studies, the majority of MST cells and about

one third to one half of FST cells were found to be directionally selective (Desimone and Ungerleider, 1986; Tanaka et al., 1986; Erickson et al., 1989), although in another study no directionally selective neurons were reported in FST (Komatsu and Wurtz, 1988a). A further classification of the macaque MST followed the observation that neurons in the anterior part had eccentrically centered larger receptive fields, while in a more lateral location neurons showed a mixture in sizes and eccentricities (Komatsu and Wurtz, 1988a). The two subregions (MSTd and MSTl, respectively) also processed different types of stimuli. In MSTd, neurons respond better to large patterns of moving stimuli. MSTl is inhabited both by neurons responding to large pattern fields and neurons preferring moving single spots of light (Komatsu and Wurtz, 1988b). The subpopulation of MSTd neurons responds to complex patterns of motion such as expansion, contraction, rotation, and spiraling patterns (Saito et al., 1986; Tanaka et al., 1986; Tanaka et al., 1993; Graziano et al., 1994), which are generated during navigation in the environment. The response of MST neurons to translational self-movement in the dark further suggests that MST neurons combine visual and vestibular signals to discriminate between self-movement and object-movement in the environment (Duffy, 1998). In addition, evidence has been provided that MSTd contributes to visuospatial orientation by encoding the preferred path of self-movement and the spatial location of the animal (Froehler and Duffy, 2002). On the other hand, it has been suggested that MSTl is involved in object motion and in controlling eye movements (Eifuku and Wurtz, 1998). Interestingly, FST has also been subdivided, albeit in the owl monkey, based on connectional data (Kaas and Morel, 1993). The dorsal part (FSTd) alone has direct connections with MT and MST, whereas the ventral part (FSTv) connects with the inferior temporal cortex.

Identified connectivity patterns support the visual and directional characteristics of MC neurons and further suggest a role in oculomotor

behavior. Area MT receives visual input directly from V1 (predominantly from layer IVB), from prestriate areas V2, V3 and V4 as well as from area V6 (Maunsell and Van Essen, 1983a; Weller and Kaas, 1983; Shipp and Zeki, 1985; Shipp and Zeki, 1989a; Shipp and Zeki, 1989b; Movshon and Newsome, 1996; Galletti et al., 2001). MST and FST are connected with VIP and V6, whereas MST has weak connections with peripheral V1, and V2 (Boussaoud et al., 1990; Lewis and Van Essen, 2000a; Galletti et al., 2001). FST shares also lateral connections with V4 (Boussaoud et al., 1990). All three areas that comprise the MC are interconnected and are also connected with LIPv (Lewis and Van Essen, 2000a). The same areas have been reported to project to the oculomotor FEF in the frontal cortex (Maioli et al., 1983; Barbas, 1988; Felleman and Van Essen, 1991; Maioli et al., 1998). Specific projections of MST/FST to the large-amplitude-saccade region of FEF (Schall et al., 1995) and to the pursuit-region of FEF have also been described (Bullier et al., 1996). Both subdivisions of the FST in the owl monkey also project to the FEF (Kaas and Morel, 1993). Among the subcortical connections of the MC, key outputs are to the SC (Maunsell and Van Essen, 1983a; Fries, 1984; Lui et al., 1995) and to the dorsolateral pontine nuclei (DLPN, Boussaoud et al., 1992; Distler et al., 2002).

Single-unit studies have identified neuronal populations in MT, MST and FST that respond during smooth tracking of a small target (Komatsu and Wurtz, 1988a; 1988b; Erickson and Dow, 1989; Thier and Erickson, 1992). In one study, pursuit-related neurons were found in the most anterior part of MT that corresponds to the representation of foveal visual field (MTf, Komatsu and Wurtz, 1988a). Engagement of MT neurons in saccade execution has been provided only indirectly. Small chemical inactivation of MT/MST produced a retinotopic error in adjusting saccade amplitude during pursuit initiation in the visual field contralateral to the lesion (Dursteler and Wurtz, 1988; Newsome et al., 1985). When the lesion was restricted to subregions of MST a directional error was observed related to pursuit maintenance. It was

characterized by a deficit in matching eye speed to target speed when the target was moving toward the lesioned side. Similar retinotopic deficits were also reported in a previous study in which the lesion was restricted to the central representation of MT (Dursteler et al., 1987). Microstimulation of MT and MST with high currents modified ongoing pursuit movements, usually yielding acceleration toward the stimulated site. (Komatsu and Wurtz, 1989). Therefore, stimulation increased retinal error and produced catch-up saccades but it had no effect when the eyes were fixating. In other experiments, microstimulation also affected both saccades and pursuit by introducing a velocity signal to the preferred direction of neurons (Groh et al., 1997; Born et al., 2000).

The execution of pursuit eye movements requires the continuous presence of a moving visual target. In contrast, saccades can be made without any visual stimulation. This tight linkage of smooth pursuit with light stimulation poses difficulties in distinguishing the visual from the motor components of pursuit responses. By transiently removing the visual motion stimulus during pursuit maintenance it was shown that MST neurons did not change their response (Newsome et al., 1988; Thier and Erickson, 1992). Even with brief target extinction, neurons could still maintain a tonic signal due to visual memory. This problem was solved with the execution of pursuit in the presence of an eccentric visual stimulus that fell outside the receptive field ("imaginary" target). Tracking neurons that responded in this task were recorded from MST. It is therefore suggested that extraretinal signals related to movement are confound to MST. However, it was reported later that for all cells in both MT and MST the response is primarily determined by the visual stimulus (Ferrera and Lisberger, 1997).

The rest of the STs comprises of: i) area V4t, in the posterior bank. This is a narrow cortical strip flanked between MT/V5 and V4 (Zeki, 1977; Maguire and Baizer, 1984), ii) the dorsal part of area TEO (von Bonin and Bailey, 1947)

that extends in the posterior bank (Distler et al., 1993), which may correspond to the posterior inferotemporal area (PIT, Felleman and Van Essen, 1991) or V4A (Zeki, 1996) in macaques, or to the FSTv of owl monkeys (Kaas and Morel, 1993), iii) the architectonic area temporo-parieto-occipital (TPO) (Cusick et al., 1995) in the upper bank, corresponding to the superior temporal polysensory cortex (STP) (Desimone and Gross, 1979).

The proposal that the areas V4t and TEO/V4A are parts of the color-coding V4-complex (Zeki, 1977; Zeki, 1996) as reflected in their similar response properties only attests to the complexity of the characterization of a cortical field as area. Perhaps the strongest pieces of evidence in treating these as distinct areas lie in their different myelination patterns and in that they contain different representations of the contralateral visual field (Desimone and Ungerleider, 1986; Boussaoud et al., 1991). TEO and V4 neurons modulated their firing in a fixation task (Watanabe and Iwai, 1991). In a comprehensive study, neurons with small receptive fields were recorded from V4t and TEO, which responded to the presentation of simple and complex objects (Kobatake and Tanaka, 1994). Both these areas share connections with V2 and V4 (Zeki, 1977; Boussaoud et al., 1991; Nakamura et al., 1993; Felleman et al., 1997), LIPd (Webster et al., 1994; Lewis and Van Essen, 2000a), the MC (Seltzer and Pandya, 1989b; Barone et al., 2000) and FEF (Webster et al., 1994; Schall et al., 1995).

In area TPO, almost all neurons are visually responsive and over half of them are modulated also by auditory and/or somatesthetic stimuli (Desimone and Gross, 1979; Bruce et al., 1981). TPO has no visuotopic organization, and visual and somesthetic receptive fields are very large usually including both hemifields (Bruce et al., 1981). Many neurons are sensitive to direction of motion and insensitive to stimulus size or shape, responding equally to moving dots and human bodies (Oram and Perrett, 1996). After striate cortex lesions, TPO neurons do not abolish their visual

properties, although directional selectivity is disrupted. Loss of visual properties of TPO neurons requires the ipsilateral removal of SC in addition to the striate cortex lesion (Bruce et al., 1986), same way as for MT (Rodman et al., 1990). TPO is connected to FEF (Barbas and Mesulam, 1981; Seltzer and Pandya, 1989a), specifically to pursuit FEF (Bullier et al., 1996), to SEF (Luppino et al., 2001) and to posterior parietal cortex (Morel and Bullier, 1990; Baizer et al., 1991). It receives projections from MST, FST (Boussaoud et al., 1990) and the inferior temporal cortex (Morel and Bullier, 1990; Baizer et al., 1991).

In summary, the caudal STs harbors multiple heterogeneous signals. The MC carries visual motion information to guide smooth-pursuit and self-motion, areas V4t and TEO analyze visual inputs for object identification and area TPO integrates visual, auditory and somatosensory signals for eye-movement execution and biological motion.

Aim of the study

We attempted to explore the visual and oculomotor patterns of IPs and STs cortical activation in rhesus monkeys performing simple repetitive saccades to visual and memorized targets. By applying the quantitative autoradiographic method of 2DG (Sokoloff et al., 1977) we investigated in detail the cortical areas activated under the two behavioral paradigms. Previous attempts to understand how neural space in the intraparietal cortex represents visual space and movement metrics have been indirect, relying on single-cell records obtained sequentially over several experimental sessions on different days and in different animals. In contrast, the technique we employed allowed us to obtain high-resolution two-dimensional activity maps throughout the intraparietal and superior temporal cortex of monkeys engaged in visuo/oculomotor tasks. Furthermore, alignment of functional data with cytoarchitectonic maps enabled us to assign distinct roles in each of the areas analyzed. In the present study, we addressed the following questions:

1) Whether saccades to visual targets activate area LIP in the intraparietal cortex, while their impact on the superior temporal areas is less pronounced, in accordance to the existing literature. To this end, we trained two monkeys to make visually-guided horizontal and oblique saccades of similar amplitudes, and we examined the patterns of glucose uptake in the IPs and STs cortices.
2) Whether, in the absence of visual targets, saccades to memorized locations affect LIP neurons but not ST cortical neurons. Accordingly, we eliminated the visual inputs and trained two monkeys to make memory-guided saccades of similar metrics as in the visually-guided paradigm. Examination of the extent and magnitude of glucose consumption revealed the cortical areas activated by execution of this

task and allowed for comparisons with the effects induced by saccades to visual targets.

3) Whether active fixation of a central visual target modulates the metabolic activity in cortical areas that represent the central visual field. To this end, we trained one monkey in a simple fixation task and we examined the effects of foveation and compared them with those induced by visually-guided saccades.

METHODS

Animals

Experiments were performed on six adult female monkeys (*Macaca mulatta*) weighing between 3 and 6kg. All animals were purpose-bred by authorized suppliers (LaborAgra, Budapest, Hungary; Deutches Primatenzentum, Goettingen, Germany). While food was fully available (Mucedola, Mi, Italy), access to water was controlled and animals received necessary fluids during daily experimental sessions. The weight and well-being of the animals were carefully monitored and, if necessary, supplementary fruit and water were provided. Monkeys had free access to water on weekends.

Housing, surgical and experimental procedures were approved by the Greek Veterinary Authorities and the FO.R.T.H animal use committee and conformed to European Council Directive 86/609/ECC.

Animal Preparation

Upon arrival, the animals were accommodated in their cages (Crist Instrument Co, Hagerstown, MD, USA) and were allowed to get accustomed to their new environment for three weeks before any operation. During this

time, they were monitored for normal behavior and eating habits and were presented with baby toys and music for stimulation.

Animals were prepared for behavioral training by stereotactically cementing (Resivy, Vence, France) a metal bolt (Crist Instrument Co, Hagerstown, MD, USA) onto mandibular plates (Synthes, Bettlach, Switzerland), secured on the cranium with titanium screws (Synthes, Bettlach, Switzerland) for head immobilization. Eye coils were sutured on the sclera [modified from Judge et al. (1980)] to record the instantaneous position of the eyes (Robinson, 1963). All surgical procedures were performed under anesthesia (ketamine hydrochloride, Imalgene 1000, Merial, France, 20mg/kg, i.m.) and aseptic conditions, with the aid of a stereo microscope. Systemic antibiotics (Rocephin, Roche, Switzerland, 70 mg/kg/d i.m.; Tobrex, Alcon, Switzerland) and analgesics (Apotel, Uni-Pharma, Hellas) were administered pre- and post-operatively. The animals were allowed to recover from surgery for at least 3 weeks before training began.

Experimental set-up

During training sessions and 2DG experiments, animals were seated in a primate chair (Crist Instrument Co, Hagerstown, MD, USA) with their upper and lower limbs restrained with Velcro® tapes. Limb restraint and head immobilization ensured that the detected activations were due to visual/oculomotor rather than skeletomotor behavior. Training was based on operant conditioning techniques and successful completion of each trial was rewarded with water, delivered by a tube placed close to the animal's mouth. Monkeys were trained for 3-10 months, until they performed ~90% accurately, before proceeding with the 2DG experiment.

The behavioral apparatus was a 21-inch video monitor (Philips, the Netherlands) placed 23 cm in front of the monkeys. Visual targets were red

spots of 1.5° diameter. Monkeys executing visually-guided saccades were required to hold eye position within an electronically defined circular window of 2.5° diameter centered on the visual target. Monkeys executing memorized saccades were required to hold eye position within a circular window of 5° diameter around the memorized location. During the memorized oculomotor tasks, auditory cues were presented through a speaker attached on top of the monitor straight ahead of the monkey. All experimental procedures took place in complete darkness.

Experimental control and data acquisition

Behavioral paradigms, data acquisition and reward were controlled by a PC running the custom written software NPV (Dr. Paul Johnson). The NPV feeded a) the behavioral monitor with the stimuli to be presented to the animal, and b) a microprocessor interface (CED1401, Cambridge, UK) with target position information (Fig. 2).

The instantaneous eye position was monitored using the search coil method (Judge et al., 1980). Electrical current flowing through paired horizontal and vertical coils (Remmel Labs, TX, USA) around the monkey's head created approximately homogeneous magnetic fields. These magnetic fields induced in the implanted search coils the signal used to measure eye position. Incoming analog eye position signals from the eye coil converged on the CED interface. Eye position was sampled at a temporal rate of 500Hz. From the CED interface, digital information about eye position was fed back to the NPV software. Incoming behavioral information was stored and, in case of accurate oculomotor behavior, reward was released, otherwise, trial was aborted and a new trial begun. Eye-position information was also fed to a second PC running the Spike2 software (Cambridge Electronics

Design,Cambridge, UK). Incoming information about eye movements was stored and analyzed off-line.

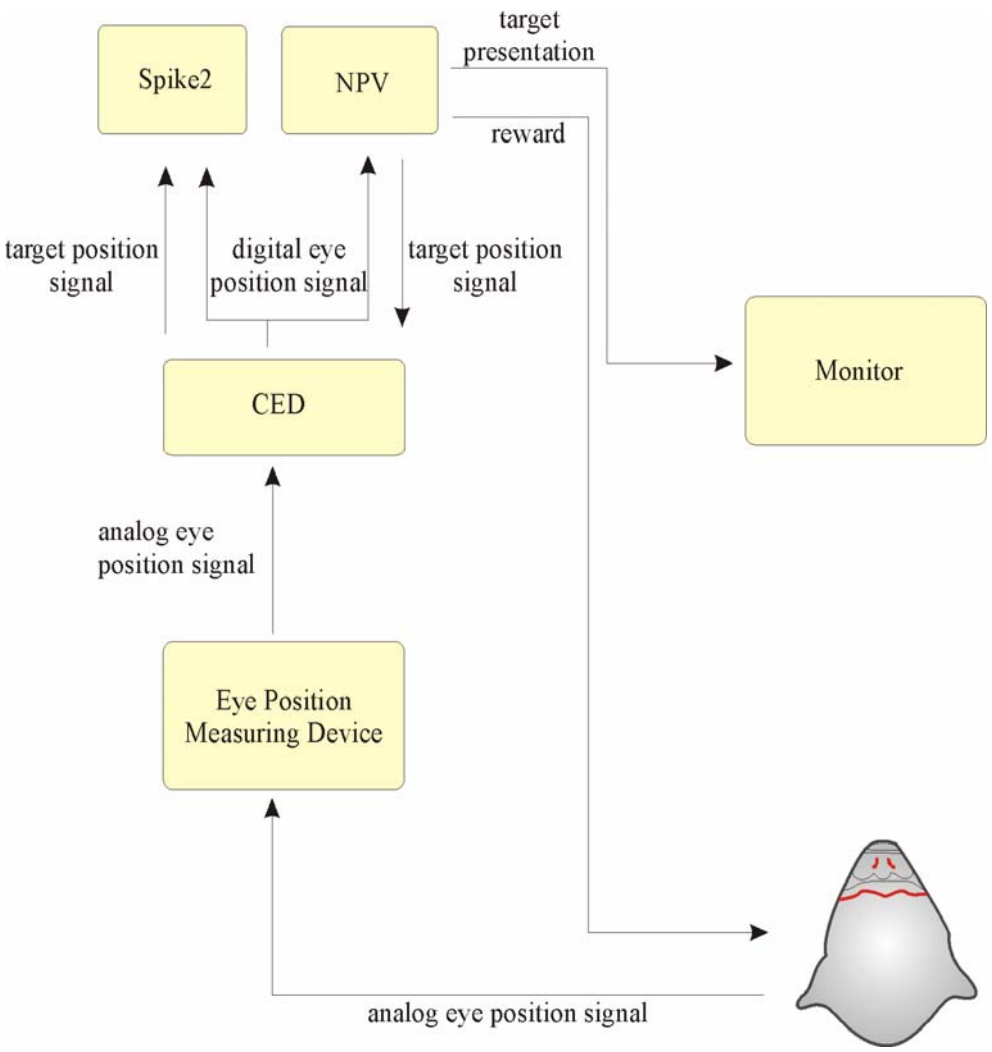

Figure 2. *Schematics of the experimental set-up. A target controlled by the NPV software was presented to the monkey on a video monitor. Through the CED box, eye position from the eye-position-measuring device was compared to target position and, in case of accurate oculomotor behavior, reward was released. If oculomotor behavior was not accurate, the trial was aborted. Furthermore, from the CED box, eye and target position signals were sent to a second computer running the Spike2 software for off-line analysis.*

Behavioral tasks

Given the European Union restrictions about the use of primates as experimental subjects, we used the minimum possible number of monkeys that allows for solid conclusions about the mechanisms of function of the primate oculomotor cortical system. We designed the experimental tasks in a way that controlled behavioral parameters (e.g. fixation, visual stimulation, saccades to memorized locations, saccades to visual targets) were gradually added (Table 1). This way, all tasks were complementary to each other, and the major metabolic findings in each monkey per task were verified by those in the monkey of the following, more complex task. Task parameters were chosen so as to ensure that the crucial variable, i.e., the total number of the stimulus triggered saccades per minute, would obtain the same value in all animals.

Visually-guided saccades. The monkey performing the visually-guided horizontal saccade task (Hl, Horizontal-light) had to maintain fixation of a central visual target for 0.3–0.6s, then to execute a saccade within 0.7s to a peripheral visual target located 30° to the right in the horizontal direction, and to fixate it for 0.3–0.6s. Intertrial intervals ranged between 0.5 and 0.8s (Fig.3B). The monkey performing the visually-guided oblique saccade task (Ol, Oblique-light) was required to execute an up-left saccade of 20° amplitude and 135° direction from the central starting position, within 0.6s, and to maintain fixation on each target for 0.4–0.6s. Intertrial intervals were between 0.3 and 0.5s (Fig. 3C).

Memory-guided saccades. The monkey performing the memory-guided horizontal saccade task (Hd, Horizontal-dark) was required to fixate straight ahead in total darkness following an auditory cue (90Hz) and hold its gaze for 0.4–0.7s, until a second auditory cue (180Hz) signaled that a memorized saccade of 20° in the horizontal direction should be executed within 1s, and

fixation should be maintained for 0.4–0.7s. Intertrial intervals ranged from 0.8–1.1s (Fig. 3D). Following an auditory cue of 90Hz, the monkey performing the memory-guided oblique saccade task (Od, Oblique-dark) had to keep its eyes straight ahead for 0.5–0.7s, until a second auditory cue of 180Hz commanded an up-left saccade of 25° in amplitude and 135° in direction within 1s. The monkey held its gaze to the memorized target position for 0.5–0.7s. Intertrial intervals were 0.5–0.7s long (Fig. 3E). Each monkey executing memory-guided saccades was initially trained to fixate a central visual target during the presentation of the 90Hz auditory cue, and to saccade to a visual target of specific amplitude (20–25°) and specific direction (either horizontal or oblique) during the 180Hz auditory cue. Later on in their training, the visual targets were removed, and the monkeys were rewarded for executing saccades to the target positions they had learned to associate with the respective sounds. Each monkey was required to execute saccades to a single memorized position. Because they were in complete darkness, monkeys executing memorized saccades were required to fixate the central and the peripheral target both within a window of 5°, in contrast to the monkeys executing visually-guided saccades, which were required to hold their gaze in a window of 2.5°.

Task	Behavioral components
Central fixation	visual stimulation, fixational eye movements
Visually guided saccades	visual stimulation, fixational eye movements, large-amplitude saccades
Memory-guided saccades	fixational eye movements, large-amplitude saccades, auditory cues
Control in the dark	auditory cues

Table 1. *Task components.*

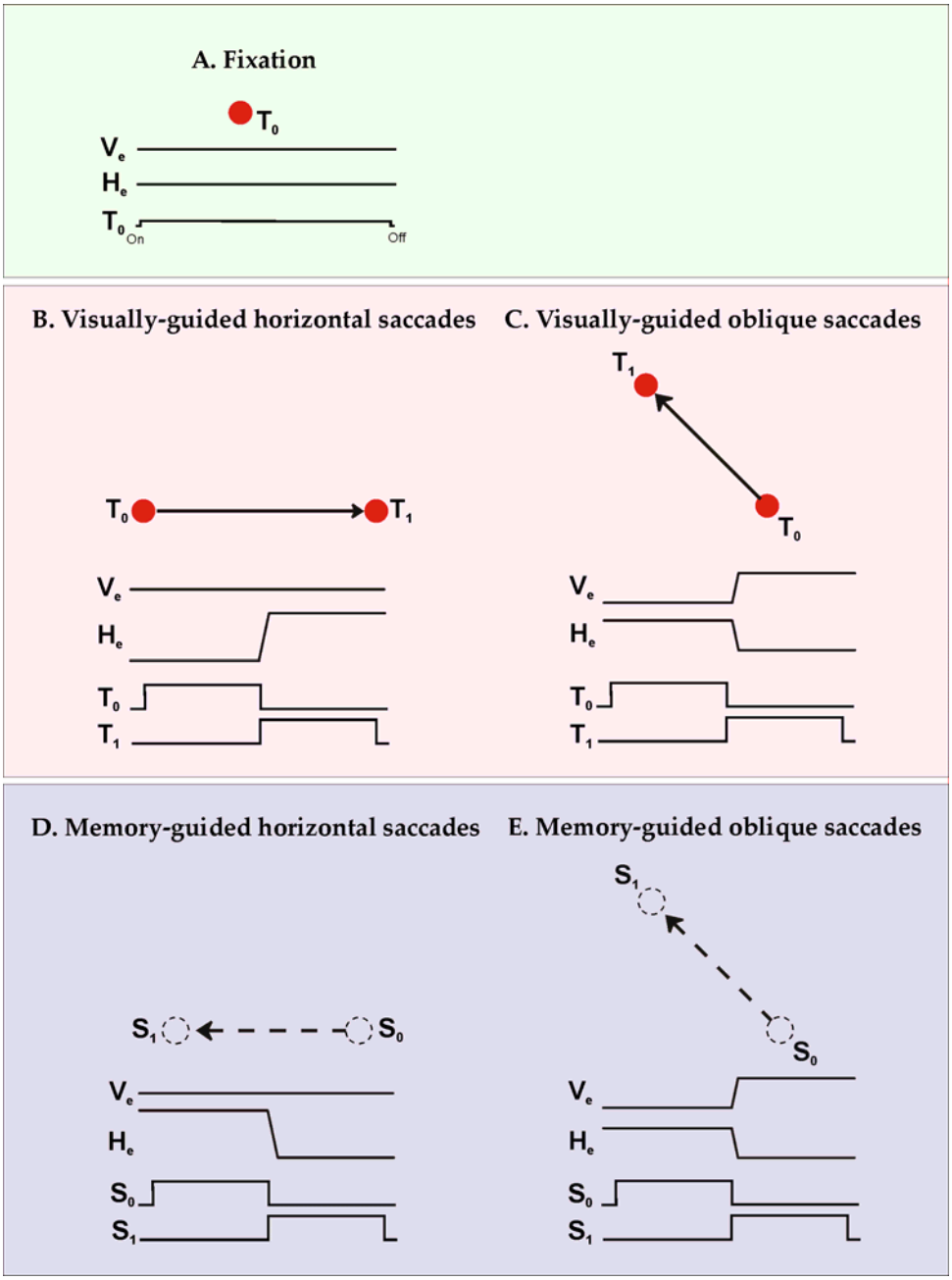

Figure 3. *Schematics of the behavioral tasks. (A) In the fixation task the monkey was rewarded for fixating a visual target (T_0) straight ahead. Ve, He, vertical and horizontal eye position, respectively. (B) The second monkey was rewarded for making visually-guided horizontal saccades of 30^0 (from T_0 to T_1) to the right. (C) The third monkey was rewarded for making visually-guided oblique saccades of 20^0 amplitude and 135^0 direction (from T_0 to T_1). (D) The fourth monkey was rewarded for making memory-guided horizontal saccades of 20^0 amplitude to the left, triggered by auditory cues (from S_0 to S_1). (E) The fifth monkey was rewarded for making memory-guided oblique saccades of 25^0 amplitude and 135^0 direction, triggered by auditory cues (from S_0 to S_1).*

Controls. The control monkey in the dark (Cd, Control in the dark) was presented with auditory stimuli similar to the acoustic cues presented to the monkeys executing memory-guided saccades. Reward was delivered randomly in order to prevent association of the auditory stimuli with reward expectancy. The monkey was alert during the whole 45min of the 2DG experiment as demonstrated by the execution of spontaneous eye movements. The fixation control (Cf, Control-fixation) monkey was trained to fixate a central light spot located straight ahead for 4s per trial. Intertrial intervals ranged between 0.2 and 0.3s (Fig. 3A).

[^{14}C]-Deoxyglucose Procedure

Theoretical basis

The tight coupling of energy metabolism to neuronal activity stands at the core of functional imaging techniques whereby local changes in brain activity can be detected by monitoring the changes in blood flow, glucose utilization or blood oxygenation. In 1977, Louis Sokoloff and co-workers developed a method to measure the local rates of energy metabolism simultaneously in all brain structures of conscious laboratory animals (Sokoloff et al., 1977). The conceptual framework of the method is based on the biochemical properties of 2-deoxyglucose, a structural analogue of glucose, enabling the mapping of brain regions involved in specific neural and cognitive processes.

The brain is an organ whose energy demands are among the highest of all body tissues. Thus, while it represents only 2% of the total body weight, it accounts for 20% of the resting total body oxygen consumption. Glucose is considered the almost exclusive blood-borne energy substrate utilized by the adult brain to fuel its activity. Energy metabolism is directly reflected in

oxygen consumption; however, the volatility of oxygen and its metabolic products and the short half-life of its radiolabeled isotopes preclude measurement of oxidative metabolism by the autoradiographic technique. Radioactive glucose is not fully satisfactory either, because its labeled products are lost too rapidly from cerebral tissues. The biochemical properties of 2DG, the labeled analogue of glucose, make it particularly appealing to trace glucose metabolism and to measure local cerebral glucose utilization by the autoradiographic technique. 2DG competes with glucose for transport across the blood-brain barrier and for hexokinase phosphorylation. Further metabolism of 2DG-6-phospate (2DG-6-P) occurs only slowly, so that it accumulates in the cerebral tissues. It is this particular feature that made 2DG an attractive glucose tracer.

If, following the administration of 2DG, the interval of time is kept short enough (less than 1 hour), the quantity of 2DG-6-P accumulated in any cerebral tissue at any time is equal to the integral of the rate of 2DG phosphorylation during that interval of time. This integral is related to the amount of glucose that has been phosphorylated over the same interval, depending on the time courses of the relative concentrations of 2DG and glucose in the precursor pools, and the Michaelis-Menten kinetic constants for hexokinase with respect to both 2DG and glucose. With cerebral glucose consumption in a steady-state, the amount of glucose phosphorylated during the interval of time equals the steady-state flux of glucose through the hexokinase-catalyzed step times the duration of the interval, and the net rate of flux of glucose through this step equals the rate of glucose utilization.

An operational equation that describes these relations has been derived, provided that: a) glucose metabolism is in a steady-state throughout the experimental period, i.e. independent of plasma glucose, b) the concentration of glucose and 2DG are homogeneous in the compartments,

and c) 2DG concentrations are low compared to their glucose counterparts, i.e. tracer kinetics apply.

The operational equation, which defines the rate of glucose utilization/unit mass of tissue, i, (Ri), is presented in Appendix. This equation is a general statement of the standard relationship by which rates of enzyme-catalyzed reactions are determined from measurements made with radioactive tracers. The numerator represents the amount of radioactive product formed in any given interval of time; it is equal to Ci*, the combined concentrations of 2DG and 2DG-6-P in the tissue at time, T, (measured by quantitative autoradiography) minus a term that represents the free (non-metabolized) 2DG still remaining in the tissue. The denominator represents the integrated specific activity (the ratio of labeled to total molecules) in the precursor pool as measured in plasma, corrected for the lag in the equilibration of the tissue precursor pool with the plasma, times a factor that corrects for kinetic differences between the labeled and natural compound (isotope effect).

Experimental session

Experiments were performed on conscious behaving animals. The day of the 2DG experiment, each animal was subjected to femoral vein and artery catheterization under anesthesia (ketamine hydrochloride, 20 mg/kg, i.m.). The catheters, plugged at one end, were filled with dilute heparin solution (100 U/ml) before insertion. Both catheters were 45 cm long, to minimize extensive flushing of dead space during the sampling period. The animals were allowed to recover from anesthesia for 4-5 hours before continuation of the experiment.

A dose of 100 μCi/kg of 2DG (specific activity 55 mCi/ml, ARC, St. Louis, MO, USA) was employed. Because the 2DG is supplied in ethanol

solution, it was evaporated to dryness and then re-dissolved in 1ml of saline. The experimental period was initiated with the infusion of a single pulse of 2DG through the venous catheter over a period of 30s. To monitor the plasma and 2DG concentrations, arterial blood samples were collected in heparinized tubes during predetermined time intervals: 0s (start of infusion), 15 s, 30 s, 45 s, 1 min, 2 min, 3 min, 5 min, 7.5 min, 10 min, 15 min, 25 min, 35 min and 45 min. Care was taken to clear the dead space of the arterial catheter prior to the collection of each sample. The samples were immediately centrifuged in a high speed Beckman centrifuge and kept on ice for analysis. After the collection of the last sample, the animal was killed by an i.v. infusion of thiopental (10 mg/ml) followed by a saturated solution of KCl for cardiac arrest.

Analysis of arterial plasma 2DG and glucose concentrations

The concentration of deoxyglucose was calculated by its ^{14}C content. Twenty μl of plasma and 3 ml of scintillation liquid (Insta-Gel, Packard Co., Illinois, USA) were introduced in a counting vial and assayed in a liquid scintillation counter (Beckmann Coulerton Inc., Foullerton, CA, USA). The efficiency (E) of the counting was estimated by internal standardization (calibrated [^{14}C]-toluene), then, the obtained counts (cpm) were transformed into disintegrations per minute (dpm) according to the equation dpm=cpm/E.

The plasma glucose concentration was assayed in a dry glucose analyzer (Spotchem, Menarini, Italy) to establish the required steady state for plasma glucose levels.

Tissue processing

The brain was rapidly removed, frozen by immersion in isopentane at −50°C, covered in embedding medium (M1, Lipshaw Manufacturing Co, Detroit, MI,

USA) to prevent dryness and stored at −80°C. Twenty-μm-thick adjacent horizontal sections were cut serially in a cryostat (Leica Microsystems, Wetzlar, Germany) at −20°C. Sections were collected on coverslips and dried on a hot plate at 60°C. Coverslips were glued to cardboard, and exposed to x-ray film (EMC1, Kodak) for about 14 days together with a set of precalibrated ^{14}C standards (Amersham plc, Little Chalfont, Buckinghamshire, UK). Films were developed in a Kodak X-OMAT 1000 automatic processor. One section in every 25 was saved on a slide and stained with thionine.

Analysis of autoradiographs

Quantitative densitometric analysis of autoradiographs was performed on a computerized image-processing system (MCID, Imaging Research, Ontario, Canada). Integrated arterial plasma specific activities for each monkey, derived from the blood concentration curves, were used to convert tissue ^{14}C concentrations to local cerebral glucose utilization (LCGU) values (Kennedy et al., 1978).

Two-dimensional reconstructions

Local cerebral glucose utilization (LCGU) values (in μmol/100g/min) were calculated from the original operational equation of the method (Sokoloff et al., 1977) using the appropriate kinetic constants for the monkey (Kennedy et al., 1978). To cover the full extent of the IPs, a total of about 550 serial horizontal sections of 20μm thickness in each hemisphere were analyzed. The full extent of the STs was analyzed in about 1700 serial horizontal sections.

The spatial distribution of metabolic activity within the rostrocaudal and the dorsoventral extent of each hemisphere was reconstructed in two dimensional (2D) maps (Dalezios et al., 1996; Savaki et al., 1997) (Fig. 4B, 5B).

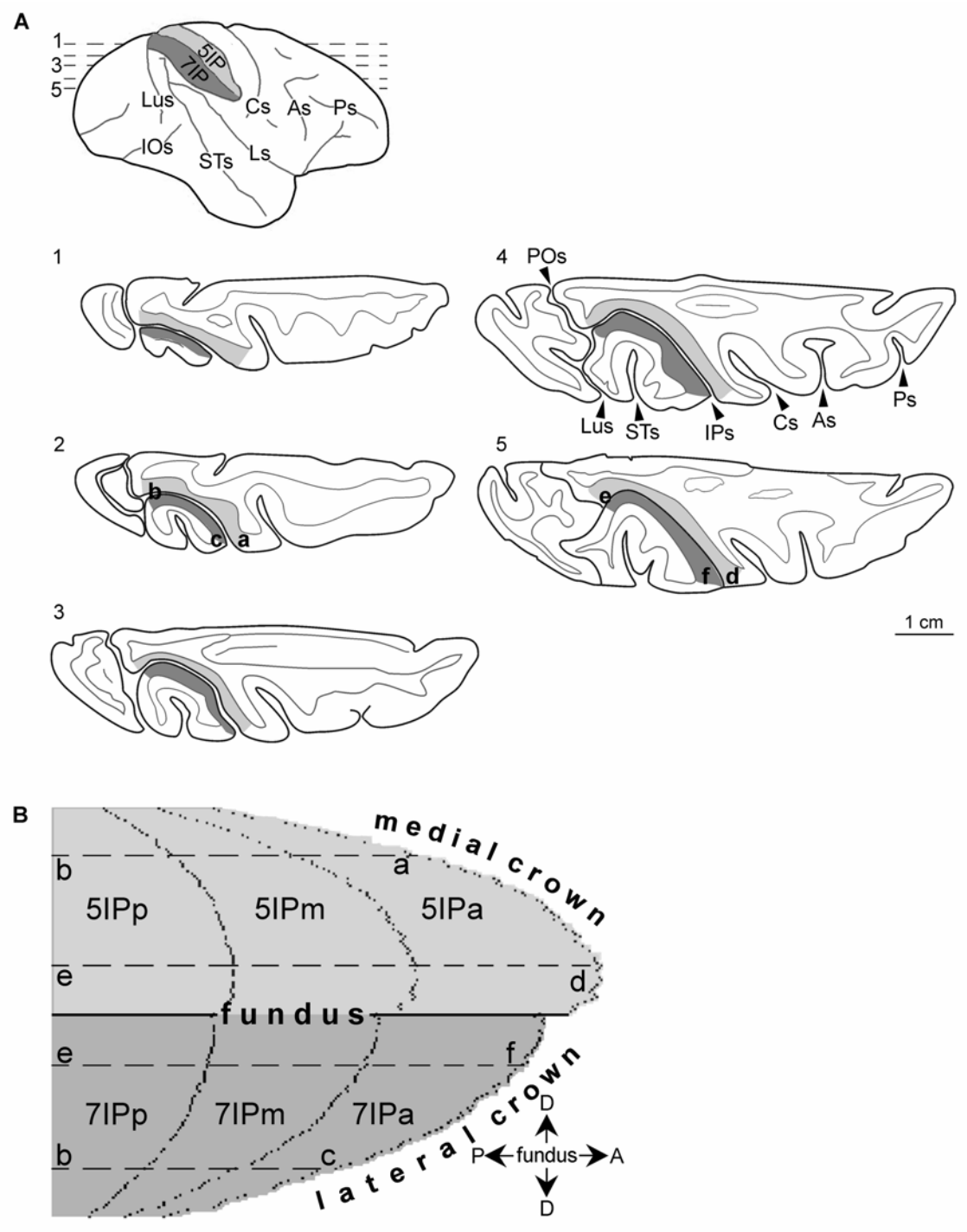

Figure 4. *(A) Lateral view of the right hemisphere of a monkey brain illustrating the unfolded IPs and the exposed medial (5IP, light grey) and lateral (7IP, dark grey) banks. Also, schematic illustration of five horizontal sections (1–5 from dorsal to ventral) at the levels indicated in the brain drawing. In all sections, the reconstructed IPs is gray-shaded. In sections 2 and 5, points a and d correspond to the crown of the medial bank of the IPs; points b and e to the intersection of the IPs with the parietoccipital (POs) and the Ls sulci used for alignment of adjacent sections; points c and f to the crown of the lateral bank of the IPs. (B) Schematic illustration of the 2D reconstructed IPs. Letters a–f correspond to the same anatomical landmarks as in sections 2 and 5 in (A); 5IPa, 5IPm, 5IPp, anterior, middle, posterior third of the medial bank of the IPs; 7IPa, 7IPm, 7IPp, anterior, middle, posterior third of the lateral bank of the IPs; A, anterior; P, posterior; D, dorsal; other abbreviations, as in Fig. 1.*

For each horizontal brain section, a data array was obtained by sampling LCGU values in the rostrocaudal extent along a line parallel to the surface of the cortex which included all cortical layers. For the intraparietal cortex, the intersection of the IPs with the parietoccipital sulcus (POs) was used for the alignment of adjacent data arrays. For the temporal cortex, the anterior tip of the floor of STs was used as the point of alignment. Given that the average of LCGU values was calculated in sets of five adjacent sections, the plotting resolution in the illustrated 2D maps is 100 μm. Normalization of LCGU values was based on the average unaffected gray matter value pooled across all hemispheres of all monkeys. The statistical significance of differences in LCGU values for the intraparietal and temporal regions in all monkeys was determined by the Student's unpaired *t*-test. Adopting a conservative criterion, only differences exceeding 10% were considered for statistical analysis given that homologous areas of the two hemispheres of a normal resting monkey can differ by up to 7% (Savaki et al., 1993).

Geometrical normalization and activity plots

Due to the inter- and intra-hemispheric variability, and to allow for the direct comparison of the sites of activation, the individual 2D maps (functional-2DG, and anatomical-cytoarchitectonic) were further processed to match a reference map [geometrical normalization according to Gregoriou and Savaki (2003)]. For the intraparietal cortex, in each horizontal section, the distances between the intersection of the IPs with the POs and the two crowns (anterior and posterior) of the IPs were averaged and used as landmarks to generate a reference surface map. For the temporal cortex, the distances between (i) the anterior crown (of the upper bank) of the STs and the anterior cytoarchitectonic border of the MC, (ii) the latter and the anterior tip of the floor of STs (point of alignment), (iii) the latter and the posterior

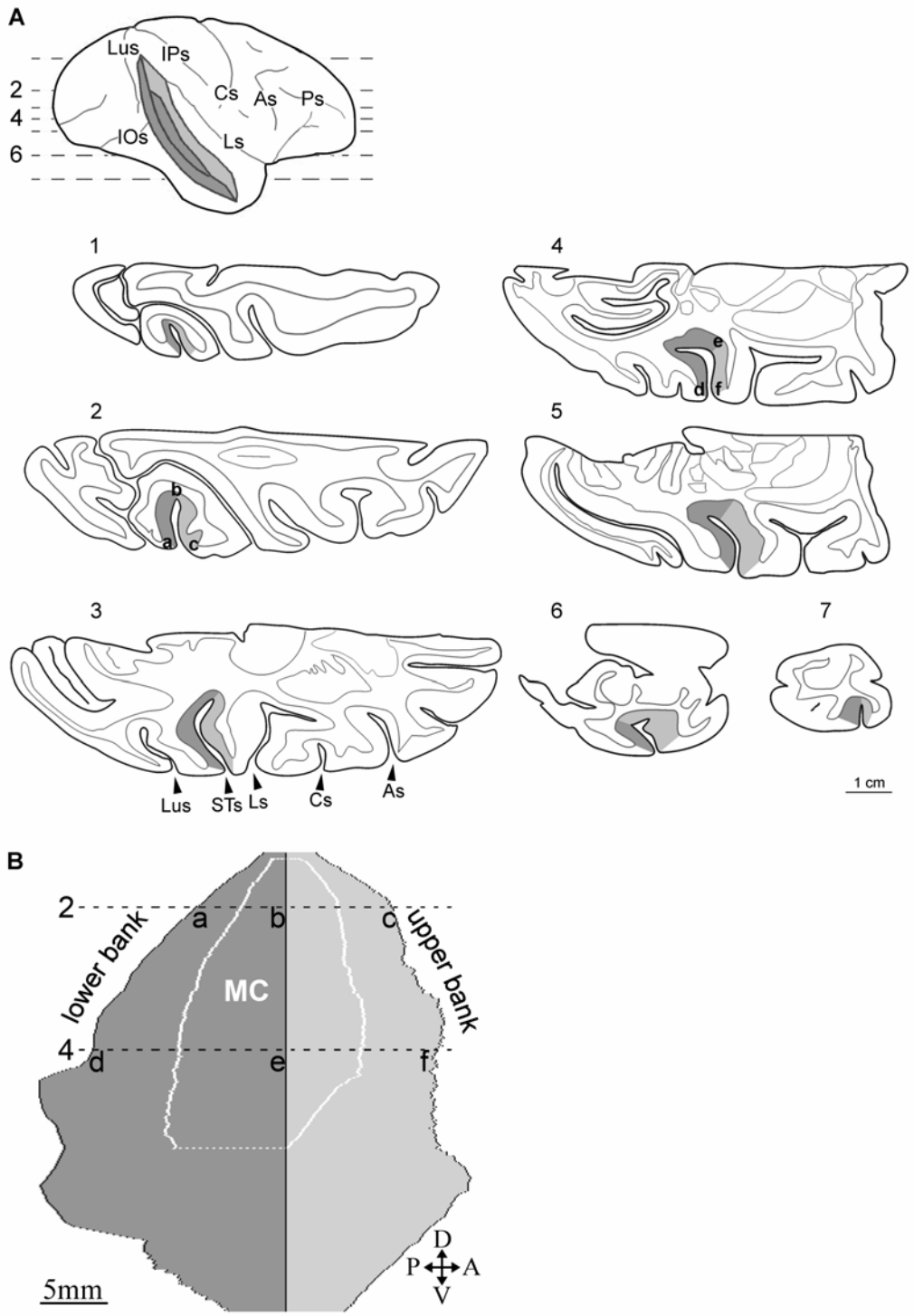

Figure 5. *(A) Lateral view of a monkey brain with the unfolded STs. Also, schematic illustration of seven horizontal sections (1–7 from dorsal to ventral) at the levels indicated in the brain drawing. In sections 2 and 4, points a and d correspond to the crown of the lower bank, respectively; points b and e to the anterior tip of the fundus (used for alignment); points c and f to the crown of the upper bank; other abbreviations, as in Fig.4. (B) Schematic illustration of the 2D reconstructed STs. MC, motion complex demarcated by white lines; letters a-f correspond to those in sections 2 and 4 in panel A; V, ventral; other abbreviations, as in Fig.1, 4.*

cytoarchitectonic borders of the MC, and (iv) the latter and the posterior crown (of the lower bank) of the STs were measured. The average of these measures was computed to produce a reference STs-map of landmarks. The 2D functional and anatomical maps of each hemisphere were then transformed using linear transformations of the plane in the Matlab software (The MathWorks, Massachusetts, USA) with custom designed routines (Dr. G.G. Gregoriou) to fit the reference surface landmark map.

Histology

One section every 500 μm was stained with thionine for the identification of cytoarchitectonic borders. In the literature, identification of areal borders for both LIP and the MC is based on the examination of myelin-stained material and/or SMI-32 (monoclonal antibody to neurofilament protein) immunocytochemistry. However, the thickness of our sections (20 μm) and the use of fresh-frozen, non-perfused tissue did not allow for the employment of these techniques.

The cytoarchitectonic boundaries in the lateral bank of the IPs were based on criteria established by Medalla and Barbas (2006). In agreement with their descriptions, it is demonstrated that (i) area 7 covers only the outermost part of the lateral bank, (ii) adjacent to area 7, the dorsal part of area LIP (LIPd) is located superficially covering about a third of the bank, and (iii) the ventral part of area LIP (LIPv) is bigger and lies deeper in the bank. The cortex lying caudal to LIPv may correspond to LOP (lateral occipitoparietal zone) of Lewis and Van Essen (Lewis and Van Essen, 2000b; Ben Hamed et al., 2001).

The MC, which is identified in the caudal STs (Fig. 5B), extends from about halfway in the lower bank along the floor and into the upper bank, and partially corresponds to Seltzer and Pandya's areas OAa and PGa (Seltzer and

Pandya, 1978). It is characterized by the presence of a more prominent layer IV, clearly distinct from the relatively poor layer V (Seltzer and Pandya, 1978; Hof and Morrison, 1995). Ventrally in the sulcal floor, it borders area IPa (Seltzer and Pandya, 1978) which is characterized by the presence of a prominent VIth layer organized in small cell clusters. The identification of the STs areas (V5/MT, MTf, MST, FST, TPOc, TPOi, TPOr, V4ta, V4tp, TEO) was based on the cytoarchitectonic borders of the MC, surface landmarks, and previously reported maps (Gattass and Gross, 1981; Desimone and Ungerleider, 1986; Boussaoud et al., 1991; Cusick et al., 1995; Lewis and Van Essen, 2000a).

RESULTS

Oculomotor performance

Figure 6 presents a broad overview of the eye movements made by all six monkeys in directions contralateral to the hemispheres studied. Because approximately 85% of the radiolabeled glucose is taken up by cells during the critical first 10 min of the experiment, this figure includes data from only this period. It includes the saccades executed by the two control monkeys, the control in the dark (Fig. 6A) and the fixation control (Fig.6B), the two monkeys executing either horizontal rightward (Fig. 6C) or oblique up-left (Fig. 6D) saccades to visual targets, and the two monkeys executing either horizontal leftward (Fig. 6E) or oblique up left (Fig. 6F) saccades to memorized target locations.

It should be noted that because areas LIP and MT are known to represent the contralateral half of visual space (Dubner and Zeki, 1971; Maunsell and Van Essen, 1983b; Blatt et al., 1990; Ben Hamed et al., 2001) only saccades contraversive to the reconstructed cortical areas are reported. After the end of each trial and during the intertrial interval, the animals made eye movements in

several directions before returning to the central position in the beginning of the new trial. These widely scattered eye movements had a small widespread effect on the activity of the contralateral hemispheres and consequently they might be expected to have an even smaller, if any, effect on the activity of the hemisphere considered.

The first experimental monkey (Hl) was being rewarded for making repeated horizontal visually-guided saccades and the second one (Ol) for making visually-guided saccades in an oblique direction 45^0 up left. The Hl monkey made 212 saccades from the central to the peripheral visual target during the critical 10 first minutes of the 2DG experiment, within an oculomotor space $10x10^0$ centered on the peripheral target. This corresponds to a density of 2.12 saccades/deg^2. The mean saccade amplitude was 29.5 ± 1^0 (mean±SD). Small eye movements ($<3^0$) mostly around the fixation window had a density of 3.88 saccades/deg^2, and mean amplitude was 1.5 ± 0.5^0. Finally, saccades executed by Hl in other directions and amplitudes had a low average density (0.02 saccades/deg^2). The distribution of end points of the saccades and the small amplitude eye movements around the fixation point executed by this monkey during the critical 10 first minutes of the experiment are illustrated in Fig. 6C. The Ol monkey made 182 saccades from the central to the peripheral visual target (density: 1.82 saccades/deg^2) during the critical 10 first minutes of the experiment (within the same $10x10^0$ window centered on the peripheral target). The mean saccade amplitude was 20.6 ± 1^0. Small eye movements ($<3^0$) around the fixation point had a density of 3.4 saccades/deg^2, and mean

Figure 6. *Three dimensional histograms of the number of saccades (Z-axis) versus horizontal (DH) and vertical (DV) eye displacements of all saccades executed by the monkeys during the critical first ten minutes of the 2DG experiment. (A) Control-in-the-dark monkey. (B) Monkey fixating a centrally located visual target. (C, D) Histograms from monkeys executing visually guided saccades, 30^0 horizontal, and 20^0 up-left oblique, respectively. (E, F) Histograms from monkeys executing memory-guided saccades, 20^0 horizontal, and 25^0 up-left oblique, respectively.*

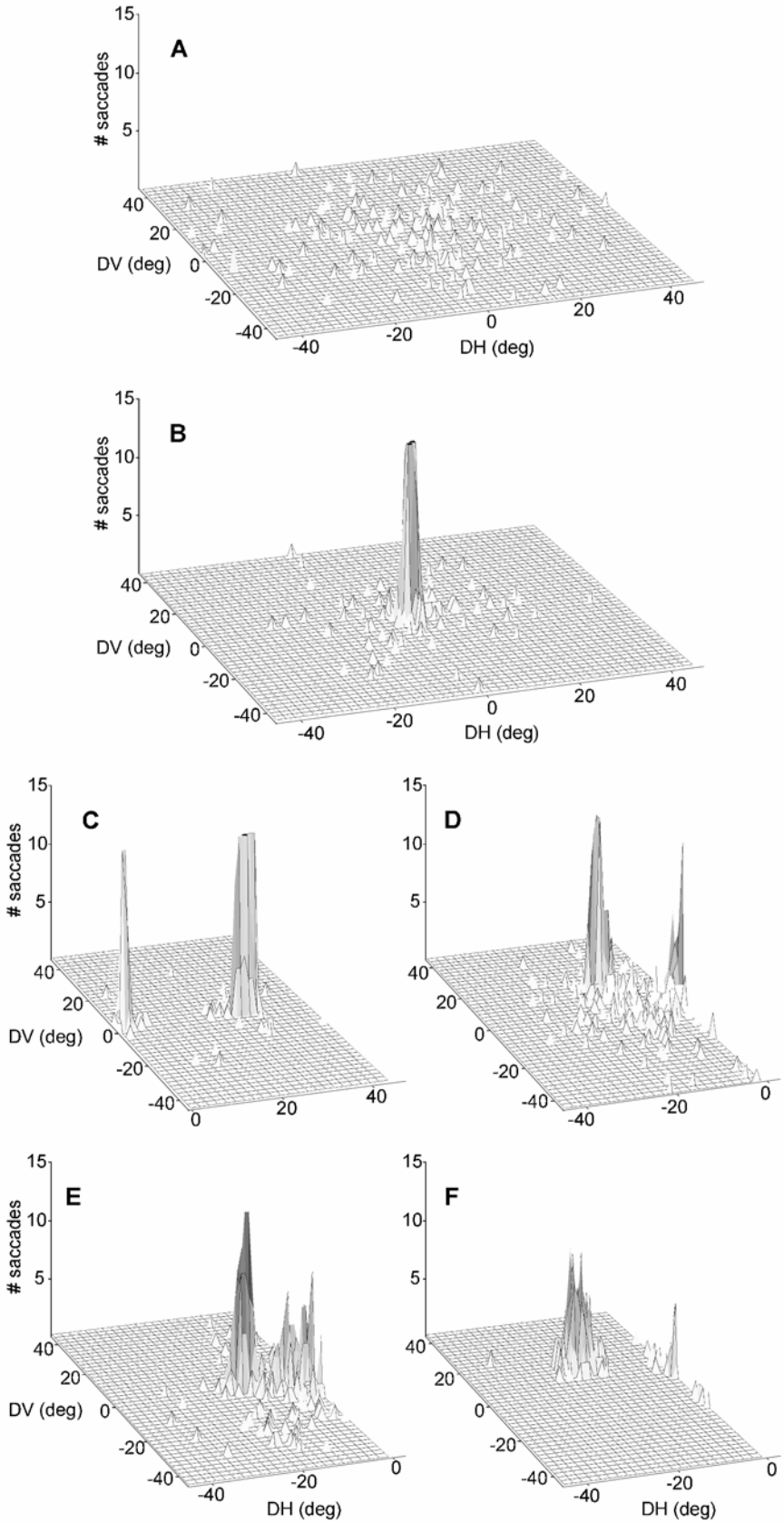
A
B
C
D
E
F
saccades
DV (deg)
DH (deg)

amplitude was 1.6±0.7^0. Saccades of other amplitudes and directions had an average density of 0.08 saccades/deg^2 (Fig. 6D). Since the end points of saccades are more widely distributed in the absence of visual stimulation, to compare the number of saccades executed by the animals in the visually-guided tasks with that executed by the animals in the memory-guided tasks we kept the sampling window at 10x10^0. However, the Hl monkey made 191 saccades and the Ol monkey made 138 saccades in a more confined oculomotor space of 5x5^0.

To obtain maps of the cortical regions activated for memory-guided saccades of amplitudes and directions similar to those of the visually-guided saccades described above, one monkey (Hd) was being rewarded for making repeated acoustically-triggered horizontal saccades to a memorized target location 20^0 away from straight ahead, and another monkey (Od) for making acoustically-triggered saccades to a memorized location 25^0 away from straight ahead in an oblique direction 45^0 up-left. The Hd monkey made 210 saccades within a window of 10x10^0 (density: 2.1 saccades/deg^2) centered on the peripheral memorized location during the critical 10 first minutes of the experiment (mean saccade amplitude: 15.9±1.8^0). The distribution of the end points of saccades and small amplitude eye movements around the fixation point made by Hd during the critical 10 first minutes of the experiment are illustrated in Fig. 6E. Small eye movements (<3^0), around the fixation window, had a density of 0.24 saccades/deg^2, and a mean amplitude of 2.5±0.2^0. Few saccades were performed outside these regions, at an average density of 0.09 saccades/deg^2. The Od monkey made 217 saccades from the central to the peripheral memorized location during the critical 10 first minutes of the experiment, within an oculomotor space of the same size (10x10^0) also centered on the peripheral memorized location (density: 2.17 saccades/deg^2). The mean saccade amplitude was 24.5±2.1^0. Eye movements smaller than 3^0 had a density of 0.64 saccades/deg^2 and a mean amplitude of 2.3±0.7^0. Saccades performed elsewhere had an average density of 0.03 saccades/deg^2 (Fig. 6F). Saccade

amplitudes reported for the Hd and Od monkeys agree with the spatial distortion during saccades to memorized locations: horizontal saccades are usually hypometric while saccades with an upward component are usually hypermetric (Gnadt et al., 1991). It should also be noted that in our analysis we included fixational movements of all animals smaller than 3^0, which are larger than those usually reported. This was done to include the fixational movements of the animals making saccades to memorized locations which are larger than those of the animals in the visually-guided paradigms (Snodderly, 1987).

The control fixation monkey (Cf) fixated the visual target for 75% of the time during the critical 10 first minutes of the 2DG experiment. Small eye movements ($<3^0$) near the fixation point had a density of 7.2 saccades/deg^2, and mean amplitude of 1.2 ± 0.7^0. The average density of eye movements executed outside the fixation window was 0.01 saccades/deg^2. The distribution of end points of eye movements made by the Cf monkey during the critical 10 first minutes is illustrated in Fig. 6B. Finally, the control in the dark monkey (Cd) made saccades that were almost evenly distributed throughout oculomotor space, with an average density equal to 0.04 saccades/deg^2 in the central visual field and 0.03 saccades/deg^2 in the peripheral field (Fig. 6A).

The characteristics of the saccades made under different conditions were further studied. In the visually-guided tasks, saccades made by the Hl monkey had a mean duration of 48±7 ms. The mean duration of saccades executed by the Ol monkey was 39±5.7 ms. In the memory-guided task, the Hd monkey made saccades with a mean duration of 65±25 ms and the Od monkey of 52±9.7 ms. As expected for memory-guided saccades (Leigh and Zee, 1999), these were slower than predicted from their amplitude (*t*-test, $p<0.001$). In the animal that maintained fixation of a central target, fixational movements had a mean duration of 33±11 ms, implying mean velocities of approximately 36^0/s. Figure 7 shows the main sequence relationships (saccade amplitude *vs.* saccade duration) for one monkey executing visually-guided saccades (Fig. 7A) and for

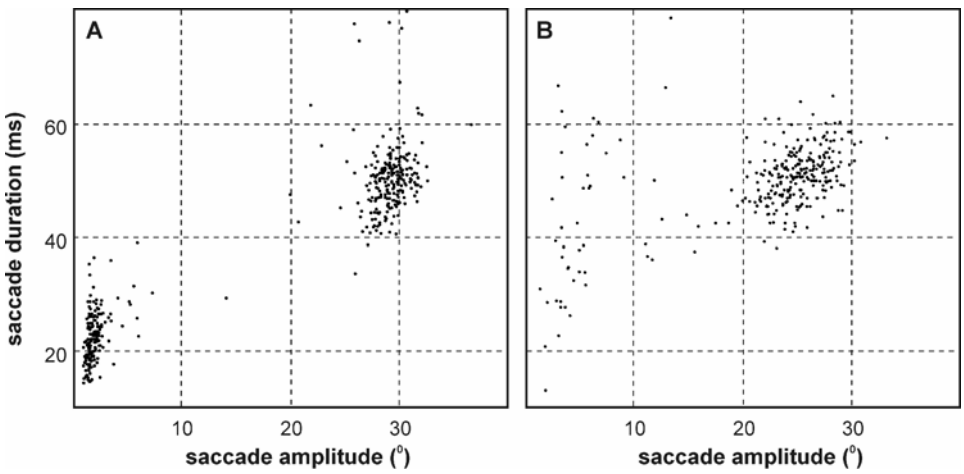

Figure 7. *Scatterplots of mean duration (ordinate) versus radial size (abscissa) for all saccades executed during the critical first ten minutes of the 2DG experiment by a monkey performing visually-guided (A) and a monkey performing memory-guided (B) saccades.*

one monkey executing memory-guided saccades (Fig. 7B). In Figure 7A, the slope of the linear regression line that fits the data is 1.1 ms/^{0}, equal to that reported in the study of Fuchs for horizontal saccades (1967). For the monkey executing oblique visually-guided saccades, the horizontal component of eye movements was slower (*t*-test, $p<0.0001$) than expected from the duration-amplitude relationships of horizontal saccades (Fuchs et al., 1985).

Intraparietal cortex

Regions activated for visually-guided saccades

The 2D maps of the intraparietal cortical regions activated for the execution of visually-guided saccades are presented in Fig. 8. An extended region of the intraparietal cortex was activated in both monkeys executing visually-guided saccades (Fig. 8C, D). To provide a more refined description of the location of the activated region, the IPs was divided into three parts (Fig. 4B), equidistant at all antero-posterior levels. The anterior third in the lateral bank (7IPa)

included most of the cytoarchitectonically defined area LIPd, the middle one (7IPm) covered most of the cytoarchitectonically delineated area LIPv, and the posterior one (7IPp) included the caudalmost segment of area 7IP (most probably including LOP). Approximately the middle and anterior thirds of the lateral bank were activated in these monkeys, covering most of areas LIPv and LIPd (Fig. 8C, D). A different pattern of activation was found in the control monkey that was rewarded for maintaining fixation of a visual target located straight ahead (Cf). Cf demonstrated increased metabolic activity in the fixation-related region of the intraparietal cortex (Gregoriou and Savaki, 2001), which is located at the border of LIPd and LIPv and extends mainly in the anterior part of the lateral bank of the IPs (Fig. 8B).

Regions activated for memory-guided saccades

The 2D maps of the intraparietal cortical regions activated for the execution of memory-guided saccades are presented in Fig. 8. In contrast to the monkeys executing visually-guided saccades, it is mainly LIPv in the middle third of the lateral bank of the IPs that was activated in both monkeys executing memory-guided saccades in the dark (Fig. 8E, F). The activation observed during the execution of memory-guided saccades is unlikely to be due to differences in the metrics of the saccades executed, since both the memory-guided and the visually-guided saccades were large in amplitude and area LIP neurons are broadly tuned for saccade amplitude (Barash et al., 1991b).

Comparison of regions activated for visually- and memory-guided saccades

To better compare the effects induced by memory-guided saccades in the dark (without any visual stimulus) to those induced by visually-guided saccades,

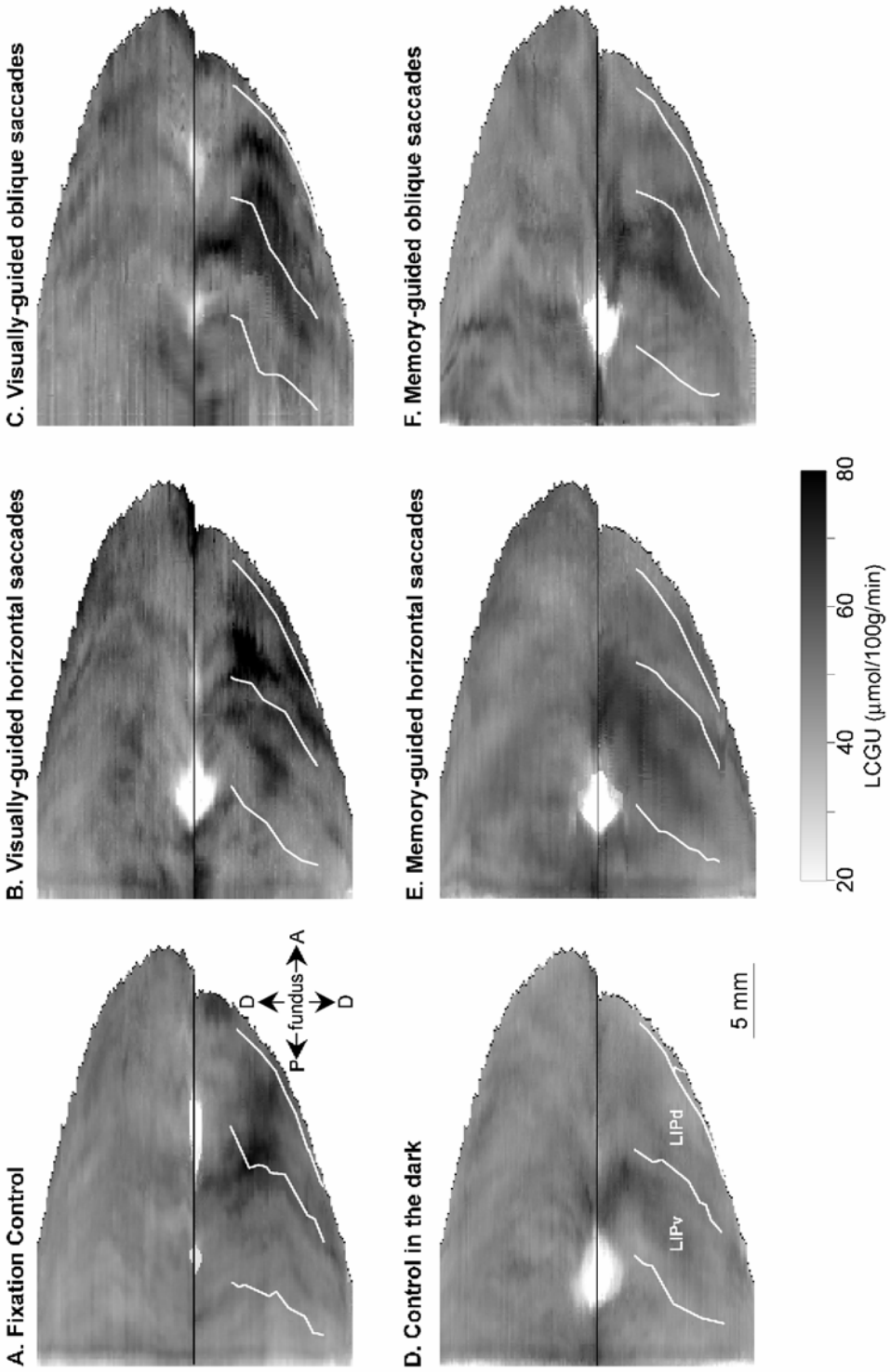
A. Fixation Control
B. Visually-guided horizontal saccades
C. Visually-guided oblique saccades
D. Control in the dark
E. Memory-guided horizontal saccades
F. Memory-guided oblique saccades
D
P
fundus
A
D
LIPv
LIPd
5 mm
20
40
60
80
LCGU (µmol/100g/min)

two average maps of metabolic activity were generated. The first one was produced by averaging the two geometrically normalized quantitative intraparietal 2D-metabolic maps in the contralateral hemispheres of the two monkeys executing saccades to visual targets (saccades in the light, Sl), and the second one by averaging the corresponding maps of the two monkeys performing saccades to memorized target locations (saccades in the darkness, Sd). Comparison of these two average quantitative glucograms indicates that the region activated for visually-guided saccades (Fig. 9A) extends more rostrally and superficially (close to the crown) in the lateral bank of the IPs whereas that activated for memory-guided saccades (Fig. 9B) is restricted to a region more posterior and deep in the lateral bank (close to the fundus).

To better define quantitatively the anteroposterior location and extent of the 7IP regions activated for visually- and memory-guided saccades, average LCGU values (in μmol/100g/min) and their 95% confidence intervals were plotted every 100 μm along the rostrocaudal extent of the lateral bank of the IPs (area 7IP). The line graph obtained from the Cd control monkey (Fig. 9C, light gray) is the average of the two lateral banks of the IPs in its two hemispheres and indicates the baseline activity of area 7IP. By comparison to it, the peak value of the line graph obtained from the two monkeys engaged in memory-guided saccades (Sd) is higher by approximately 15%, and is located in the

Figure 8. *Quantitative two-dimensional (2D) maps of metabolic activity in the IPs. (A) Average IPs map from both hemispheres of the monkey executing visual fixation; abbreviations, as in Fig.4. (B) Map of the IPs from the left hemisphere of the monkey executing visually-guided horizontal saccades to the right. (C) IPs map of the right hemisphere of the monkey executing visually-guided oblique saccades to the left. (D) Average map of the IPs from the left and right hemispheres of the control monkey in the dark. LIPd and LIPv, dorsal and ventral part of the lateral intraparietal area, respectively; 7, area 7. (E) Map of the IPs from the right hemisphere of the monkey executing leftward memory-guided horizontal saccades. (F) IPs map of the right hemisphere of the monkey executing up-left memory-guided oblique saccades. In all reconstructions, white lines indicate, from left to right, (i) the posterior border of LIPv, (ii) the boundary between LIPv and LIPd, and (iii) the boundary between LIPd and area 7. Gray scale bar indicates LCGU values.*

middle third of the lateral bank of the IPs (Fig. 9C, dark gray). Again by comparison to Cd, the peak value of the line graph obtained from the two monkeys engaged in visually-guided saccades (Sl) is similarly increased by approximately 15% as far as the middle third of their area 7IP is concerned (Fig. 9C, intermediate gray). However, the peak value of this line graph is considerably higher (by approximately 35%) and is located in the anterior third of area 7IP in the lateral bank of IPs.

To illustrate the spatial distribution of the LCGU differences between experimental and control monkeys, we subtracted the average metabolic maps of different groups from each other. The IPs map obtained after averaging the two hemispheres of monkey Cd was subtracted from the average Sl map. The resulting quantitative image (Fig. 10A) indicates that the intraparietal area devoted to visually-guided saccades (i.e., to visuo-spatial and visuo-movement processes) extends through the anterior and middle thirds of the lateral bank, covering parts of both areas LIPd and LIPv. Visually-guided and memory-guided saccades induced similar activations in LIPv of the middle third of the IPs (by an average of 19% and 17%, respectively) as compared to the Cd monkey (Table 2, 7IPm). On the other hand, the anterior part of the IPs, including LIPd, (Table 2, 7IPa) was activated markedly (by an average of 35% as compared to the Cd) for visually-guided saccades and much less for memory-guided saccades (10% higher than the Cd). To elucidate the IPs region responsible for visuo-spatial saccade-related processing, the average Sd map was subtracted from the average Sl map. The resulting image (Fig. 10B) indicates that this visuo-spatial, saccade-related region is confined to a portion of the anterior third of the lateral bank of the IPs, it remains superficial within the bank and covers mainly area LIPd.

Figure 11 shows the spatial relationship of 7IP regions activated for distinct facets of oculomotor behavior. Firstly, the geometrically normalized IPs metabolic maps of both hemispheres of the monkey executing visual fixation

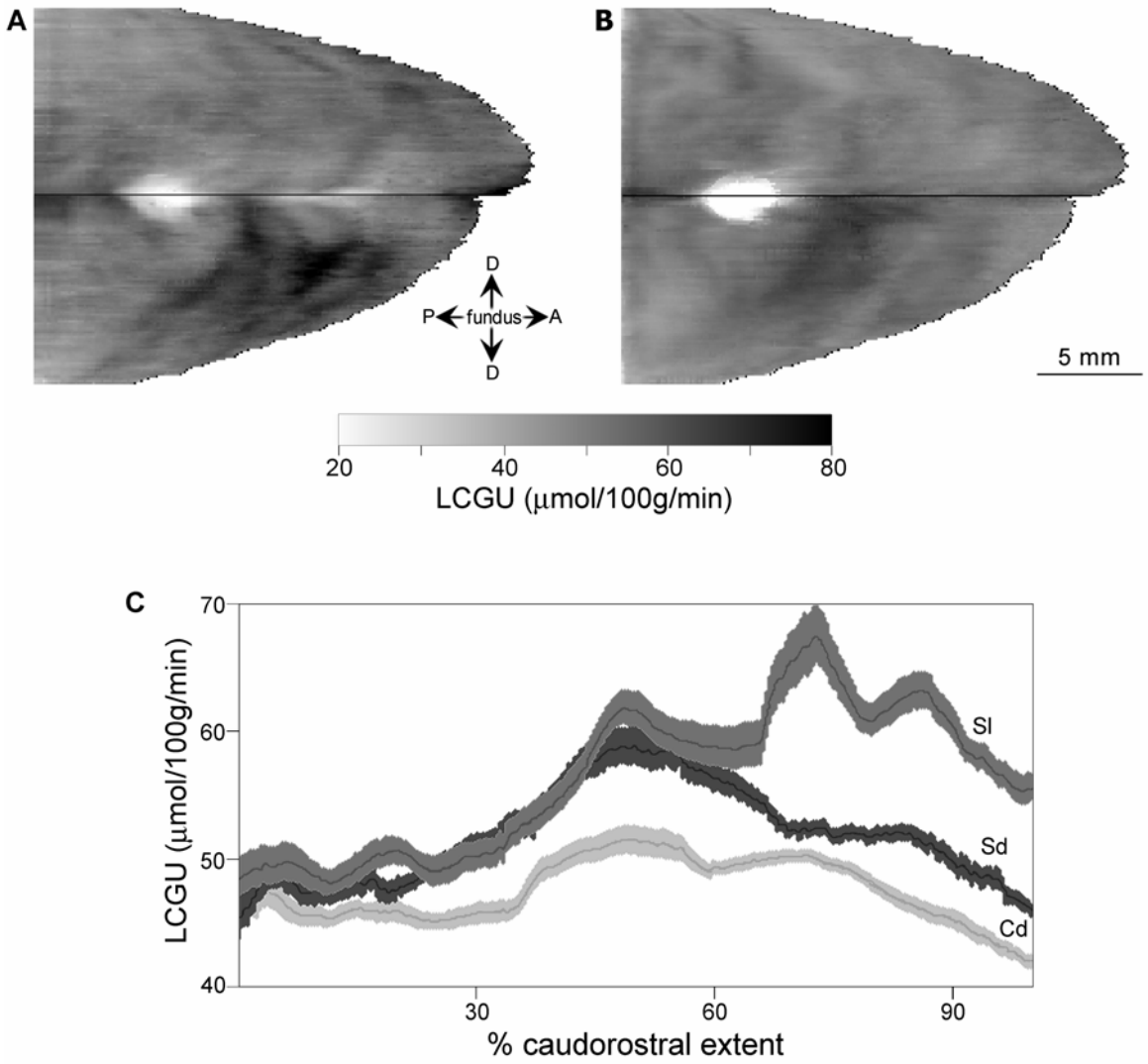

Figure 9. *Comparison of IPs regions activated by visually- and memory-guided saccades. (A) Average quantitative map of IPs metabolic activity from the two contralateral hemispheres of the animals executing visually-guided saccades. (B) Average quantitative map of IPs activity from the two contralateral hemispheres of the animals executing memory-guided saccades. Gray scale bar indicates LCGU values (μmol/100g/min). (C) Plot of IPs activity along the caudorostral extent of the sulcus (abscissa). Each line represents average glucose consumption (LCGU) values and 95% confidence intervals/ 100μ. Cd, average from the two hemispheres of the Control-dark monkey; Sd, average from the monkeys executing horizontal and oblique memory-guided saccades; Sl, average from the monkeys executing horizontal and oblique visually-guided saccades.*

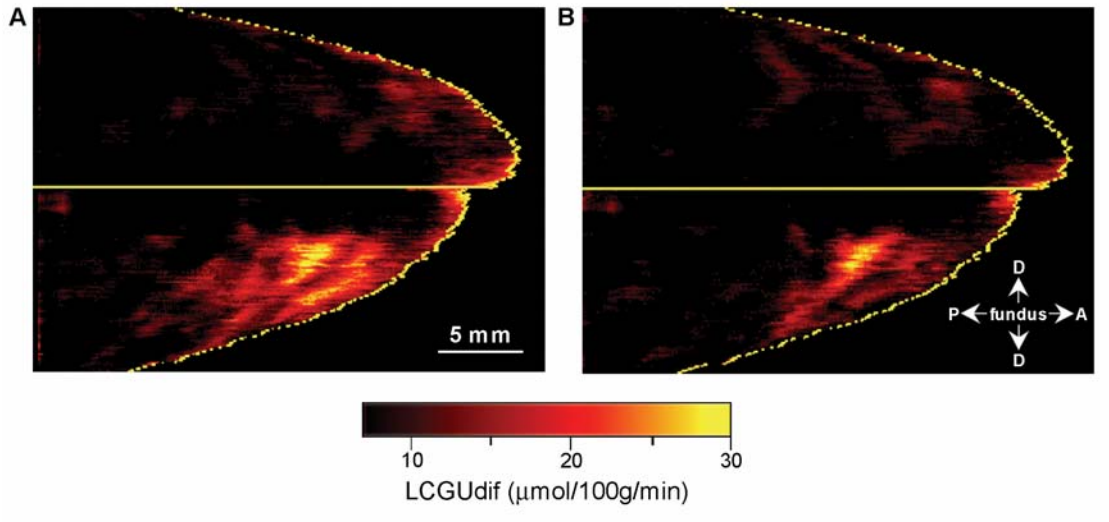

Figure 10. *Differential activations induced by visually- and memory-guided saccades. (A) Subtraction of the average quantitative IPs map of the control monkey in the dark from that of the two monkeys executing visually-guided saccades illustrates the entire intraparietal region related to visuo-spatial and visuo-movement activity. (B) Subtraction of the average quantitative map of the animals executing memory-guided saccades from that of the animals executing visually-guided saccades illustrates the intraparietal region related to visuo-spatial processing during saccade execution. Color scale indicates LCGU differences in µmol/100g/min.*

were averaged, and all pixels in the lateral bank with LCGU values higher (by 10% or more) than those of the Cd were color coded green. The resulting map (Fig. 11A) was superimposed on the average IPs map of the two monkeys executing saccades to visual targets, which was generated with the same 10% threshold and was color-coded red. The region of overlap (green+red=yellow) indicates that about one third of the neural space of area 7IP devoted to visually-guided saccades also participates in visual fixation (Fig. 11B). In a similar manner, we explored the spatial relationship of the intraparietal regions devoted to visually- and memory-guided saccades. The average metabolic IPs map of the two monkeys executing saccades to visual targets (whose activated regions were color coded red) were overlaid on the corresponding map of the two monkeys executing saccades to memorized targets whose activated regions were color coded blue. Clearly, the region of overlap (Fig. 11C, blue+red=magenta) indicates that most of the 7IP area activated by saccades to

Area *(n)*	**Cd**	**Sd**		**Cf**		**Sl**		
	LCGU±SD	LCGU±SD	%Cd	LCGU±SD	%Cd	LCGU±SD	%Cd	%Sd
5IPp *(81)*	48±2	50±3	4	47±2	-2	50±4	4	0
5IPm *(72)*	49±2	51±2	4	50±2	2	51±3	4	0
5IPa *(50)*	47±0	50±1	6	50±2	6	53±4	**13**	6
7IPp *(79)*	46±1	48±3	4	48±1	4	49±3	7	2
7IPm *(62)*	53±2	62±3	**17**	57±2	8	63±3	**19**	2
7IPa *(40)*	49±2	54±1	**10**	59±7	**20**	66±8	**35**	**22**

Table 2. *Metabolic effects in the intraparietal cortical regions. Values represent the mean normalized glucose utilization (LCGU) in μmol/100g/min (± Standard Deviation). Cd, average of distinct IPs regions in the two hemispheres of the control monkey in the dark. Sd, values from the monkeys executing memory-guided saccades. Cf, average of the IPs regions in the two hemispheres of the fixating monkey. Sl, values from the monkeys executing visually guided saccades. n, number of sets of five adjacent horizontal sections used to obtain the mean LCGU values for each region in each hemisphere. %Cd, percent difference between the experimental and the Cd, monkey, calculated as (experimental-Cd)/Cd*100. %Sd, percent difference between the Sl and the Sd, monkey, calculated as (Sl-Sd)/Sd*100. Values in bold indicate statistically significant differences by the Student's unpaired t-test at the level of p<0.001. 5IPa, 5IPm, 5IPp, anterior, middle, posterior part of the medial bank of the IPs, respectively. 7IPa, 7IPm, 7IPp, anterior, middle, posterior part of the lateral bank of the IPs, respectively.*

memorized target locations, in the absence of any visual stimulus, extends through the caudalmost and deepest portion of the region activated for saccades to visual targets, and is confined to area LIPv. In addition, there is widespread activation related exclusively to the visually-guided saccades (Fig. 11C, red) within area LIPd, and a small region in the depth of the sulcus (close to the fundus of the IPs) which is activated exclusively by memory-guided saccades (Fig. 11C, blue). In view of the large extent of the fixation-related area of 7IP (Fig. 11A, green), the fact that the region activated for visually-guided saccades (Fig. 11C, red+magenta) is more widespread and significantly more intense (Table 2) than that activated for memory-guided saccades (Fig. 11C, blue+magenta) must be partly due to the fact that monkeys executing visually-

guided saccades devoted some of their time into fixating visual targets. It should be noted that the fixation of visual targets implies not only exposure to intense sensory stimulation but also more marked oculomotricity, as demonstrated by numerous small eye movements executed around the fixation target (our Fig. 4B, Martinez-Conde et al., 2004). Figure 11D summarizes the 7IP regions activated for the distinct facets of oculomotor behavior. Besides those shown in green, red, yellow, blue, and magenta according to the color coding scheme described above, the region in white (=green+red+blue) apparently participates in all these behaviors (fixation, visual-saccades, and memory-saccades).

Figure 11. *Qualitative imaging of the functional parcellation of area 7IP. (A) Averaged, geometrically normalized IPs metabolic maps from both hemispheres of the monkey executing visual fixation. All pixels contained within area 7IP with LCGU values higher than those of the control monkey in the dark (by 10% or more) are color coded green. (B) Superimposition of fixation-related (from A) and visual-saccade-related pattern of activity in area 7IP. The latter is color coded red, and was obtained from the two monkeys executing saccades to visual targets using the same 10% threshold. The yellow color of the region of overlap results from the presence of both green (fixation-related) and red (visual-saccade-related) color in the same pixels. (C) Superimposition of visual-saccade-related (from B) and memory-saccade-related pattern of activity. The latter is color coded blue, and was obtained from the two monkeys executing saccades to memorized target locations using the same 10% threshold. The magenta color of the region of overlap results from the presence of both red (visual-saccade-related) and blue (memory-saccade-related) color in the same pixels. (D) Functional parcellation of area 7IP resulting from the superimposition of fixation-related (green), visual-saccade-related (red) and memory-saccade-related (blue) patterns of activity. The white color of the region of overlap results from the presence of green, red and blue color in the same pixels.*

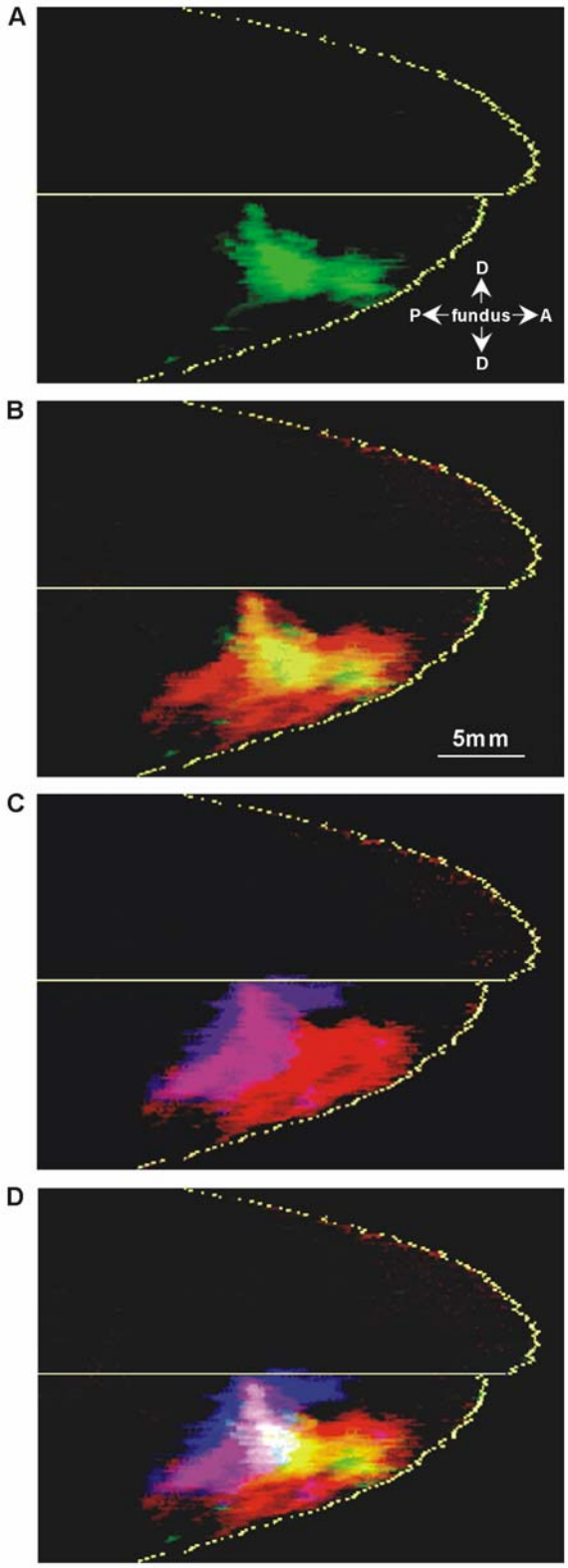
A
D
P
fundus
A
D
B
5mm
C
D

Temporal cortex

Regions activated for visually-guided saccades

Figure 12 provides high resolution 2D functional maps of the STs reconstructed from serial horizontal sections through the whole extent of the sulcus. Functional (2DG) and anatomical (cytoarchitectonic) reconstructions are superimposed. In agreement with previous descriptions, the MC we identified histologically includes parts of the upper (anterior) and lower (posterior) banks and the fundus of the caudal (dorsal) portion of the STs. Areas MT/V5 in the posterior bank, MST in the anterior bank, and FST in the fundus of the STs were activated in both monkeys executing visually-guided saccades (Fig. 12B, C; Table 3, Sl) as compared to Cf (Fig. 12A). The areas in both banks of the STs have been traditionally assigned as visual, due to almost exclusive stimulation by photic stimuli and, in the case of MT/V5, due to its direct connection with the striate cortex. Therefore, in our analysis, we compared the metabolic effects between the animals executing visually-guided saccades and the control animal that maintained fixation of a central visual target. Visually-guided saccades activated MT/V5 including its ventralmost posterior part, which corresponds to area MTf and represents

Figure 12. *Quantitative 2D maps of metabolic activity in STs. (A). Average STs map from the two hemispheres of the Cf monkey. (B) STs map from the monkey executing visually-guided horizontal saccades. (C) STs map from the monkey executing visually-guided oblique saccades. (D) Average STs map from the two hemispheres of the Cd monkey. (E) STs map from the monkey executing memory-guided horizontal saccades. (F) STs map from the monkey executing memory-guided oblique saccades. Gray-scale bar indicates LCGU values (μmol/100g/min); c, area temporal-parietal-occipital, caudal; i, area temporal-parietal-occipital, intermediate; tp, V4 transitional, posterior; TPOr, area temporal-parietal-occipital, rostral; V4ta, V4 transitional, anterior; other abbreviations, as in Fig.1, 4, 5.*

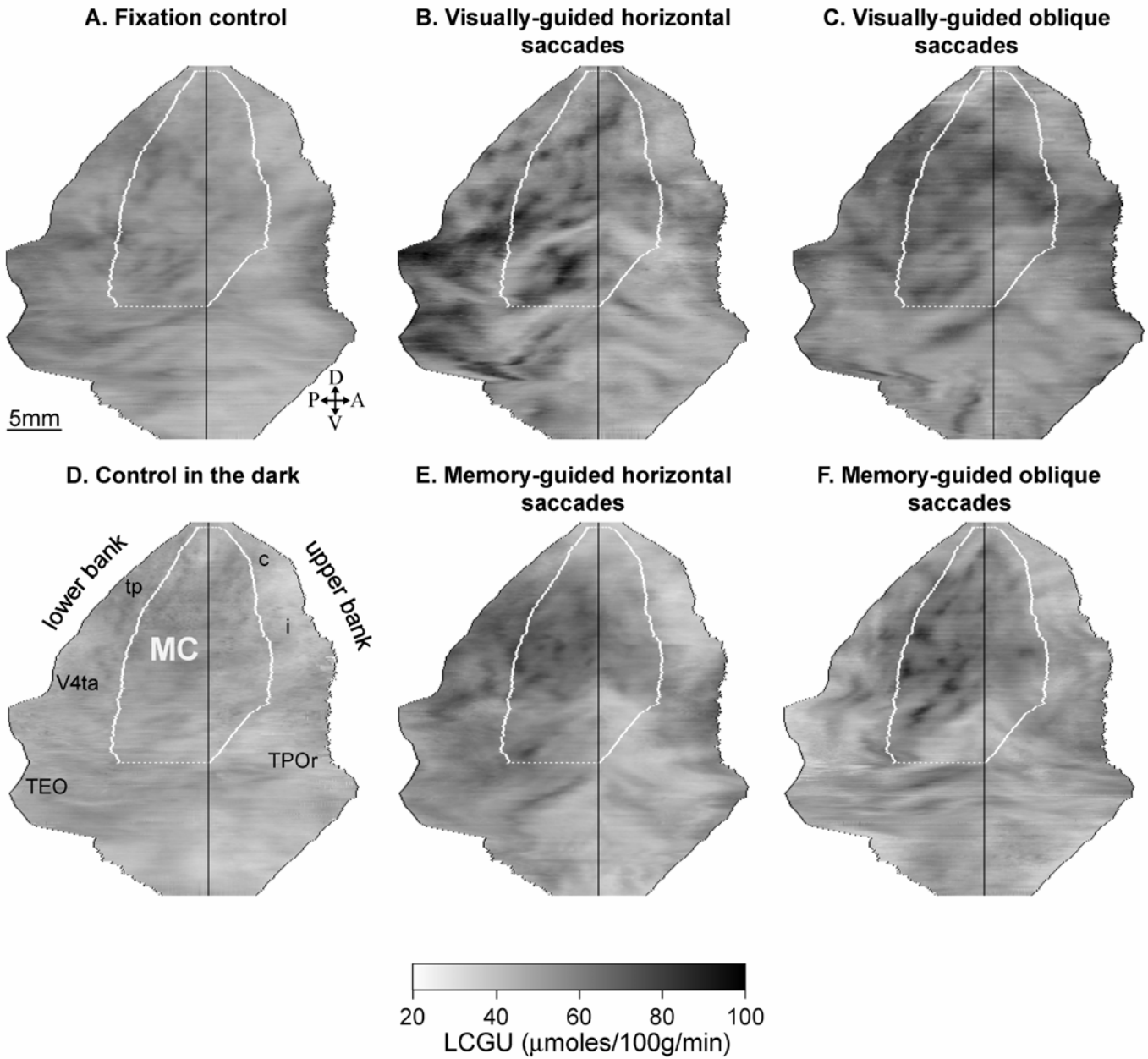
A. Fixation control
B. Visually-guided horizontal saccades
C. Visually-guided oblique saccades
D. Control in the dark
E. Memory-guided horizontal saccades
F. Memory-guided oblique saccades
5mm
D
P
A
V
lower bank
upper bank
tp
c
i
MC
V4ta
TPOr
TEO
20
40
60
80
100
LCGU (μmoles/100g/min)

Area *(n)*	**Cd**	**Sd**		**Cf**		**Sl**		
	LCGU±SD	LCGU±SD	%Cd	LCGU±SD	%Cd	LCGU±SD	%Cf	%Sd
V5/MT *(72)*	54±3	68±4	**26**	57±2	6	67±4	**18**	-1
MTf *(25)*	53±3	67±6	**26**	61±5	**15**	74±3	**21**	**10**
MST *(50)*	50±3	60±4	**20**	54±4	8	66±4	**22**	**10**
FST *(40)*	46±4	48±4	4	56±5	**22**	64±8	**14**	**33**
TPOr *(110)*	45±3	47±4	4	47±3	4	50±2	6	6
TPOi *(50)*	42±6	43±4	2	45±4	7	53±7	**18**	**23**
TPOc *(50)*	42±6	42±5	0	45±3	7	49±5	9	**17**
V4tp *(145)*	51±4	59±6	**16**	54±4	6	64±6	**19**	8
V4ta *(75)*	48±3	54±6	**13**	59±4	**23**	67±8	**14**	**24**
TEO *(50)*	50±3	53±3	6	59±3	**18**	64±4	8	**21**

Table 3. *Metabolic effects in the superior temporal cortical areas. %Cf, percent difference between the experimental and the Cf, monkey, calculated as (experimental-Cf)/Cf*100; other abbreviations, as in Fig. 1, 12 and Table 2.*

central vision (Gattass and Gross, 1981). Moreover, visually-guided saccades induced activation in area TPOi, anterior to the MST, in subareas V4tp and V4ta posterior to MT/FST, and in the higher order visual area TEO (Fig. 12B, C; Table 3). Visual fixation activated areas MTf, FST, V4ta and TEO (Table 3, Cf, %Cd). Thus, some of the regions activated for visually-guided saccades were also activated for fixation, as expected by the notion that the fixation of visual targets engenders not only exposure to sensory stimulation but also a considerable number of small eye movements (Martinez-Conde et al., 2004).

Regions activated for memory-guided saccades

As in the Sl monkeys, areas V5/MT, MTf, MST, V4tp and V4ta were activated in both monkeys executing memory-guided saccades (Fig. 12E, F; Table 3, Sd) as compared with the Cd monkey (Fig. 12D). In contrast to the Sl monkeys, areas FST, TEO and TPOi were not significantly activated in the Sd monkeys (Table 3). The observed activations in the STs of the monkeys executing memory-guided saccades are unlikely to be due to differences in the metrics or the directions of the saccades executed, because both the memory-guided and the visually-guided saccades were large in amplitude and MT/V5 neurons have large receptive fields and broad directional tuning (Maunsell and Van Essen, 1983b; Albright, 1984).

Comparison of regions activated for visually- and memory-guided saccades

To better compare the effects of visually- and memory-guided saccades, two average quantitative maps of metabolic activity were obtained. The first one was produced by averaging the STs maps of the two Sl monkeys (Fig. 13A), and the second by averaging the corresponding maps of the two Sd monkeys (Fig. 13B). The region that remains activated when the latter is subtracted from the former (Fig. 13C) extends to TPOc and TPOi in the rostral bank, to FST in the floor and to TEO in the caudal bank.

To correct for differences due to oculomotor performance, we normalized the activity patterns observed in different monkeys to that observed in the monkey with the smallest number of executed saccades. To this end, we divided the LCGU values in the metabolic map of each monkey by the number of saccades it executed (to obtain an estimate of LCGU/pixel/movement) and multiplied it by the number of saccades (182) executed by the monkey with the poorest performance (Ol). Figure 13D

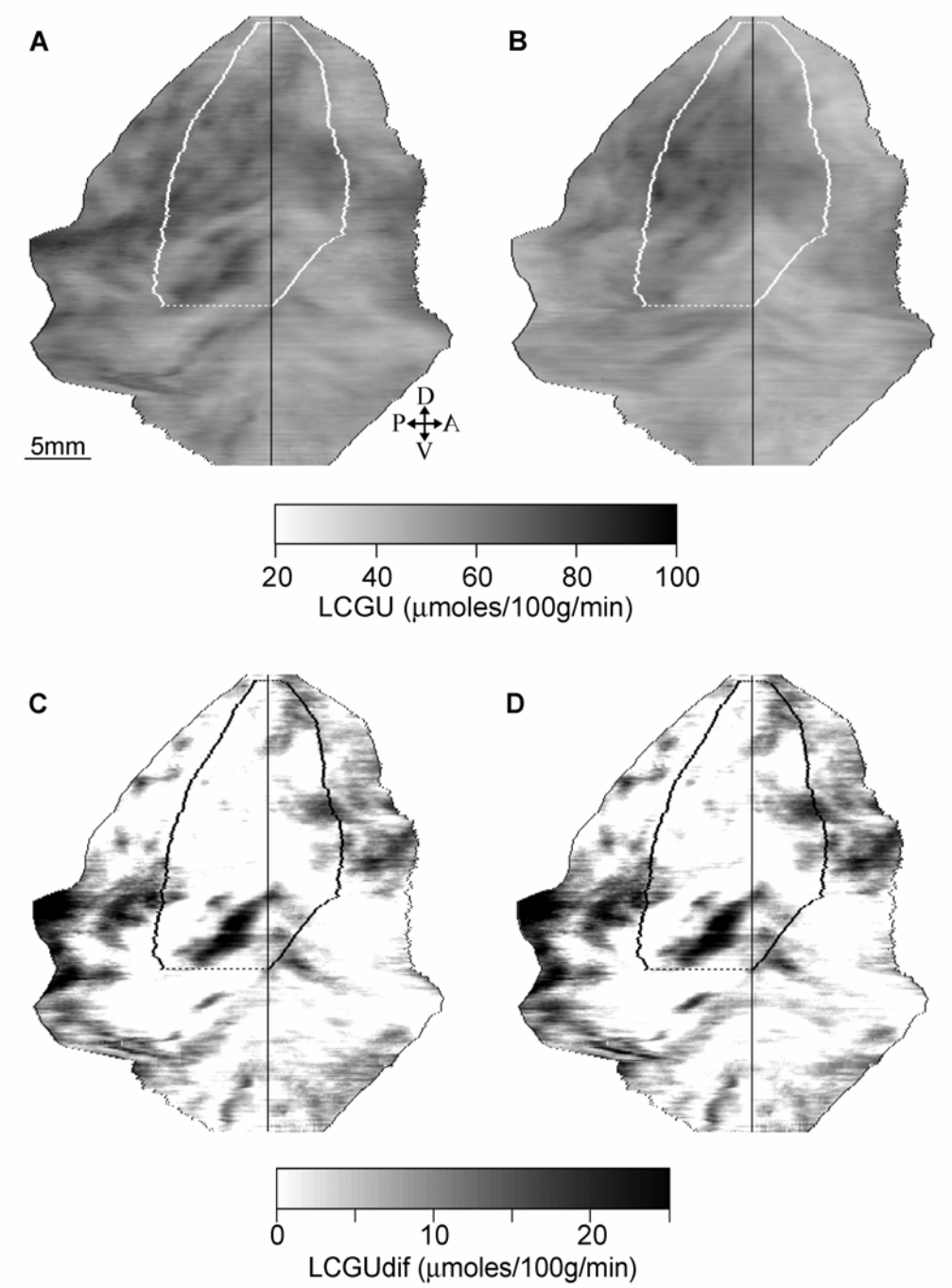

Figure 13. *(A) Average quantitative map of metabolic activity in the STs from the two animals executing visually-guided saccades. (B) Average STs map from the monkeys executing memory-guided saccades. Gray-scale bar indicates LCGU values. (C) Subtraction of map B from map A. (D) Subtraction of weighted map B from weighted map A. Gray-scale bar indicates LCGU.*

illustrates the quantitative map of metabolic activity obtained after subtracting the average map obtained from the weighted STs maps of the two monkeys executing memory-guided saccades from the average map obtained from the weighted STs maps of the two monkeys executing visually-guided saccades. Visual inspection of the activity patterns before (Fig. 13C) and after normalization (Fig. 13D) shows that relatively small differences in oculomotor performance (e.g., the number of saccades executed by our monkeys) did not contribute appreciably to the STs activity patterns.

Figure 14 illustrates the spatial relationship of STs activations in the two conditions. Firstly, the geometrically normalized STs activity maps of the two Sl monkeys were averaged, and all pixels with LCGU values higher (by 10% or more) than those of the Cf were color-coded red. The resulting map (Fig. 14A) was superimposed on the average STs map of the two Sd monkeys, again using the same 10% threshold but color-coded blue (Fig. 14B). The region of overlap (red + blue = magenta) indicates that about one third of the neural space devoted to visually-guided saccades (corresponding to areas V5/MT, MST and V4t) also participates in memory-guided saccades in complete darkness (Fig. 14C).

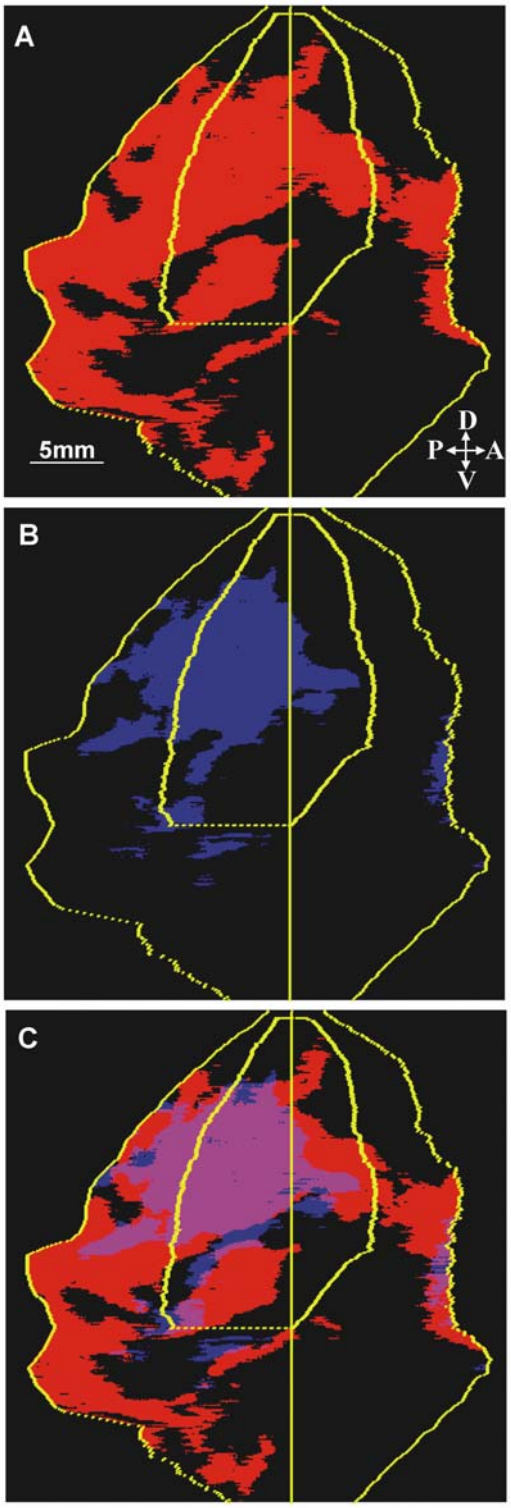

Figure 14. *(A) Averaged qualitative STs map from two Sl monkeys. Pixels with LCGU values higher than those of the control by more than 10% are shown in red. (B) Averaged STs map from two Sd monkeys. Pixels with LCGU values higher than the control by more than 10% are color-coded blue. (C) Superimposition of A and B. The region of overlap (magenta) results from the presence of both red and blue.*

DISCUSSION

In the current study, we demonstrate the modulation of metabolic demands in the intraparietal and superior temporal cortical areas of rhesus monkeys under different behavioral paradigms. Employment of the quantitative autoradiographic method of 2DG enable us to present for the first time high-resolution quantitative functional images of the location and extent of activated regions during i) fixation of a central visual target, ii) execution of saccades to visual targets, and iii) execution of saccades to memorized target locations in the dark. In addition, we provide the anatomical localization of metabolic effects by aligning our activity maps with cytoarchitectonically defined cortical areas. In the following sections, we discuss our findings in relation to the existing literature implicating the intraparietal and superior temporal cortex in oculomotor function.

Intraparietal cortex

Our study demonstrates the extended and differential activation of area LIP in the lateral bank of the intraparietal cortex during eye movement tasks. We provide evidence that the ventral subdivision of LIP (area LIPv) is activated for both visually-guided and memory-guided saccades, whereas the dorsal one

(area LIPd) is activated only for visually-guided saccades. This result suggests that topographically distinct, though partially overlapping, neuronal populations process visuo-spatial and memory-related oculomotor signals.

The present data indicate that the anteroposterior extent and the location of the 7IP region activated for visually-guided saccades and fixation differ from those of the traditionally defined area LIP. The latter has been variously described as occupying the middle-posterior fourth [Fig. 1 in Gnadt and Andersen (1988); Fig. 1 in Barash et al. (1991a)], the posterior two-thirds [Fig. 2 in Andersen et al. (1990)], the middle third [Fig. 2 in Colby (1998), Fig. 5 in Tanné-Gariépy (2002)], and the middle two-fourths [Fig. 10 in Lewis and Van Essen (2000b), Ben Hamed et al. (2001)] of the lateral bank of the IPs. In contrast, our high-resolution quantitative maps show that the 7IP region activated for visually-guided saccades extends more rostrally than previously reported, in approximately the anterior and middle two thirds of the lateral bank of the IPs. This activation lies within both subareas LIPv and LIPd, as confirmed by histological analysis.

Consistent with previous reports (Barash et al., 1991b; Colby et al., 1996; Ben Hamed et al., 2001), our metabolic findings indicate that area 7IP is significantly activated during the execution of visually-guided saccades. The fact that horizontal 30^0 and oblique 20^0 visually-guided saccades induced roughly similar patterns of activation within 7IP may be due to the coarse visual field topography of area LIP (Blatt et al., 1990; Ben Hamed et al., 2001) and to the broad tuning of LIP neurons (Barash et al., 1991b).

Our quantitative functional results also demonstrate that a considerable part of area 7IP, confined to area LIPv, is activated for both visually-guided and memory-guided saccades. The demonstration that the middle third of area 7IP is markedly activated for saccades executed to memorized locations in the absence of visual stimulation is consistent with the fact that LIP neurons discharge for delayed saccades to a recently

extinguished target (Gnadt and Andersen, 1988; Colby et al., 1996) and for saccades to memorized locations in the absence of visual stimuli (Colby et al., 1996). The much weaker activation we observed in the anterior third of area 7IP during memory-guided saccades is compatible with the weak oculomotor signals carried by relatively rostral 7IP neurons (Ben Hamed and Duhamel, 2002). The present report is the first to demonstrate that the extent of the region activated for memory-guided saccades is smaller, and the intensity of its activation weaker than that activated for visually-guided saccades of similar direction and amplitude. The weaker activation accompanying memory-guided saccades is consistent with the fact that, to discharge maximally, LIP neurons require both the presence of visual stimuli and the execution of saccades towards them (Colby and Duhamel, 1996; Paré and Wurtz, 1997; Colby and Goldberg, 1999; Kusunoki et al., 2000). Unexpectedly, the region activated for memory-guided saccades extends to the fundus of the IPs into some of the traditional area VIP (Colby et al., 1993). Nevertheless, this finding confirms a previous report indicating that the saccade related part of the IPs extends beyond the traditional LIP, rostral and ventral to it, into area VIP (Thier and Andersen, 1998).

In contrast to the region activated for memory-guided saccades, which was located fairly deeply in the middle third of the lateral bank of the IPs and was confined to LIPv, the region activated for saccades to visual targets occupied both deeper and superficial territories of both its anterior and middle thirds and extended through both the LIPv and the LIPd. The activation in LIPd displayed the most pronounced effects we observed in the lateral bank of the IPs. The level of activation in LIPv was the same in the monkeys executing visually-guided saccades and monkeys performing memory-guided saccades, in both cases displaying about 18% higher glucose consumption than that of the Cd monkey. The activation induced by visually-guided saccades and extending to LIPd was even higher (by about 35%) as

compared to the Cd monkey. Apparently, LIPd requires visual stimulation in addition to saccades to be maximally activated.

The functional parcellation of the lateral IPs we propose, is in agreement with existing anatomical and neurophysiological evidence. Firstly, the posterior part of the lateral bank of the IPs projects to the frontal eye field (FEF) and contains a high proportion of neurons related to memory-guided saccades (Blatt et al., 1990), whereas the more anterior part contains a representation of the visual field (Ben Hamed et al., 2001). Also, LIPv close to the fundus of IPs, is strongly connected with the core FEF and the superior colliculi whereas LIPd, close to the crown, is not (Lynch et al., 1985; Blatt et al., 1990; Schall et al., 1995). Moreover, LIPv receives projections mostly from the action-related dorsal stream areas whereas LIPd from both the dorsal and ventral (feature recognition) streams (Ungerleider and Desimone, 1986; Andersen et al., 1990; Blatt et al., 1990; Boussaoud et al., 1990; Stanton et al., 1995).

Such a functional parcellation of area LIP into subareas related to memory- and visually- guided saccades could settle certain apparently conflicting results regarding the response properties of its neurons and the deficits resulting from its lesions. In one study, almost the entire neuronal population of LIP were shown to respond to visual stimulation (Colby et al., 1996). In contrast, only about half of the LIP neurons were shown to respond to visual stimulation in two other studies [49% in Gnadt and Andersen (1988) and 63% in Barash et al. (1991a)]. Our findings can explain the discrepancy mentioned above if the three studies focused on different subregions of area LIP, namely if the neurons studied in the former study were located more rostrally than the neurons studied in the latter two studies. Unfortunately, no map of the recording sites was provided by Colby and her colleagues (Colby et al., 1996). However, in a later publication of this group (Colby, 1998) recording sites are indeed reported to lie in more anterior locations than those of Gnadt

and Andersen (1988) and Barash (1991a). Moreover, the recording sites in the study by Gnadt and Andersen (1988) and Barash (1991a) are also more rostral than their descriptions lead one to expect, and roughly correspond to the middle third of our study, because (i) the location of their electrode tracks was projected onto the parasagittal plane (a procedure which underestimates the length of segments normal to the horizontal plane, such as the caudal part of the IPs), whereas we unfolded the entire IPs, and (ii) our reconstructed 2D maps extend more caudally, up to the intersection of the IPs with the parietoccipital and the lunate sulci. Similarly conflicting are the results from lesion studies. Visual perception deficits rather than saccade execution deficits were reported following reversible chemical inactivation of area LIP in one study (Wardak et al., 2002) whereas memory-guided saccades (but not visually-guided ones) were compromised in another (Li et al., 1999). Again, our data could help reconcile these conflicting results if the lesion was more severe in the middle third and in the depth of the lateral bank of IPs in the latter study (thus impairing the region we found activated for memory-guided saccades), and in the rostral third and more superficially within the bank in the former study (thus impairing a region more intensely activated for visually-guided saccades).

Finally, our data could help reconcile the long-standing debate between two alternative hypotheses concerning the elemental functional role of area LIP during saccadic movements. On the one hand, area LIP has been proposed to participate in selective spatial attention and to embody a salience map of the visible world (Goldberg et al., 1990; Colby and Duhamel, 1996; Gottlieb et al., 1998; Gottlieb and Goldberg, 1999; Kusunoki et al., 2000). On the other hand, it is considered to directly reflect saccade-related movement plans in a variety of conditions (Gnadt and Andersen, 1988; Barash et al., 1991b; Mazzoni et al., 1996a; Snyder et al., 1998). The present study favors both hypotheses by suggesting the existence of two functional subregions in the lateral bank of the IPs, each entrusted with a different role. A rostral subregion located

superficially (close to the crown) within the anatomically defined area LIPd is mainly dedicated to the visuo-spatial aspect of saccade activity. A caudal one deeper in the bank (close to the fundus) within the anatomically defined area LIPv is primarily associated with the motor component of oculomotor behavior.

Overall, our findings illustrate that the lateral bank of the IPs is a mosaic of the following segregated, albeit partially overlapping, regions: (i) a centrally placed fixation-related region at the border of LIPv and LIPd (Fig. 11A, green). (ii). This is surrounded by a widespread region extending in both LIPv and LIPd, which is activated for visually-guided saccades and possibly encodes visuo-spatial and saccade-related parameters (Fig. 11B, red). (iii) A more caudal region confined to LIPv, which is activated for memory-guided saccades and possibly encodes the remembered locations of saccade targets and/or saccade metrics. The area of overlap between regions ii & iii (Fig. 11C, magenta) lying in LIPv may correspond to the representation of oculomotor space in area 7IP, while the area of overlap between all three regions (fixation, visual- and memory-saccade related) lying in the middle of the bank around the border of LIPv and LIPd may correspond to the representation of the central part of oculomotor space in area 7IP (Fig. 11D, white). To the subdivisions of area LIP that present high metabolic demands for visually- and memory-guided saccades in the current study, we should add the regions activated for visually-guided forelimb reaching described in previous studies of our laboratory. Besides occupying a large part of area 5IP in the medial bank of the IPs, the region activated for visually-guided forelimb reaching also extended within area 7IP in the lateral bank of the IPs (Gregoriou and Savaki, 2001; 2003). Consistent with previous reports (Snyder et al., 1998; 2000; Oristaglio et al., 2006), our present and previous data demonstrate that there is overlap, albeit minimal, between the eye movement saccade-related and forelimb reach-related regions of area 7IP. Common activation is largely confined to a portion of the saccade-related region of the present study in the depth of the sulcus.

This notion suggests that LIPv neurons discharge for movement-related signals, irrespectively of the effector employed (eye *vs.* forelimb), while LIPd neurons respond more strongly to visual stimuli serving as targets for the impending movements in the contralateral extrapersonal space.

Temporal cortex

The current study demonstrates for the first time that the superior temporal cortical areas that comprise the MC (MT/V5, MST and FST) display significant metabolic effects during the execution of visually- and memory-guided saccades. More specifically, our findings demonstrate that areas MT/V5 and MST, traditionally thought to process visuo-motion signals for smooth-pursuit eye movements, also carry extraretinal oculomotor signals.

In our study, the three areas that comprise the MC, MT/V5, MST and FST, occupied an area of approximately 200 mm^2, and extended from the posterior bank of the STs, through the floor of the sulcus to its anterior bank. This cortical surface, as defined in our Nissl-stained sections, compares to 125 mm^2 in one study (Cusick et al., 1995) and to 175 mm^2 in another report (Desimone and Ungerleider, 1986). It has also been reported that the areal size of MT that contains a complete representation of the visual field ranges between 76 mm^2 (Ungerleider and Desimone, 1986) and 83 mm^2 (Gattass and Gross, 1981) for monkeys of about the same weight as ours. However, in a recent study, the fMRI estimates of solely the central 11^0 in monkey MT were 100-150 mm^2 (Brewer et al., 2002).

In addition to directionally selective neurons displaying sensory (retinal) discharges, both MT/V5 and MST contain neurons displaying extraretinal signals associated to the maintenance of pursuit (Newsome et al., 1988; Bremmer et al., 1997b; Ferrera and Lisberger, 1997; Squatrito and Maioli, 1997). Nonetheless, the visual and oculomotor components of MC neuronal

discharge have always been assigned a role in smooth pursuit rather than rapid eye movements. Our data demonstrate that the MC is activated for saccades as well. This agrees with descriptions of neurons that respond to fast moving stimuli (Baker et al., 1981; Tanaka et al., 1993; Duffy and Wurtz, 1997). Our data are also in line with previous imaging studies that have consistently shown activation of the superior temporal cortex for visually-guided (Sweeney et al., 1996; Petit and Haxby, 1999; Koyama et al., 2004) and memory-guided saccades (Anderson et al., 1994; Luna et al., 1998; Ozyurt et al., 2006). However, it should be noted that we provided no visual stimulation whatever during the execution of the memory-guided task, whereas previous studies relied on retinal stimulation, albeit minimal, due to the presence of visual targets extinguished before movement onset. In addition, our method provides higher sampling resolution (20 micron sections) and histological confirmation of the anatomical borders of the MC. Our study is in better agreement with a more recent, well controlled fMRI study (Baker et al., 2005) of monkeys executing visually-guided saccades, showing activation of the superior temporal cortex, including areas MT, MST, FST, STP and V4. In this study, the robust activation of the MT/MST/FST complex was considered unexpected and was attributed to the visual motion induced on the retina by saccades. Indeed, motion signals accompanying saccades are as effective in eliciting responses from V1 neurons as the motion of objects in the visual field (Wurtz, 1969). Consequently, part of the visually-guided saccade-related activation of the MC we observed could be due to the shear of the visual scene on the retina. Such a mechanism is doubtful for areas MT/V5 and MST, though, since they contain neurons with oppositely directed motion signals that could annul each other (Thiele et al., 2002). More importantly, such a mechanism can not explain the herein documented activation of areas MT and MST for memory-guided saccades in total darkness, which was equally robust to that for visually-guided saccades, and could only reflect the presence of

extraretinal saccade-related signals. To our knowledge, this is the first study to implicate conclusively the pursuit-associated areas MT/V5 and MST in saccadic behavior.

Our findings provide evidence that areas FST (the ventralmost portion of the MC in the floor of STs) and TPOi (anterior to MST) are activated only for saccades to visual targets and not for saccades to memorized locations. Activation of FST in pursuit eye movements has only been reported in one previous study (Erickson and Dow, 1989). Given that area FST in macaques lies deeply in the floor of the STs, its access becomes difficult and physiological data on its response properties are scant. It was shown that FST neurons in the owl monkey connect to the part of MT which integrates motion cues over wide areas of the visual field (Berezovskii and Born, 2000). Accordingly, the saccadic information that FST neurons carry may be useful for orientation in the environment.

The region anatomically defined as temporal–parietal–occipital (TPO) (Padberg et al., 2003) largely corresponds to the superior temporal polysensory area occupying the rest of the anterior bank of the STs (Cusick et al., 1995). In our analysis, we adopted the three caudal-to-rostral chemoarchitectonic subdivisions, TPOc, TPOi and TPOr, suggested before (Cusick et al., 1995). Single-unit recordings revealed that almost all of TPO neurons are visually responsive, preferring peripheral stimulation (Desimone and Gross, 1979; Bruce et al., 1981). Compared to the parietal and MT/V5, area TPO neurons are not visuotopically organized with large receptive fields that usually encompass both hemifields (Bruce et al., 1981). A common property shared by TPO and MT/V5 neurons is directional selectivity for moving visual stimuli. In addition, TPO neurons respond to more complex forms of movement, such as movement in depth and radial movement, features reported also for MST (Bruce et al., 1981). Although the described characteristics of area TPO imply involvement in oculomotor behavior, this

has only been reported in abstract form (Colby and Miller, 1986). The connectivity patterns of TPO with oculomotor centers of the frontal and the posterior parietal cortex can provide the anatomical substrate of eye-movement-related activity. Of interest is that the TPOi subdivision activated by visually-guided saccades in our study is reciprocally connected to the eye-movement-related areas of the prefrontal and the posterior parietal, same way as areas V5/MT and MST (Seltzer and Pandya, 1989a; Seltzer et al., 1996). Consistent with our findings, TPO has been implicated in the control of visually-guided saccades, because its damage prolongs their latency (Scalaidhe et al., 1995). In the same study, removal of TPO had no effect in the execution of saccades to auditory targets, suggesting that the impairment was not purely motor. Given that TPO neurons respond better to moving than stationary stimuli (Bruce et al., 1981), we cannot exclude the possibility that TPO activation relates to the visual motion induced in the retina by saccades. On the other hand, the anterior/ventral part of STs (TPOr), which has been associated with integration of animate form, motion and location (Jellema et al., 2004), remained unaffected in our study.

Our data also demonstrate that both saccades to visual targets and to memorized locations activated area V4t (V4 transitional), located posterior to MT in the STs and corresponding to the homonymous area described before (Desimone and Ungerleider, 1986). The anterior and posterior subdivisions of area V4t (V4ta and V4tp, respectively) in our study are based on their relative location on the STs maps according to the anatomical maps of Lewis and Van Essen (Lewis and Van Essen, 2000b). Both subdivisions displayed enhanced metabolic effects during visually- and memory-guided saccades, with the only difference being that V4ta was also activated for fixation. In agreement with our findings, V4 neurons have been reported to enhance their discharge before saccades (Fischer and Boch, 1981a; Tolias et al., 2001). Moreover, V4 codes extra-retinal signals related to the direction of stimulus motion more

reliably than MT (Ferrera et al., 1994). Finally, V4 neurons shift their receptive fields towards the saccadic goal prior to eye movement initiation (Tolias et al., 2001).

Fixational Effects

Our study indicates selective metabolic effects in the intraparietal and superior temporal cortical areas that represent the foveal visual field, during active fixation of a centrally located visual target. These effects were significantly higher as compared to the basal condition; however, consistent with a previous report (Corbetta et al., 1998), they were weaker than those induced during visually-guided saccades.

In the intraparietal cortex, enhanced neuronal activity in area LIP during visual fixation of a stationary target is in agreement with previous studies (e.g. Andersen et al., 1990; Colby et al., 1995; Robinson et al., 1995; Ben Hamed et al., 2001; Gregoriou and Savaki, 2001). In the current study, we provide the anatomical localization of the observed activation as circumscribing the border of LIPd and LIPv and extending rostrally into LIPd. Our finding is consistent with the recording of fixation-related neurons at an anterior location of the lateral intraparietal bank (Murata et al., 2000). The relatively large extent of the intraparietal-fixation region conforms with the reported overrepresentation of the central visual field (Ben Hamed et al., 2001; Ben Hamed and Duhamel, 2002) and may be due to the enlargement of the neural space allocated to central vision during fixation (Ben Hamed et al., 2002). On the other hand, the middle part of 7IP that includes LIPv was only marginally activated during the fixation task by 8% compared to the baseline condition. This finding supports the suggestion that LIPv is engaged in the execution of large-amplitude saccades.

In the superior temporal cortex, fixation-related activity was observed in the foveal region of MT/V5, in FST and in areas V4ta and TEO. Our results are in agreement with reports demonstrating that these areas represent the central visual field (Gattass and Gross, 1981; Desimone and Ungerleider, 1986; Komatsu and Wurtz, 1988a; Boussaoud et al., 1991). Small saccades during fixation have been shown to modulate the firing of MT neurons by injecting visual motion signals (Bair and O'Keefe, 1998). In that study, as in ours, small fixational eye movements had an average velocity of approximately 30^0/sec, in the range of sensitivities for MT neurons. The fixational effects we report could be attributed to the recruitment of the low-pass cells described in MT (Lagae et al., 1993), which have foveal receptive fields and show preference for slow speeds. MT neurons with small foveal receptive fields and similar preference for speed have also been described in another study (Rodman and Albright, 1987). Area TEO of our study corresponds to the portion of TEO around the posterior lip of the STs that contains a representation of the foveal and parafoveal visual field (Boussaoud et al., 1991). This area connects principally with the inferior temporal areas that constitute the pathway for fine discrimination analysis (Boussaoud et al., 1991) and also projects to the small-amplitude-saccade FEF and to LIPd (Baizer et al., 1991; Webster et al., 1994). Compatible with the fixation-induced activation of V4ta and TEO in our study are the reports that 41% of TEO and 34% of V4 neurons were activated during a spot-fixation task (Watanabe and Iwai, 1991), and that focal attention to a visual stimulus enhanced processing in V4 neurons (Moran and Desimone, 1985).

Our finding that areas LIP and MT are activated during fixation and saccades (in addition to smooth-pursuit) conforms with the report of Krauzlis et al. (1997; 2000) that a population of fixation neurons in rostral SC discharge both during smooth-pursuit and small-amplitude saccades. These neurons are distinct from the saccade-related neurons recorded in caudal SC (Munoz and

Wurtz, 1995). The activity of SC fixation neurons does not depend on the presence of visual stimulation, as it is sustained even in the absence of visual target (Munoz and Wurtz, 1993). Krauzlis et al. (1997; 2000) suggest that the rostral SC provides a position-error signal that can be used by both saccades and pursuit and which "*might act to coordinate the two types of movements, thereby avoiding the deleterious visual consequences that would follow if the two systems operated completely independently*". Our results cannot indicate whether the same neuron carries information about fixation and eye movements. Conceivably, there exists a continuum of cortical motor maps, with fixation (and possibly smooth-pursuit) in the foveal/parafoveal representations of the visual field, and large-amplitude saccades in the peripheral ones. Segregation of neural responses along a center-to-periphery organization allows faster and more efficient oculomotor processing (Gattass et al., 2005).

Comparison between the intraparietal and superior temporal activations

The present findings indicate that all areas of the IPs and the STs activated during memory-guided saccades are also active in the visually-guided condition. Interestingly, both the foveal and extrafoveal parts of areas with known central-peripheral topography (LIP, MT/V5, V4t) are activated during visually-guided and memory-guided saccades. In the case of extrafoveal MT/V5, glucose consumption was approximately the same under the two behavioral paradigms (Table 3, Sd, Sl). In a similar way, LIPv and V4tp representing peripheral vision displayed equally robust activations in both the light and the dark conditions (LIPv: Table 2, Sd, Sl; V4tp: Table 3, Sd, Sl). Taken together, our results suggest that oculomotor behavior in the light as well as in the dark exerts similar metabolic effects in areas with eccentric representations of the visual field. In the subdivisions of MT, LIP and V4t that represent the central visual field, i.e. MTf , LIPd and V4ta, activation was

significantly higher in the monkeys executing visually-guided saccades as compared to those executing memory-guided saccades (by 10%, 22% and 24%, respectively). Therefore, subregions representing the central visual field require visual stimulation, in addition to eye movements, to be maximally activated.

Surprisingly, the current results imply that, in the studied areas, the relative load of motor *vs.* sensory activation (as expressed in activation during memory-guided saccades and the difference in activation between visually- and memory-guided saccades) has a rather systematic pattern. Originally, Felleman and van Essen (1991) proposed a hierarchical scheme of cortical organization based on the laminar patterns of connectivity among different areas. Accordingly, MT and V4t occupy a lower level in the hierarchy compared to LIP, MST and FST. Similarly, by quantitative comparison of the proportion of supragranular projecting neurons in V1 and V4 afferents, Barone et al (2000) suggested that area MT lies at a lower level compared to LIP and FST which occupy progressively higher positions. Other studies describe stronger attentional modulation of incoming sensory information in later stages of cortical processing (Ferrera et al., 1994; Treue and Maunsell, 1999), a striking observation which has not yet been accounted for (Maunsell and Cook, 2002).

Our functional results of the differential cortical activations during simple saccade tasks largely comply with the anatomical schemata of Felleman and van Essen (1991) and Barone et al (2000). In addition, we propose that these need to expand to include the subdivisions of areas with discrete representations for central and peripheral fields. As we have shown, area MT and subareas LIPv and V4tp were equally activated in the visually- and memory-guided-saccade tasks. The subareas MTf, LIPd, V4ta and area MST display significant effects during the execution of memory-guided saccades; they also carry a load of sensory activation. In the case of MTf and

LIPd, the weaker enhancement of the former in the visually-guided task compared to the memory-guided one may reflect its earlier engagement in visuo-motor function. The same is already evident in the fixating condition with MTf displaying weaker activation than LIPd (15% *vs.* 20%). Finally, area FST singled out by displaying enhanced activation in the visually-guided and the fixation task but not in the memory-guided condition. According to the current data, MT, LIPv and V4tp should be placed in an earlier level of cortical processing. MTf and MST should occupy a higher tier, followed by LIPd and V4ta. The latest stage should be occupied by area FST. It is tempting then to suggest that lower order areas assume an executional role while higher order areas are involved in the transformation of their heavy load of sensory inputs to more abstract representations of visual space (Freedman and Assad, 2006).

SUMMARY

We applied the quantitative autoradiographic method of [^{14}C]-deoxyglucose to study the location and extent of intraparietal and superior temporal cortical activation in monkeys performing: i) fixation of a central visual target, ii) visually-guided saccades, and iii) memory-guided saccades, of similar amplitude and direction as in the visually-guided paradigms, in complete darkness. By eliminating visual stimulation in the memory-guided task, we dissociated the effects related to the sensory component from the effects related to the motor component of saccadic behavior. This is the first study to provide high-resolution two-dimensional functional and anatomical maps of metabolic activity of the intraparietal and the superior temporal cortices that allowed for direct comparisons between different experimental conditions.

In the intraparietal cortex, visually-guided saccades induced enhanced metabolic activation in approximately the middle and anterior third of the lateral bank of the IPs. The effect spread in both the ventral and dorsal subdivisions of area LIP (LIPv and LIPd, respectively), as we confirmed with histological examination. Our results demonstrate that the oculomotor-related area LIP extends further rostrally than traditionally reported to include most of the anterior part of the bank. Besides saccade execution, area LIPd requires visual stimulation for maximal activation. The effect induced by memory-guided saccades was equally robust as that induced in the visual-guided paradigm, but was confined to the middle third of the lateral bank within LIPv. Active fixation of a visual target induced significant metabolic activation in the border of LIPd/LIPv and extended in the anterior part of the lateral bank within area LIPd, covering approximately one-third of the neuronal space allocated to visually-guided saccades. We propose that the lateral intraparietal cortex represents visual and motor space in functionally segregated subregions. A rostral subregion located superficially (close to the crown) within the

cytoarchitectonically-defined area LIPd is mainly dedicated to the visuo-spatial aspect of oculomotor behavior. A caudal one deeper in the bank (close to the fundus) within the cytoarchitectonically-defined area LIPv is predominantly associated with the motor component of saccadic activity.

In the superior temporal cortex, oculomotor behavior activated a constellation of brain areas, providing evidence for their involvement in saccadic eye movements. All areas that comprise the motion-complex network traditionally implicated in the analysis of visual motion and in smooth-pursuit execution i.e., MT/V5, in the lower bank of the STs, MST, in the upper bank of the STs, and FST, in the floor of the STs, were significantly activated during visually-guided saccades. Areas MT/V5 and MST were also activated during memory-guided saccades. Interestingly, we observed enhanced metabolic activation in the rest of the regions of the caudal STs, which are not usually implicated in oculomotor/fixational behavior. Both the posterior and the anterior subdivisions of area V4t in the lower bank were activated during the execution of visually- and memory-guided saccades, whereas the intermediate part of polysensory area TPO (TPOi) in the upper bank displayed significant activation in the visually-guided saccade task. Fixation-related metabolic increases were observed in the areas with central field representations, i.e. the foveal part of MT (MTf), ventrally, in the anterior part of V4t (V4ta), in FST and in area TEO. Our findings demonstrate that areas MT/V5, MST and V4t receive and/or process extra-retinal saccade-related information.

ΠΕΡΙΛΗΨΗ

Με την ποσοτική αυτοραδιογραφική μέθοδο της [^{14}C]-δεοξυγλυκόζης χαρτογραφήθηκε η μεταβολική δραστηριότητα στην ενδοβρεγματική και άνω κροταφική αύλακα πιθήκων που εκτελούσαν i) εστίαση βλέμματος σε κεντρικό οπτικό στόχο, ii) σακκαδικές κινήσεις προς οπτικούς στόχους και iii) σακκαδικές κινήσεις προς απομνημονευμένους στόχους στο σκοτάδι, ώστε να διαχωριστεί η κινητική από την αισθητική (οπτική) συνιστώσα της συμπεριφοράς. Η τοπική κατανάλωση γλυκόζης κατά μήκος των υπό εξέταση περιοχών υπολογίστηκε σε αυτοραδιογραφικές εικόνες οριζόντιων σειριακών τομών, με τη βοήθεια συστήματος ανάλυσης εικόνας. Η κατανομή της μεταβολικής δραστηριότητας καθ'όλη την προσθιοπίσθια και ραχιαιοκοιλιακή έκταση των υπό ανάλυση περιοχών αναπαραστήθηκε σε δισδιάστατους χάρτες υψηλής διακρισιμότητας. Οι χάρτες όλων των ημισφαιρίων ευθυγραμμίστηκαν ώστε να συμπέσουν με πρότυπο χάρτη, επιτρέποντας την άμεση σύγκριση μεταβολικών δεδομένων που προήλθαν από διαφορετικούς εγκεφάλους.

Εντός της ενδοβρεγματικής αύλακας, στα ημισφαίρεια αντίπλευρα από τις εκτελούμενες κινήσεις, ενεργοποιήθηκαν διαφορετικές, μερικώς επικαλυπτόμενες υποπεριοχές κατά την εκτέλεση σακκαδικών κινήσεων προς οπτικούς και προς απομνημονευμένους στόχους. Αυξημένη μεταβολική δραστηριότητα παρατηρήθηκε σε εκτενές τμήμα της πλάγιας όχθης κατά την εκτέλεση σακκαδικών κινήσεων προς οπτικούς στόχους. Η ενεργοποίηση κάλυπτε το μεσαίο και πρόσθιο τρίτο της αύλακας που αντιστοιχούν στην κοιλιακή και ραχιαία πλάγια ενδοβρεγματική υποπεριοχή, όπως επιβεβαίωσε η ιστολογική παρατήρηση. Για την μέγιστη ενεργοποίηση του πρόσθιου τμήματος της αύλακας απαιτείται οπτικός ερεθισμός. Κατά την εκτέλεση σακκαδικών κινήσεων προς απομνημονευμένους στόχους, απουσία οπτικού ερεθισμού, η μεταβολική δραστηριότητα περιορίστηκε στο μεσαίο τρίτο της αύλακας στην κοιλιακή πλάγια ενδοβρεγματική υποπεριοχή. Κατά την εστίαση βλέμματος σε κεντρικό οπτικό στόχο, η μεταβολική δραστηριότητα εκτεινόταν από το όριο μεταξύ της κοιλιακής και της ραχιαίας πλάγιας ενδοβρεγματικής υποπεριοχής

μέχρι το πρόσθιο τμήμα της αύλακας και κατελάμβανε περίπου το ένα τρίτο του νευρωνικού χώρου που ενεργοποιήθηκε κατά την εκτέλεση οπτικά καθοδηγούμενων σακκαδικών κινήσεων. Προτείνουμε συνεπώς ότι η οφθαλμοκινητική περιοχή στην πλάγια όχθη της ενδοβρεγματικής αύλακας εκτείνεται από το μεσαίο μέχρι το πρόσθιο τρίτο της αύλακας. Η ραχιαία πλάγια ενδοβρεγματική υποπεριοχή ενεργοποιείται κυρίως λόγω παρουσίας οπτικού ερεθισμού, ενώ η κοιλιακή πλάγια ενδοβρεγματική υποπεριοχή ενεργοποιείται κυρίως λόγω των εκτελούμενων σακκαδικών κινήσεων.

Εντός της οπίσθιας άνω κροταφικής αύλακας, στα ημισφαίρεια αντίπλευρα από τις εκτελούμενες κινήσεις, παρατηρήθηκε σημαντική ενεργοποίηση διαφόρων φλοιικών περιοχών. Κατά την εκτέλεση σακκαδικών κινήσεων προς οπτικούς στόχους ενεργοποιήθηκαν οι περιοχές μέση κροταφική, στην οπίσθια όχθη, έσω άνω κροταφική, στην πρόσθια όχθη, και η περιοχή στο δάπεδο της αύλακας, που συνολικά αποτελούν το σύστημα ανάλυσης κινούμενων οπτικών ερεθισμάτων. Αυξημένη μεταβολική δραστηριότητα παρατηρήθηκε επίσης στο πρόσθιο και οπίσθιο τμήμα της μεταβατικής οπτικής περιοχής 4, στην οπίσθια όχθη της αύλακας, και στο ενδιάμεσο τμήμα της περιοχής κροταφική-βρεγματική-οπτική, στην πρόσθια όχθη της αύλακας. Κατά την εκτέλεση σακκαδικών κινήσεων προς απομνημονευμένους στόχους ενεργοποιήθηκαν οι περιοχές μέση κροταφική, έσω άνω κροταφική, καθώς και το πρόσθιο και οπίσθιο τμήμα της μεταβατικής οπτικής περιοχής 4. Κατά την εστίαση βλέμματος σε οπτικό στόχο σημειώθηκε αυξημένη μεταβολική δραστηριότητα στις περιοχές που σχετίζονται με την αντιπροσώπευση του κεντρικού οπτικού πεδίου, συγκεκριμένα στο τμήμα κεντρικής αντιπροσώπευσης της μέσης κροταφικής περιοχής, στην περιοχή του δαπέδου της αύλακας, στο πρόσθιο τμήμα της μεταβατικής οπτικής περιοχής 4 και στην περιοχή κροταφική-ινιακή. Συμπερασματικά, στην άνω κροταφική αύλακα, οι περιοχές μέση κροταφική, έσω άνω κροταφική, και η μεταβατική οπτική περιοχή 4 ενεργοποιούνται κατά την εκτέλεση σακκαδικών κινήσεων, ανεξάρτητα από την παρουσία οπτικού ερεθίσματος.

REFERENCES

Albright TD. (1984). Direction and Orientation Selectivity of Neurons in Visual Area MT of the Macaque. *J Neurophysiol* **52**:1106-30.

Albright TD, Desimone R and Gross CG. (1984). Columnar organization of directionally selective cells in visual area MT of the macaque. *J. Neurophysiol.* **51**:16-31.

Allman JM and Kaas JH. (1971). A representation of the visual field in the caudal third of the middle tempral gyrus of the owl monkey (*Aotus trivirgatus*). *Brain Research* **31**:85-105.

Andersen RA, Asanuma C, Essick G and Siegel RM. (1990). Corticocortical connections of anatomically and physiologically defined subdivisions within the inferior parietal lobule. *J. Comp. Neurol.* **296**:65-113.

Andersen RA and Buneo CA. (2002). Intentional maps in posterior parietal cortex. *Annu Rev Neorosci* **25**:189-220.

Anderson TJ, Jenkins IH, Brooks DJ, Hawken MB, Frackowiak RSJ and Kennard C. (1994). Cortical control of saccades and fixation in man. A PET study. *Brain* **117**:1073-84.

Asanuma C, Andersen RA and Cowan WM. (1985). The thalamic relations of the caudal inferior parietal lobule and the lateral prefrontal cortex in monkeys: divergent cortical projections from the cell clusters in the medial pulvinar nucleus. *J. Comp. Neurol.* **241**:357-81.

Bair W and O'Keefe LP. (1998). The influence of fixational eye movements on the response of neurons in area MT of the macaque. *Vis Neurosci* **15**:779-86.

Baizer JS, Ungerleider LG and Desimone R. (1991). Organization of visual inputs to the inferior temporal and posterior cortex in macaques. *J. Neurosci.* **11**:168-90.

Baker JF, Petersen SE, Newsome WT and Allman JM. (1981). Visual response properties of neurons in four extrastriate visual areas of the owl monkey (Aotus trivirgatus): A quantitative comparison of medial, dorsomedial, dorsolateral, and middle temporal areas. *J. Neurophysiol.* **45**:397-416.

Baker JT, Patel GH, Corbetta M and Snyder LH. (2005). Distribution of Activity Across the Monkey Cerebral Cortical Surface, Thalamus and Midbrain during Rapid, Visually Guided Saccades. *Cereb Cortex.* **2005**.

Barash S, Bracewell RM, Fogassi L, Gnadt JW and Andersen RA. (1991a). Saccade-related activity in the lateral intraparietal area. I. Temporal properties; comparison with area 7a. *J. Neurophysiol.* **66**:1095-108.

Barash S, Bracewell RM, Fogassi L, Gnadt JW and Andersen RA. (1991b). Saccade-related activity in the lateral intraparietal area. II. Spatial properties. *J. Neurophysiol.* **66**:1109-24.

Barbas H. (1988). Anatomic organization of basoventral and mediodorsal visual recipient prefrontal regions in the rhesus monkey. *J. Comp. Neurol.* **276**:313-42.

Barbas H and Mesulam MM. (1981). Organization of afferent input to subdivisions of area 8 in the rhesus monkey. *J. Comp. Neurol.* **200**:407-31.

Barone P, Batardiere A, Knoblauch K and Kennedy H. (2000). Laminar Distribution of Neurons in Extrastriate Areas Projecting to Visual Areas V1 and V4 Correlates with the Hierarchical Rank and Indicates the Operation of a Distance Rule. *J. Neurosci.* **20**:3263-81.

Ben Hamed S and Duhamel J-R. (2002). Ocular fixation and visual activity in the monkey lateral intraparietal area. *Exp. Brain Res.* **142**:512-28.

Ben Hamed S, Duhamel J-R and Bremmer F. (2001). Representation of the visual field in the lateral intraparietal area of macaque monkeys: a quantitative receptive field analysis. *Exp. Brain Res.* **140**:127-44.

Ben Hamed S, Duhamel J-R and Bremmer F. (2002). Visual receptive field modulation in the lateral intraparietal area during attentive fixation and free gaze. *Cereb Cortex* **12**:234-45.

Berezovskii VK and Born RT. (2000). Specificity of Projections from Wide-Field and Local Motion-Processing Regions within the Middle Temporal Visual Area of the Owl Monkey. *J. Neurosci.* **20**:1157-69.

Blatt GJ, Andersen RA and Stoner GR. (1990). Visual receptive field organization and cortico-cortical connections of the lateral intraparietal area (area LIP) in the macaque. *J. Comp. Neurol.* **299**:421-45.

Born RT, Groh JM, Zhao R and Lukasewycz SL. (2000). Segregation of Object and Background Motion in Visual Area MT: Effects of Microstimulation on Eye Movements. *Neuron* **26**:725-34.

Boussaoud D, Desimone R and Ungerleider LG. (1991). Visual topography of area TEO in the macaque. *J. Comp. Neurol.* **306**:554-75.

Boussaoud D, Desimone R and Ungerleider LG. (1992). Subcortical connections of visual areas MST and FST in macaques. *Vis Neurosci.* **9**:291-302.

Boussaoud D, Ungerleider LG and Desimone R. (1990). Pathways for motion analysis: Cortical connections of the medial superior temporal and fundus of the superior temporal visual areas in the macaque. *J. Comp. Neurol.* **296**:462-95.

Bracewell RM, Mazzoni P, Barash S and Andersen RA. (1996). Motor intention activity in the Macaque's lateral intraparietal area.II. Changes of motor plan. *J. Neurophysiol.* **76**:1457-64.

Bremmer F, Distler C and Hoffmann K-P. (1997a). Eye-position effects in monkey cortex. II: Pursuit and fixation related activity in posterior parietal areas LIP and 7A. *J. Neurophysiol.* **77**:962-77.

Bremmer F, Ilg UJ, Thiele A, Distler C and Hoffmann K-P. (1997b). Eye-position effects in monkey cortex. I: Visual and pursuit related activity in extrastriate areas MT and MST. *J. Neurophysiol.* **77**:944-61.

Brewer AA, Press WA, Logothetis NK and Wandell BA. (2002). Visual areas in macaque cortex measured using functional magnetic resonance imaging. *J. Neurosci.* **22**:10416-26.

Bruce CJ, Desimone R and Gross CG. (1981). Visual properties of neurons in a polysensory area in superior temporal sulcus of the macaque. *J. Neurophysiol.* **46**:369-84.

Bruce CJ, Desimone R and Gross CG. (1986). Both striate cortex and superior colliculus contribute to visual properties of neurons in superior temporal polysensory area of Macaque monkey. *J. Neurophysiol.* **55**:1057-75.

Bullier J, Schall JD and Morel A. (1996). Functional streams in occipito-frontal connections in the monkey. *Behavioral Brain Research* **76**:89-97.

Bushnell MC, Goldberg ME and Robinson DL. (1981). Behavioral enhancement of visual responses in monkey cerebral cortex. I. Modulation in posterior parietal cortex related to selective visual attention. *J. Neurophysiol.* **46**:755-72.

Cavada C and Goldman-Rakic PS. (1989a). Posterior parietal cortex in rhesus monkey: I. Parcellation of areas based on distinctive limbic and sensory corticocortical connections. *J. Comp. Neurol.* **287**:393-421.

Cavada C and Goldman-Rakic PS. (1989b). Posterior parietal cortex in rhesus monkey: II. Evidence for segregated corticocortical networks linking sensory and limbic areas with the frontal lobe. *J. Comp. Neurol.* **287**:422-45.

Cheng K, Hasegawa T, Saleem KS and Tanaka K. (1994). Comparison of neuronal selectivity for stimulus speed, length, and contrast in the prestriate visual cortical areas V4 and MT of the maqaque monkey. *J. Neurophysiol.* **71**:2269-80.

Colby CL. (1998). Action-oriented spatial reference frames in cortex. *Neuron* **20**:15-24.

Colby CL, Duhamel J-R and Goldberg ME. (1993). Ventral intraparietal area of the Macaque: Anatomic location and Visual response Properties. *J. Neurophysiol.* **69**:902-14.

Colby CL, Duhamel J-R and Goldberg ME. (1995). Oculocentric spatial representation in parietal cortex. *Cereb. Cortex* **5**:470-81.

Colby CL, Duhamel J and Goldberg ME. (1996). Visual, presaccadic, and cognitive activation of single neurons in monkey lateral intraparietal area. *J. Neurophysiol.* **76**:2841-52.

Colby CL and Duhamel JR. (1996). Spatial representations for action in parietal cortex. *Cogn. Brain Res.* **5**:105-15.

Colby CL, Gattass R, Olson CR and Gross CG. (1988). Topographical organization of cortical afferents to extrastriate visual area PO in the macaque: a dual tracer study. *J. Comp. Neurol.* **269**:392-413.

Colby CL and Goldberg ME. (1999). Space and attention in parietal cortex. *Annu. Rev. Neurosci.* **22**:319-49.

Colby CL and Miller EK. (1986). Eye movement related responses of neurons in superior temporal polysensory area of macaque. *Soc. Neurosci. Abstr.* **12**:11.

Connolly JD, Goodale MA, Desouza JFX, Menon RS and Vilis T. (2000). A comparison of frontoparietal fMRI activation during anti-saccades and anti-pointing. *J. Neurophysiol.* **84**:1645-55.

Corbetta M, Akbudak E, Conturo TE, Snyder AZ, Ollinger JM, Drury HA, Linenweber MR, Petersen SE, Raichle ME, VanEssen DC and Shulman GL. (1998). A common network of functional areas for attention and eye movements. *Neuron* **21**:761-73.

Cusick CG, B. S, Cola M and Griggs E. (1995). Chemoarchitectonics and corticocortical terminations within the superior temporal sulcus of the rhesus monkey: evidence for subdivisions of superior temporal polysensory cortex. *J. Comp. Neurol.* **360**:513-35.

Dalezios Y, Raos VC and Savaki HE. (1996). Metabolic activity pattern in the motor and somatosensory cortex of monkeys performing a visually guided reaching task with one forelimb. *Neuroscience* **72**:325-33.

Desimone R and Gross CG. (1979). Visual areas in the temporal cortex of the macaque. *Brain Res.* **178**:363-80.

Desimone R and Ungerleider LG. (1986). Multiple visual areas in the caudal superior temporal sulcus of the macaque. *J. Comp. Neurol.* **248**:164-89.

DeSouza JFX, Dukelow SP, Gati JS, Menon RS, Andersen RA and Vilis T. (2000). Eye Position Signal Modulates a Human Parietal Pointing Region during Memory-Guided Movements. *J. Neurosci.* **20**:5835-40.

Distler C, Boussaoud D, Desimone R and Ungerleider LG. (1993). Cortical connections of inferior temporal area TEO in macaque monkeys. *J. Comp. Neurol.* **334**:125-50.

Distler C, Mustari MJ and Hoffmann KP. (2002). Cortical projections to the nucleus of the optic tract and dorsal terminal nucleus and to the dorsolateral pontine nucleus in macaques: a dual retrograde tracing study. *J. Comp. Neurol.* **444**:144-58.

Dodge R. (1903). Five types of eye movements in the horizontal meridian plane of the field of regard. . *Amer. J. Physiol.* **8**:307-29.

Dubner R and Zeki SM. (1971). Response properties and receptive fields of cells in an anatomically defined region of the superior temporal sulcus in the monkey. *Brain Res.* **34**:528-32.

Duffy CJ. (1998). MST neurons respond to optic flow and translational movement. *J Neurophysiol* **80**:1816-27.

Duffy CJ and Wurtz RH. (1997). Medial Superior Temporal Area Neurons Respond to Speed Patterns in Optic Flow. *J. Neurosci.* **17**:2839-51.

Dursteler MR and Wurtz RH. (1988). Pursuit and optokinetic deficits following chemical lesions of cortical areas MT and MST. *J. Neurophysiol.* **60**:940-65.

Dursteler MR, Wurtz RH and Newsome WT. (1987). Directional pursuit deficits following lesions of the foveal representation within the superior temporal sulcus of the macaque monkey. *J Neurophysiol.* **57**:1262-87.

Eifuku S and Wurtz RH. (1998). Response to Motion in Extrastriate Area MSTl: Center-Surround Interactions. *J Neurophysiol* **80**:282-96.

Erickson RG and Dow BM. (1989). Foveal Tracking Cells in the Superior Temporal Sulcus of the Macaque Monkey. *Exp Brain Res* **78**:113-31.

Erickson RG, Dow BM and Snyder AZ. (1989). Representation of the fovea in the superior temporal sulcus of the macaque monkey. *Exp Brain Res* **78**:90-112.

Felleman DJ and Van Essen DC. (1991). Distributed hierarchical processing in the primate cerebral cortex. *Cereb. Cortex* **1**:1-47.

Felleman DJ, Xiao Y and McClendon E. (1997). Modular Organization of Occipito-Temporal Pathways: Cortical Connections between Visual Area 4 and Visual Area 2 and Posterior Inferotemporal Ventral Area in Macaque Monkeys. *J. Neurosci.* **17**:3185-200.

Ferrera VP and Lisberger SG. (1997). Neuronal responses in visual areas MT and MST during smooth pursuit target selection. *J. Neurophysiol.* **78**:1433-46.

Ferrera VP, Rudolph KK and Maunsell JH. (1994). Responses of neurons in the parietal and temporal visual pathways during a motion task. *J. Neurosci.* **14**:6171-86.

Fiorani MJ, Gattass R, Rosa MG and Sousa AP. (1989). Visual area MT in the Cebus monkey: location, visuotopic organization, and variability. *J. Comp. Neurol.* **287**:98-118.

Fischer B and Boch R. (1981a). Enhanced activation of neurons in prelunate cortex before visually guided saccades of trained rhesus monkeys. *Exp Brain Res* **44**:129-37.

Freedman DJ and Assad JA. (2006). Experience-dependent representation of visual categories in parietal cortex. *Nature* **443**:85-88.

Fries W. (1984). Cortical projections to the superior colliculus in the macaque monkey: a retrograde study using horseradish peroxidase. *J. Comp. Neurol.* **230**:55-76.

Froehler MT and Duffy CJ. (2002). Cortical neurons encoding path and place: where you go is where you are. *Science* **295**:2462-65.

Fuchs AF. (1967). Saccadic and smooth pursuit eye movements in the monkey. *J Neurophysiol* **191**:609-31.

Fuchs AF, Kaneko CR and Scudder CA. (1985). Brainstem control of saccadic eye movements. *Annu Rev Neurosci.* **8**:307-37.

Galletti C, Gamberini M, Kutz DF, Fattori P, Luppino G and Matelli M. (2001). The cortical connections of area V6: occipito- parietal network processing visual information. *Eur. J. Neurosci.* **13**:1-18.

Garey JL. (1999). *Brodmann's localization in the cerebral cortex*. London: Imperial College Press.

Gattass R and Gross CG. (1981). Visual topography of striate projection zone (MT) in posterior superior temporal sulcus of the macaque. *J. Neurophysiol.* **46**:621-28.

Gattass R, Nascimento-Silva S, Soares J, Lima B, Jansen A, Diogo A, Farias M, Botelho M, Mariani O, Azzi J and Fiorani M. (2005). Cortical visual areas in monkeys: location, topography, connections, columns, plasticity and cortical dynamics. *Philos Trans R Soc Lond B: Biol Sci* **360**:709-31.

Geesamen BJ, Born RT, Andersen RA and Tootel RBH. (1997). Maps of complex motion selectivity in the superior temporal cortex of the alert macaque monkey: a double-label 2-deoxyglucose study. *Cereb. Cortex* **7**:749-57.

Gnadt JW and Andersen RA. (1988). Memory related motor planning activity in posterior parietal cortex of macaque. *Exp. Brain Res.* **70**:216-20.

Gnadt JW, Bracewell RM and Andersen RA. (1991). Sensorimotor transformation during eye movements to remembered targets. *Vision Res.* **31**:693-715.

Goldberg ME, Colby CL and Duhamel J-R. 1990. Representation of visuomotor space in the parietal lobe of the monkey. In: Cold Spring Harbor Symposia on Quantitative Biology: Cold Spring Harbor Laboratory Press. p 729-39.

Gottlieb J and Goldberg ME. (1999). Activity of neurons in the lateral intraparietal area of the monkey during an antisaccade task. *Nature Neurosci.* **2**:906-12.

Gottlieb JP, Bruce CJ and MacAvoy MG. (1993). Smooth eye movements elicited by microstimulation in the primate frontal eye field. *J. Neurophysiol.* **69**:786-99.

Gottlieb JP, Kusunoki M and Goldberg ME. (1998). The representation of visual salience in monkey parietal cortex. *Nature* **391**:481-84.

Graziano MS, Andersen RA and Snowden RJ. (1994). Tuning of MST neurons to spiral motions. *J Neurosci* **14**:54-67.

Gregoriou GG and Savaki HE. (2001). The intraparietal cortex: Subregions involved in fixation, saccades, and in the visual and somatosensory guidance of reaching. *J. Cereb. Blood Flow Metab.* **21**:671-82.

Gregoriou GG and Savaki HE. (2003). When vision guides movement: A functional imaging study of the monkey brain. *NeuroImage* **19**:959-67.

Groh JM, Born RT and Newsome WT. (1997). How Is a Sensory Map Read Out? Effects of Microstimulation in Visual Area MT on Saccades and Smooth Pursuit Eye Movements. *J Neurosci* **17**:4312-30.

Grunewald A, Linden JF and Andersen RA. (1999). Responses to auditory stimuli in macaque lateral intraparietal area. I. Effects of training. *J. Neurophysiol.* **82**:330-42.

Hecaen H and de Ajuriaguerra J. (1954). Balint's syndrome (psychic paralysis of visual fixation) and its minor forms. *Brain* **77**:373-400.

Heinen SJ. (1995). Single neuron activity in the dorsomedial frontal cortex during smooth pursuit eye movements. *Exp. Brain Res.* **104**:357-61.

Hof PR and Morrison JH. (1995). Neurofilament Protein Defines Regional Patterns of Cortical Organization in the Macaque Monkey Visual System: A Quantitative Immunohistochemical Analysis. *J. Comp. Neurol.* **352**:161-86.

Ilg UJ. (1997). Slow eye movements. *Prog Neurobiol* **53**:293-329.

Jellema T, Maassen G and Perrett DI. (2004). Single cell integration of animate form, motion and location in the superior temporal cortex of the macaque monkey. *Cereb Cortex* **2004**:781-90.

Judge SJ, Richmond BJ and Chu FC. (1980). Implantation of magnetic search coils for measurements of eye position: An improved method. *Vision Res.* **20**:535-38.

Kaas JH and Morel A. (1993). Connections of visual areas of the upper temporal lobe of owl monkeys: the MT crescent and dorsal and ventral subdivisions of FST. *J. Neurosci.* **13**:534-46.

Kennedy C, Sakurada O, Shinohara M, Jehle J and Sokoloff L. (1978). Local cerebral glucose utilization in the normal conscious macaque monkey. *Ann. Neurol.* **4**:293-301.

Kobatake E and Tanaka K. (1994). Neuronal selectivities to complex object features in the ventral visual pathway of the macaque cerebral cortex. *J. Neurophysiol.* **71**:856-67.

Komatsu H and Wurtz RH. (1988a). Relation of cortical areas MT and MST to pursit eye movements. I. Localization and visual properties of neurons. *J. Neurophysiol.* **60**:580-603.

Komatsu H and Wurtz RH. (1988b). Relation of cortical areas MT and MST to pursit eye movements. III. Interaction with full-field visual stimulation. *J. Neurophysiol.* **60**:621-44.

Komatsu H and Wurtz RH. (1989). Modulation of pursuit eye movements by stimulation of cortical areas MT and MST. *J Neurophysiol* **62**:31-47.

Koyama M, Hasegawa I, Osada T, Adachi Y, Nakahara K and Miyashita Y. (2004). Functional magnetic resonance imaging of macaque monkeys performing visually guided saccade tasks: comparison of cortical eye fields with humans. *Neuron* **41**:795--807.

Krauzlis RJ. (2004). Recasting the smooth pursuit eye movement system. *J Neurophysiol* **91**:591-603.

Krauzlis RJ. (2005). The Control of Voluntary Eye Movements: New Perspectives. *Neurocientist* **11**:124-37.

Krauzlis RJ, Basso MA and Wurtz RH. (1997). Shared motor error for multiple eye movements. *Science* **276**:1693-95.

Krauzlis RJ, Basso MA and Wurtz RH. (2000). Discharge Properties of Neurons in the Rostral Superior Colliculus of the Monkey During Smooth-Pursuit Eye Movements. *J Neurophysiol* **84**:876-91.

Kruse W, Dannenberg S, Kleiser R and Hoffmann KP. (2002). Temporal relation of population activity in visual areas MT/MST and in primary motor cortex during visually guided tracking movements. *Cereb Cortex* **12**:466-76.

Kusunoki M, Gottlieb J and Goldberg ME. (2000). The lateral intraparietal area as a salience map: the representation of abrupt onset, stimulus motion, and task relevance. *Vision Res.*:1459-68.

Lagae L, Raiguel S and Orban GA. (1993). Speed and direction selectivity of macaque middle temporal neurons. *J. Neurophysiol.* **69**:19-39.

Leigh RJ and Zee DS. (1999). *The Neurology of Eye Movements*, 3rd ed. New York: Oxford University Press.

Lewis JW and Van Essen DC. (2000a). Corticocortical connections of visual, sensorimotor, and multimodal processing area in the parietal lobe of the macaque monkey. *J. Comp. Neurol.* **428**:112-37.

Lewis JW and Van Essen DC. (2000b). Mapping of architectonic subdivisions in the macaque monkey, with emphasis on parieto- occipital cortex. *J. Comp. Neurol.* **428**:79-111.

Li C-SR, Mazzoni P and Andersen RA. (1999). Effect of reversible inactivation of macaque lateral intraparietal area on visual and memory saccades. *J. Neurophysiol.* **81**:1827-38.

Liu J and Newsome WT. (2003). Functional Organization of Speed Tuned Neurons in Visual Area MT. *J Neurophysiol* **89**:246-56.

Lui F, Gregory KM, Blanks RHI and Giolli RA. (1995). Projections from Visual areas of the Cerebral Cortex to Pretectal Nuclear Complex, Terminal Accessory Optic Nuclei, and Superior Colliculus in the Macaque Monkey. *J. Comp. Neurol.* **363**:439-60.

Luna B, Thulborn KR, Strojwas MH, McCurtain BJ, Berman R, A., Genovese CR and Sweeney JA. (1998). Dorsal cortical regions subserving visually guided saccades in humans: an fMRI study. *Cereb. Cortex* **8**:40-47.

Luppino G, Rozzi S, Calzavara R and Matelli M. (2001). Prefrontal and agranular cingulate projections to the dorsal premotor areas F2 and F7 in the macaque monkey. *Eur. J. Neurosci.* **17**:559-78.

Lynch JC, Graybiel AM and Lobeck LJ. (1985). The differential projection of two cytoarchitectonic subregions of the inferior parietal lobule of macaque upon the deep layers of the superior colliculus. *J. Comp. Neurol.* **235**:241-54.

Lynch JC, Mountcastle VB, Talbot WH and Yin TCT. (1977). Parietal lobe mechanisms for direct attention. *J. Neurophysiol.* **40**:362-89.

Maguire WM and Baizer JS. (1984). Visuotopic organization of the prelunate gyrus in rhesus monkey. *J. Neurosci.* **4**:1690-704.

Maioli MG, Squatrito S, Galletti C, Battaglini PP and Sanseverino ER. (1983). Cortico-cortical Connections from the Visual Region of the Superior Temporal Sulcus to Frontal Eye Field in the Macaque. *Brain Research* **265**:294-99.

Maioli MG, Squatrito S, Samolsky-Dekel BG and Sanseverino ER. (1998). Corticocortical Connections between Frontal Periarcuate Regions and Visual Areas of the Superior Temporal Sulcus and the adjoining Inferior Parietal Lobule in the Macaque Monkey. *Brain Research* **789**:118-25.

Martinez-Conde S, Macknik DL and Hubel DH. (2004). The Role of Fixational Eye Movements in Visual Perception. *Nat Rev Neurosci.* **5**:229-40.

Maunsell JHR and Cook EP. (2002). The role of attention in visual processing. *Philos Trans R Soc Lond B: Biol Sci* **357**:1063-72.

Maunsell JHR and Van Essen DC. (1983a). The connections of the middle temporal visual area (MT) and their relationship to a cortical hierarchy in the macaque monkey. *J. Neurosci.* **3**:2563-86.

Maunsell JHR and Van Essen DC. (1983b). Functional properties of neurons in middle temporal visual area of the macaque monkey. I. Selectivity for stimulus direction, speed, and orientation. *J. Neurophysiol.* **49**:1127-47.

May JG and Andersen RA. (1986). Different patterns of corticopontine projections from separate cortical fields within the inferior parietal lobule and dorsal prelunate gyrus of the macaque. *Exp. Brain Res.* **63**:265-78.

Mays LE and Sparks DL. (1980). Dissociation of visual and saccade-related responses in superior colliculus neurons. *J. Neurophysiol.* **43**:207-32.

Mazzoni P, Bracewell RM, Barash S and Andersen RA. (1996a). Motor intention activity in the Macaque's lateral intraparietal area I. Dissociation of motor plan from sensory memory. *J. Neurophysiol.* **76**:1439-56.

Mazzoni P, Bracewell RM, Barash S and Andersen RA. (1996b). Spatially tuned auditory responses in area LIP of macaques performing delayed memory saccades to acoustic targets. *J. Neurophysiol.* **75**:1233-41.

Medalla M and Barbas H. (2006). Diversity of laminar connections linking periarcuate and lateral intraparietal areas depends on cortical structure. *Eur J Neurosci* **23**:161-79.

Mikami A, Newsome WT and Wurtz RH. (1986). Motion selectivity in macaque visual cortex. I. Mechanisms of direction and speed selectivity in extrastriate area MT. *J Neurophysiol* **55**:1308-27.

Moran J and Desimone R. (1985). Selective attention gates visual processing in the extrastriate cortex. *Science* **229**:782-84.

Morel A and Bullier J. (1990). Anatomical segregation of two cortical visual pathways in the macaque monkey. *Vis. Neurosci* **4**:555-78.

Moschovakis AK, Gregoriou GG, Ugolini G, Doldan M, Graf W, Guldin W, Hadjidimitrakis K and Savaki HE. (2004). Oculomotor areas of the primate frontal lobes: A transneuronal transfer of rabies virus and [14C]-2-Deoxyglucose functional imaging study. *J. Neurosci.*

Moschovakis AK, Scudder CA and Highstein SM. (1996). The microscopic anatomy and physiology of the mammalian saccadic system. *Progr. Neurobiol.* **50**:133-524.

Mountcastle VB, Lynch JC, Georgopoulos AP, Sakata H and Acuna C. (1975). Posterior parietal association cortex of the monkey: Command function for operations within extrapersonal space. *J. Neurophysiol.* **38**:871-908.

Movshon JA and Newsome WT. (1996). Visual Response Properties of Striate Cortical Neurons Projecting to Area MT in Macaque Monkeys. *J Neurosci* **16**:7733-41.

Munoz DP and Wurtz RH. (1993). Fixation cells in monkey superior colliculus. I. Characteristics of cell discharge. *J Neurophysiol* **70**:559-75.

Munoz DP and Wurtz RH. (1995). Saccade-related activity in monkey superior colliculus I. characteristics of burst and buildup cells. *J. Neurophysiol.* **73**:2313-33.

Murata A, Gallese V, Luppino G, Kaseda M and Sakata H. (2000). Selectivity for the shape, size, and orientation of objects for grasping in neurons of monkey parietal area AIP. *J. Neurophysiol.* **83**:2580-601.

Muri RM, Vermersch A-I, Rivaud S, Gaymard B and Pierrot-Deseilligny C. (1996). Effects of Single-Pulse Transcrdnial Magnetic Stimulation Over the Prefrontal and Posterior Parietal Cortices During Memory-Guided Saccades in Humans. *J Neurophysiol* **76**:2102-06.

Nakamura H, Gattass R, Desimone R and Ungerleider LG. (1993). The modular organization of projections from areas V1 and V2 to areas V4 and TEO in macaques. *J. Neurosci.* **13**:3681-91.

Newsome WT, Wurtz RH, Dursteler MR and Mikami A. (1985). Deficits in visual motion processing following ibotenic acid lesions of the middle temporal visual area of the macaque monkey. *J Neurosci.* **5**:825-40.

Newsome WT, Wurtz RH, Dursteler MR and Mikami A. (1985). Deficits in visual motion processing following ibotenic acid lesions of the middle temporal visual area of the macaque monkey. *J Neurosci.* **5**:825-40.

Newsome WT, Wurtz RH and Komatsu H. (1988). Relation of cortical areas MT and MST to pursuit eye movements. II. Differentation of retinal from extraretinal inputs. *J. Neurophysiol.* **5**:825-40.

Oram MW and Perrett DI. (1996). Integration of form and motion in the anterior superior temporal polysensory area (STPa) of the macaque monkey. *J Neurophysiol* **76**:109-29.

Oristaglio J, Schneider DM, Balan PF and Gottlieb J. (2006). Integration of Visuospatial and Effector Information during Symbolically Cued Limb Movements in Monkey Lateral Intraparietal Area. *J. Neurosci.* **26**:8310-19.

Ozyurt J, Rutschmann RM and Greenlee MW. (2006). Cortical activation during memory-guided saccades. *Neuroreport* **17**:1005-9.

Padberg J, Seltzer B and Cusick CG. (2003). Architectonics and cortical connections of the upper bank of the superior temporal sulcus in the rhesus monkey: an analysis in the tangential plane. *J Comp Neurol* **467**:418-34.

Paré M and Wurtz RH. (1997). Monkey posterior parietal cortex neurons antidromically activated from surerior colliculus. *J Neurophysiol.* **78**:3493-97.

Paus T, Marrett S, Worsley KJ and Evans AC. (1995). Extraretinal modulation of cerebral blood flow in the human visual cortex: implications for saccadic suppression. *J Neurophysiol* **74**:2179-83.

Petit L and Haxby JV. (1999). Functional anatomy of pursuit eye movements in humans as revealed by fMRI. *J Neurophysiol* **82**:463-71.

Petrides M and Pandya DN. (1999). Dorsolateral prefrontal cortex: comparative cytoarchitectonic analysis in the human and the macaque

brain and corticocortical connection patterns. *Eur. J. Neurosci.* **11**:1011-36.

Pierrot-Deseilligny C, Milea D and Muri R. (2004). Eye movement control by the cerebral cortex. *Curr Opin Neurol.* **17**:17-25.

Platt ML and Glimcher PW. (1997). Responses of intraparietal neurons to saccadic targets and visual distractors. *J. Neurophysiol.* **78**:1574-89.

Raiguel S, Van Hulle MM, Xiao DK, Marcar VL, Lagae L and Orban GA. (1997). Size and shape of receptive fields in the medial superior temporal area (MST) of the macaque. *Neuroreport* **8**:2803-08.

Rashbass C. (1961). The relationship between saccadic and smooth tracking eye movements. *J Physiol.* **159**:326-38.

Recanzone GH, Wurtz RH and Schwarz U. (1997). Responses of MT and MST neurons to one and two moving objects in the receptive field. *J, Neurophysiol.* **78**:2904-15.

Robinson DA. (1963). A method of measuring eye movement using a scleral search coil in a magnetic field. *Trans. Biomed. Engin.* **10**:137-45.

Robinson DA and Fuchs AF. (1969). Eye movements evoked by stimulation of frontal eye fields. *J. Neurophysiol.* **32**:637-48.

Robinson DL, Bowman E and Kertzman C. (1995). Covert orienting of attention in macaques. II. Contributions of parietal cortex. *J Neurophysiol* **74**:698-712.

Robinson DL, Goldberg ME and Stanton GB. (1978). Parietal association cortex in the primate: Sensory mechanisms and behavioral modulations. *J. Neurophysiol.* **41**:910-32.

Rodman HR and Albright TD. (1987). Coding of Visual Stimulus Velocity in area MT of the Macaque. *Vision Res.* **27**:2035-48.

Rodman HR, Gross CG and Albright TD. (1990). Afferent basis of visual response properties in area MT of the macaque. II. Effects of superior colliculus removal. *J. Neurosci.* **10**:1154-64.

Saito H, Yukie M, Tanaka K, Hikosaka K, Fukada Y and Iwai E. (1986). Integration of direction signals of image motion in the superior temporal sulcus of the macaque monkey. *J. Neurosci.* **6**:145-57.

Savaki HE. (1999). Sokoloff's 14C-deoxyglucose method. *Brain Res Bull* **50**:405-07.

Savaki HE, Kennedy C, Sokoloff L and Mishkin M. (1993). Visually guided reaching with the forelimb contralateral to a "blind" hemisphere: A metabolic mapping study in monkeys. *J. Neurosci.* **13**:2772-89.

Savaki HE, Raos VC and Dalezios Y. (1997). Spatial cortical patterns of metabolic activity in monkeys performing a visually guided reaching task with one forelimb. *Neuroscience* **76**:1007-34.

Scalaidhe SPÖ, Albright TD, Rodman HR and Gross CG. (1995). Effects of superior temporal polysensory area lesions on eye movements in the Macaque monkey. *J. Neurophysiol.* **73**:1-19.

Schall JD. (2004). On Building a Bridge Between Brain and Behavior. *Annu. Rev. Psychol.* **55**:23-50.

Schall JD, Morel A, King DJ and Bullier J. (1995). Topography of visual cortex connections with frontal eye field in macaque: Convergence and segregation of processing streams. *J. Neurosci.* **15**:4464-87.

Schiller PH and Lee K. (1994). The effects of lateral geniculate nucleus, area V4, and middle temporal (MT) lesions on visually guided eye movements. *Vis Neurosci.* **11**:229-41.

Schlag J and Schlag-Rey M. (1987). Evidence for a supplementary eye field. *J. Neurophysiol.* **57**:179-200.

Seltzer B, Cola MG, Gutierrez C, Massee M, Weldon C and Cusick CG. (1996). Overlapping and nonoverlapping cortical projections to cortex of the superior temporal sulcus in the rhesus monkey: double anterograde tracer studies. *J Comp Neurol* **370**:173-90.

Seltzer B and Pandya DN. (1978). Afferent cortical connections and architectonics of the superior temporal sulcus and surrounding cortex in the rhesus monkey. *Brain Res.* **149**:1-24.

Seltzer B and Pandya DN. (1986). Posterior parietal projections to the intraparietal sulcus of the rhesus monkey. *Exp. Brain Res.* **62**:459-69.

Seltzer B and Pandya DN. (1989a). Frontal lobe connections of the superior temporal sulcus in the rhesus monkey. *J. Comp. Neurol.* **281**:97-113.

Seltzer B and Pandya DN. (1989b). Intrinsic connections and architectonics of the superior temporal sulcus in the macaque monkey. *J. Comp. Neurol.* **290**:451-71.

Shadlen MN and Newsome WT. (1996). Motion perception- seeing and deciding. *Proc. Natl. Acad. Sci. USA* **93**:628-33.

Shibutani H, Sakata H and Hyvarinen J. (1984). Saccade and blinking evoked by microstimulation of the posterior parietal association cortex in monkey. *Exp. Brain Res.* **55**:1-8.

Shipp S and Zeki S. (1985). Segregation of the pathways leading from area V2 to areas V4 and V5 of macaque monkey visual cortex. *Nature (Lond.)* **315**:322-25.

Shipp S and Zeki S. (1989a). The organization of connections between areas V1 and V5 of monkey visual cortex. *Eur. J. Neurosci.* **1**:309-32.

Shipp S and Zeki S. (1989b). The organization of connections between areas V5 and V2 in macaque monkey visual cortex. *Eur. J. Neurosci.* **1**:333-54.

Snodderly DM. (1987). Effects of light and dark environments on macaque and human fixational eye movements. . *Vision Res.* **27**:401-15.

Snyder LH, Batista AP and Andersen RA. (1997). Coding of intention in the posterior parietal cortex. *Nature* **386**:167-70.

Snyder LH, Batista AP and Andersen RA. (1998). Change in motor plan, without a change in the spatial locus of attention, modulates activity in posterior parietal cortex. *J. Neurophysiol.* **79**:2814-19.

Snyder LH, Batista AP and Andersen RA. (2000). Saccade-related activity in the parietal reach region. *J. Neurophysiol.* **83**:1099-102.

Sokoloff L, Reivich M, Kennedy C, Des Rosiers MH, Patlak CS, Pettigrew KS, Sakurada O and Shinohara M. (1977). The [^{14}C]-deoxyglucose method for the measurement of local cerebral glugose utilization: Theory, procedure, and normal values in the conscious and anesthetized albino rat. *J. Neurochem.* **28**:879-916.

Squatrito S and Maioli MG. (1997). Encoding of Smooth Pursuit Direction and Eye Position by Neurons of Area MSTd of the Macaque Monkey. *J Neurosci.* **17**:3847-60.

Stanton GB, Bruce CJ and Goldberg ME. (1995). Topography of projections to posterior cortical areas from the macaque frontal eye fields. *J. Comp. Neurol.* **353**:291-305.

Suzuki WA and Amaral DG. (1994). Perirhinal and parahippocampal cortices of the macaque monkey: cortical afferents. *J. Comp. Neurol.* **350**:497-533.

Sweeney JA, Mintun MA, Kwee S, Wiseman MB, Brown DL, Rosenberg DR and Carl JR. (1996). Positron emission tomography study of voluntary saccadic eye movements and spatial working memory. *J. Neurophysiol.* **75**:454-68.

Tanaka K, Hikosaka K, Saito H, Yukie M, Fukada Y and Iwai E. (1986). Analysis of local and wide-field movements in the superior temporal visual areas of the macaque monkey. *J. Neurosci.* **6**:134-44.

Tanaka K, Sugita Y, Moriya M and Saito H-A. (1993). Analysis of object motion in the ventral part of the medial superior temporal area of the macaque visual cortex. *J. Neurophysiol.* **69**:128-42.

Tanaka M and Lisberger SG. (2002). Role of arcuate frontal cortex of monkeys in smooth pursuit eye movements: I. Basic response properties to retinal image motion and position. *J Neurophysiol* **87**:2684-99.

Tanne-Gariepy J, Rouiller EM and Boussaoud D. (2002). Parietal inputs to dorsal versus ventral premotor areas in the macaque monkey: evidence for largely segregated visuomotor pathways. *Exp. Brain Res.* **145**:91-103.

Tehovnik EJ, Sommer MA, Chou I-h, W.M. S and Schiller PH. (2000). Eye fields in the frontal lobes of primates. *Brain Res. Rev.* **32**:413-48.

Thiele A, Henning P, Kubischik M and Hoffmann K-P. (2002). Neural mechanisms of saccadic suppression. *Science* **295**:2460-64.

Thier P and Andersen A. (1998). Electrial microstimulation distinguishes distinct saccade-related areas in the posterior parietal cortex. *J. Neurophysiol.* **80**:1713-35.

Thier P and Erickson RG. (1992). Responses of visual-tracking neurons from cortical area MST-l to visual, eye and head motion. *Eur. J. Neurosci.* **4**:539-53.

Tobler PN, Felblingerb J, Bürkic M, Nirkkob AC, Ozdobac C and René M. Müri RM. (2001). Functional organisation of the saccadic reference system processing extraretinal signals in humans *Vision Res* **41**:1351-58.

Tolias AS, Moore T, Smirnakis SM, Tehovnik EJ, Siapas AG and Schiller PH. (2001). Eye Movements Modulate Visual Receptive Fields of V4 Neurons. *Neron* **29**:757-67.

Tootell RBH, Silverman MS, Switkes E and DeValois RL. (1982). Deoxyglucose analysis of retinotopic organization in primate striate cortex. *Science* **218**:902-04.

Treue S and Maunsell JHR. (1996). Attentional modulation of visual motion processing in cortical areas MT and MST. *Nature* **382**:539-41.

Treue S and Maunsell JHR. (1999). Effects of attention on the processing of motion in macaque middle temporal and medial superior temporal visual cortical areas. *J. Neurosci.* **19**:7591-602.

Ungerleider LG and Desimone R. (1986). Cortical projections of visual area MT in the maqaque. *J. Comp. Neurol.* **248**:190-222.

Van Essen DC, Maunsell JHR and Bixby JL. (1981). The middle temporal visual area in the macaque: myeloarchitecture, connections, functional properties and topographic representation. *J. Comp. Neurol.* **199**:293-326.

van Wezel RJH and Britten KH. (2002). Multiple uses for visual motion. The case for stability in visual cortex. *Neuroscience* **111**:739-59.

Vanduffel W, Tootell RB, Schoups AA and Orban GA. (2002). The organization of orientation selectivity throughout macaque visual cortex. *Cereb Cortex* **12**:647-62.

von Bonin G and Bailey P. (1947). *The neocortex of Macaca mulatta*. Urbana, Illinois: University of Illinois Press.

Wardak C, Etienne O and Duhamel J-R. (2002). Saccadic target selection deficits after lateral intraparietal area inactivation in monkeys. *J. Neurosci.* **22**:9877-84.

Watanabe J and Iwai E. (1991). Neuronal activity in visual, auditory and polysensory areas in the monkey temporal cortex during visual fixation task. *Brain Res. Bull.* **26**:583-92.

Webster MJ, Bachevalier J and Ungerleider LG. (1994). Connections of inferior temporal areas TEO and TE with parietal and frontal cortex in maqaque monkeys. *Cereb. Cortex* **4**:470-83.

Weller RE and Kaas JH. (1983). Retinotopic Patterns of Connections of Area 17 With Visual Areas V-I1 and MT in Macaque Monkeys. *J. Comp. Neurol.* **220**:253-79.

Wurtz RH. (1969). Comparison of effects of eye movements and stimulus movements on striate cortex neurons of the monkey. *J. Neurophysiol.* **32**:987-94.

Wurtz RH and Goldberg ME. (1972). Activity of superior colliculus in behaving monkey. 3. Cells discharging before eye movements. *J Neurophysiol* **35**:575-86.

Zeki S. (1996). Are areas TEO and PIT of monkey visual cortex wholly distinct from the fourth visual complex (V4 complex)? *Proc Biol Sci.* **263**:1539-44.

Zeki SM. (1971a). Convergent input from the striate cortex (area17) to the cortex of the superior temporal sulcus in the rhesus monkey. *Brain Res.* **28**:338-40.

Zeki SM. (1971b). Cortical projections from two prestriate areas in the monkey. *Brain Res.* **34**:19-35.

Zeki SM. (1974). Functional organization of a visual area in the posterior bank of the superior temporal sulcus of the rhesus monkey. *J. Physiol. (London)* **236**:549-73.

Zeki SM. (1977). Color coding in the superior temporal sulcus of rhesus monkey visual cortex. *Proc. R. Soc. Lond.* **197**:195-223.

APPENDIX

$$R_i = \frac{\overbrace{C_i^*(T)}^{\text{Total } {}^{14}C \text{ in tissue at time, T}} - \overbrace{k_1^* e^{-(k_2^*+k_3^*)T} \int_0^T C_p e^{(k_2^*+k_3^*)t}\, dt}^{{}^{14}C \text{ in precursor remaining in tissue at time, T}}}{\underbrace{\left[\frac{\lambda \cdot V_m^* \cdot k_m}{\phi \cdot V_m \cdot k_m^*}\right]}_{\text{Isotope effect correction factor}} \underbrace{\left[\underbrace{\int_0^T \left(\frac{C_p^*}{C_p}\right) dt}_{\text{Integrated plasma specific activity}} - \underbrace{e^{-(k_2^*+k_3^*)T} \int_0^T \left(\frac{C_p^*}{C_p}\right) e^{(k_2^*+k_3^*)t}\, dt}_{\text{Correction for lag in tissue equilibration with plasma}}\right]}_{\text{Integrated precursor specific activity in tissue}}}$$

Operational equation of the radioactive deoxyglucose method. Ci*, total ^{14}C concentration in a single homogenous tissue of the brain; Cp*, Cp, concentrations of [^{14}]deoxyglucose and glucose in the arterial plasma, respectively; Ce*, Ce, their respective concentrations in the tissue pools that serve as substrates for hexokinase; Cm*, concentration of [^{14}]deoxyglucose-6-phosphate in the tissue; k1*, k2*, k3*, rate constants for carrier-mediated transport of [^{14}]deoxyglucose from plasma to tissue, for carrier-mediated transport back from tissue to plasma, and for phosphorylation by hexokinase, respectively; k1, k2, k3, equivalent rate constants for glucose; T, time of termination of the experimental period; λ, ratio of the distribution space of deoxyglucose in the tissue to that of glucose; ϕ, the fraction of glucose that, once phosphorylated, continues down the glucolytic pathway; km*, Vm*, km, Vm, Michaelis-Menten kinetic constants of hexokinase for deoxyglucose and glucose, respectively.

The Labyrinth
W.H. Auden

Anthropos apteros for days
Walked whistling round and round the Maze,
Relying happily upon
His temperment for getting on.

The hundredth time he sighted, though,
A bush he left an hour ago,
He halted where four alleys crossed,
And recognised that he was lost.

"Where am I? Metaphysics say
No question can be asked unless
It has an answer, so I can
Assume this maze has got a plan.

If theologians are correct,
A Plan implies an Architect:
A God-built maze would be, I'm sure,
The Universe in miniature.

Are data from the world of Sense,
In that case, valid evidence?
What in the universe I know
Can give directions how to go?

All Mathematics would suggest
A steady straight line as the best,
But left and right alternately
Is consonant with History.

Aesthetics, though, believes all Art
Intends to gratify the Heart:
Rejecting disciplines like these,
Must I, then, go which way I please?

Such reasoning is only true
If we accept the classic view,
Which we have no right to assert,
According to the Introvert.

His absolute pre-supposition
Is - Man creates his own condition:
This maze was not divinely built,
But is secreted by my guilt.

The centre that I cannot find
Is known to my Unconscious Mind;
I have no reason to despair
Because I am already there.

My problem is how *not* to will;
They move most quickly who stand still;
I'm only lost until I see
I'm lost because I want to be.

If this should fail, perhaps I should,
As certain educators would,
Content myself with the conclusion;
In theory there is no solution.

All statements about what I feel,
Like I-am-lost, are quite unreal:
My knowledge ends where it began;
A hedge is taller than a man."

Anthropos apteros, perplexed
To know which turning to take next,
Looked up and wished he were the bird
To whom such doubts must seem absurd.